

## **ABSTRACT**

CHEN, KEN. Studies of Enhanced Instructional Modalities and Biosignals on User Performance in Virtual Reality Systems. (Under the direction of Dr. Karen Boru Chen)

Virtual reality (VR) is a computer-generated environment that can provide simulated experience of the real world through varied channels of sensory feedback. Visual feedback is the most deployed display in VR systems, which focuses on delivering information and stimuli to the visual sensory channel. In specific, current VR technology can display 3-D instructors and agents to guide users to perform various tasks. While conventional studies on 2-D instructors in desktop applications revealed that users tended to trust the instructors that exhibited similarities with them on appearances and personality, studies on 3-D instructors in VR applications were lacking. For haptic feedback, the interaction with VR objects is usually achieved through controllers and joysticks, which does not require forceful exertions that are necessary in the real world. Therefore, users may perceive less physical fidelity when interacting with the VR objects, which can impede the skill transfer from VR training to the real world. Previous study on pseudo-haptic brought up the concept of “virtual exertions” and used electromyography (EMG) as the haptic cue for VR interactions in a simple virtual dumbbell lifting task. It is worth investigating the idea of virtual exertions in more complicated movements that involved muscles across the full body.

The research purpose of this dissertation included: (1) studying the utility of 3-D virtual instructors in VR systems where different ways of designing 3-D humanoid instructors were examined and compared; (2) examining the concept of virtual exertions in a simulated patient transfer task using multi-binary criteria; and (3) applying the methods of virtual exertions in manual material handling (MMH) tasks and exploring new approaches for establishing virtual exertions threshold.

Two humanoid instructors were designed and examined in two extended reality (XR) applications. A 3-D humanoid model was developed and implemented in a virtual reality exercise program to guide participants to perform pick and place movements; A point-cloud generated humanoid instructor was built in an augmented reality (AR) posture training platform to demonstrate common manual material handling postures. Both humanoid instructors achieved their instructional functions as expected while demonstrated different characteristics: 3-D model based virtual instructor was more flexible and could be easily animated to convey dynamic movement information to the participants; point cloud generated virtual instructor shared more similarities with real humans on appearances but was difficult to be edited and animated.

A simulated patient transfer task was studied in a laboratory setting with EMG sensors attached to participants' muscles across the whole body. Principal component analysis was utilized to select the major contributing muscles of the task. A virtual patient transfer task was conducted targeting the selected major muscles, participants needed to contract all muscles to reach the respective calibration threshold obtained during the physical transfer tasks. The results showed that participants could only finish the tasks with adjusting factors that scaled down the lifting thresholds, which suggested that the multi-binary criterion was difficult to achieve.

The third study used psychophysical methods to evaluate MMH tasks, examined the potential of classifying MMH movements using EMG signal, and finally designed a virtual squat lifting task using regression-based criterion. The results showed that the program could evoke comparable sense of perceived exertions in the virtual lifting task against the physical lifting task.

Studies of Enhanced Instructional Modalities and Biosignals on User Performance in Virtual Reality Systems

by  
Ken Chen

A dissertation submitted to the Graduate Faculty of  
North Carolina State University  
in partial fulfillment of the  
requirements for the Degree of  
Doctor of Philosophy

Industrial Engineering

Raleigh, North Carolina

2022

APPROVED BY:

---

Dr. Karen Boru Chen  
Committee Chair

---

Dr. Xu Xu

---

Dr. Xiaolei Fang

---

Dr. Daowen Zhang

## **BIOGRAPHY**

Ken Chen obtained a Bachelor of Engineering in Quality and Reliability Engineering from Beihang University in 2017. In the same year, he was enrolled into the Ph.D. program of Industrial and Systems Engineering at North Carolina State University with a research focus on human factors. Apart from majoring in Industrial Engineering, he also developed an interest in Statistics and began to pursue a minor in Statistics. Ken's research interests included biosignal feedback in virtual reality system, human-system interactions, and electromyography signal processing. To date, he has completed several research projects that were supported in part by US National Science Foundation grants and US National Institute for Occupational Safety and Health grants. After graduation, he plans to continue his research in human factors in academia or industry.

## ACKNOWLEDGEMENTS

There are many people that I must thank during the process of pursuing a Ph.D. Foremost, I would like to thank my families for their continuous and selfless support throughout my life. They always stand by my side and makes me feel loved and cared during the difficult times. When I made the decision to go abroad and pursue a Ph.D. in a totally different environment, their unconditional support and encouragement gave me courage and confidence to start the journey.

Next, I want to express my sincere thanks to my advisor, Dr. Karen Boru Chen, for her guidance, support, and encouragement during my research and life. Particularly, her warm concern for me and my family during the pandemic really inspired and touched me. I've learnt a lot from her, and I enjoyed doing research under her supervision.

I would like to thank my committee members, Dr. Xu Xu, Dr. Daowen Zhang, Dr. Xiaolei Fang and Dr. Jing Feng for their valuable suggestions on my research, which helped to improve my work. In specific, I want to thank Dr. Xu for his continuous advice on my research projects and career development.

I would like to thank my research colleagues in the labs, Li Li, Rebecca Widmayer, Gimantha Perera, Nathan Sanders, Ziyang Xie, Linfeng Wu, HanwenWang and Lu Lu for their support and contribution to my studies. They are my research partners and friends.

Lastly, I would like to thank National Science Foundation for providing financial fundings to complete my research.

# TABLE OF CONTENTS

<b>LIST OF TABLES</b> .....	<b>vi</b>
<b>LIST OF FIGURES</b> .....	<b>viii</b>
<b>Chapter 1 Introduction</b> .....	<b>1</b>
<b>Chapter 2 Background and literature review</b> .....	<b>4</b>
2.1 Virtual reality.....	4
2.1.1 Human experiences in Virtual reality.....	6
2.1.2 Augmented feedback in Virtual reality .....	8
2.1.3 Limitations of VR system.....	10
2.2 Electromyography (EMG).....	11
2.2.1 Normalization of EMG.....	12
2.2.2 EMG feature extractions.....	14
2.2.3 EMG based movement classification.....	17
2.2.4 EMG based force estimation.....	20
<b>Chapter 3 The study of instructional modalities in XR applications</b> .....	<b>23</b>
3.1 Motivation.....	23
3.2 Evaluation of an instructor-guided virtual reality exercise (VRE) program .....	25
3.2.1 Introduction.....	25
3.2.2 Methods .....	29
3.2.3 Results .....	35
3.2.4 Discussion.....	38
3.2.5 Conclusions.....	43
3.3 Design of an augmented reality (AR) based posture training tool .....	44
3.3.1 Introduction.....	44
3.3.2 Methods .....	46
3.3.3 Results .....	53
3.3.4 Discussion.....	55
3.3.5 Conclusions.....	58
3.4 Summary .....	58
<b>Chapter 4 Effects of EMG feedback for simulated patient transfer task in VR system</b> .....	<b>60</b>
4.1 Motivation.....	60
4.2 Identify major contributing muscles in a simulated patient transfer task .....	61
4.2.1 Introduction.....	61
4.2.2 Methods .....	64
4.2.3 Results .....	70
4.2.4 Discussion.....	74

4.2.5 Conclusions .....	79
4.3 Simulate forceful exertions during virtual patient transfer tasks .....	80
4.3.1 Introduction .....	80
4.3.2 Methods .....	81
4.3.3 Results .....	86
4.3.4 Discussion and conclusions .....	89
4.4 Summary .....	92
<b>Chapter 5 Effects of EMG feedback for generalized gross movements in VR system.....</b>	<b>94</b>
5.1 Motivation .....	94
5.2 Examine human’s just noticeable differences (JND) for weight perception.....	94
5.2.1 Introduction.....	94
5.2.2 Methods .....	97
5.2.3 Results .....	100
5.2.4 Discussion.....	104
5.3 Examine EMG based classification for manual material handling tasks.....	106
5.3.1 Introduction.....	106
5.3.2 Methods .....	108
5.3.3 Results .....	113
5.3.4 Discussion.....	115
5.4 Examine EMG guided virtual exertions for manual lifting task.....	118
5.4.1 Introduction.....	118
5.4.2 Methods .....	119
5.4.3 Results & Discussion .....	127
5.5 Summary .....	131
<b>Chapter 6 Conclusion .....</b>	<b>132</b>
<b>REFERENCES.....</b>	<b>135</b>
<b>APPENDICES .....</b>	<b>172</b>
Appendix A.....	173
Appendix B .....	174
Appendix C .....	175

## LIST OF TABLES

Table 2-1	Different types of VR visual display devices. ....	5
Table 2-2	EMG features in time domain. ....	15
Table 2-3	EMG features in frequency domain.....	16
Table 2-4	EMG classification features and methods. ....	20
Table 2-5	EMG force prediction methods and performance. ....	22
Table 3-1	Overall mean ( $\pm 1SD$ ) of maximum shoulder flexion angle for the 3 $\times$ 2 conditions in different VR scenarios. ....	35
Table 3-2	Items from PSSUQ received ratings greater than 4 (“neutral”) from more than two participants. Frequency refers to the number of participants gave a rating greater than 4. ....	53
Table 3-3	Post-task responses related to four general open-ended questions (count of recurring comments listed as frequency. ....	54
Table 3-4	Post-task responses related to four general open-ended questions (count of recurring comments listed as frequency. ....	55
Table 4-1	The three regions of muscles and the muscles of interest within each group. ....	65
Table 4-2	Mean and standard deviation of body discomfort score of the different body sections. ....	74
Table 5-1	Movement/posture decoding number. ....	112
Table 5-2	Results of intra-participant classification from Experiment I (static lifting postures). LDA = linear discriminant analysis; kNN = k-nearest neighbor; SVM = support vector machine. ....	113
Table 5-3	Results of inter-participant classification from Experiment I (static lifting postures). LDA = linear discriminant analysis; kNN = k-nearest neighbor; SVM = support vector machine. ....	114
Table 5-4	Results of intra-participant classification for Experiment II (dynamic lifting movements). ....	114

Table 5-5	Confusion matrix for SVM classifier with normalized feature sets. ....	115
Table 5-6	Results of inter-participant classification for Experiment II (dynamic lifting movements). ....	115
Table 5-7	Rated perceived exertion (RPE) scores for the physical lifting task. There were three lifting weights and three lifting heights. ....	127
Table 5-8	Rated perceived exertion (RPE) scores for the virtual lifting task. If the participants failed to reach the threshold in 5 seconds, they were given a second chance to try to exert their muscles to reach the threshold. ....	128
Table 5-9	Maximum virtual lifting weight. ....	129
Table 5-10	Comparison between the virtual exertion studies. ....	130

## LIST OF FIGURES

Figure 2-1	The Reality-Virtuality (RV) Continuum, which consists of the real environment (RE) and the virtual environment (VE) on both ends, and augmented reality (AR) and augmented virtuality (AV) in between. Both AR and AV make up mixed reality (MR). (Milgram & Colquhoun, 1999).....	4
Figure 2-2	Different VR display systems. A) TV monitor; B) Head-mounter display (HMD); C) Cave automatic virtual environment (CAVE).....	5
Figure 2-3	Sample plot of EMG signal. ....	11
Figure 2-4	Flowchart of the EMG based movement. ....	17
Figure 2-5	Extract actual EMG pattern through threshold technique. Blue plots denote the raw EMG; black curves denote the RMS plot of the raw EMG; orange arrows denote the extraction threshold (e.g. $0.1 * \text{peak RMS}$ ). ....	18
Figure 2-6	Feature extractions through overlap windowing technique with window length (WL) and step length (SL). In this figure, $WL = 2000$ samples, and $SL = 500$ samples. ....	19
Figure 3-1	Example of a conventional humanoid agent (Oertel et al., 2020). ....	23
Figure 3-2	(A) 3-D humanoid model, (B) point cloud reconstructed humanoid model. ....	25
Figure 3-3	(a) Experimental setup and participant. A participant with EMG sensors and motion-tracking sensors attached on upper body in a fixed standing position holding the controller while looking into a head-mounted display. The EMG sensors are attached to the deltoid (1), the supraspinatus (2), and infraspinatus (3); (b) A snapshot of the real-time joint data captured by the motion capture system at the same posture of (a). The labeled marker regions are as follows: right wrist (A), right elbow (B), right acromion (C), incisura jugularis (D), C7 (E), T8 marker cluster (F), xiphoid process marker cluster (G), left acromion (H), left elbow (I), and left wrist (J); (c) The joint data mapped to humanoid model for generating instructor animations. ....	31

Figure 3-4	Exercise scenarios from the virtual environment, where the white camera icon depicts the location of the participant and thus “camera view”. (a) The imitation-oriented practice condition had a virtual instructor standing in front of the participant’s avatar, where the participant controlled the avatar’s movement to mimic the movement of the virtual instructor. (b) The task-oriented practice condition was to perform a pick-and-place task, where the participant controlled an avatar to pick up books and placed them on the shelf. ....	33
Figure 3-5	Three levels of game like feature for task-oriented practice condition: (a) low level, (b) middle level, (c) high level. The white camera icon depicts the location of the participant and thus “camera view”. The white circles depict the sophisticated lighting elements in the high game like feature level. ....	34
Figure 3-6	Activity of the deltoid across different game feature levels ( $\pm 1$ S.E.). The muscle activities were not statistically significantly across different scenarios. ....	36
Figure 3-7	Activity of the supraspinatus across different VR scenarios ( $\pm 1$ S.E.). The muscle activities are statistically different between task-oriented and imitation-oriented scenarios. $**p < 0.001$ . ....	37
Figure 3-8	Activity of the infraspinatus across different VR scenarios ( $\pm 1$ S.E.). The muscle activities were not statistically significantly across different scenarios. ....	38
Figure 3-9	Placement of RGB-D cameras. ....	47
Figure 3-10	The front, back, left-side, and right-side views, capture by the four RGB-D cameras (starting from the leftmost one). ....	47
Figure 3-11	Point cloud before noise removal (left) and after noise removal (middle), and the pink/purple regions depict the noise removed (right). ....	48
Figure 3-12	The registered and reconstructed point cloud human from a different view to depict the merged point clouds. ....	49
Figure 3-13	(A) The UI (virtual instructor at the center and information panel). The top center area has the dropdown menu and the series of play/pause icons, as well as date and time elements. The upper right section shows factual information and the	

	description of the task being performed. The lower right has toggle checkboxes to hide/unhide task description. (B) Participant using HoloLens.....	51
Figure 4-1	Locations of EMG sensors across three muscle groups, adapted from <a href="https://www.healthline.com/human-body-maps/muscular-system#1">https://www.healthline.com/human-body-maps/muscular-system#1</a> .....	66
Figure 4-2	Participants performed the two-step patient transfer task with the researcher. (a) Begin to lift patient. (b) Lift Patient to backboard height. (c) Move patient laterally. (d) Place patient on the backboard. (e) Lift the weighed backboard to ambulance loading height.....	68
Figure 4-3	Cumulative variances of PC1 and PC2. PCA with RMS input demonstrated significant higher cumulative variances compared to PCA with MDF input.....	71
Figure 4-4	Muscles in the extremities muscle region that were tested and analyzed. The y-axis (count) is the total count of major muscles across all trials. Muscles in this group were: Biceps Femoris (BF), Biceps Brachium (BI), Extensor Carpi Radialis (ECR), Flexor Carpi Radialis (FCR), Hamstring (HAM), Triceps (TRI), Vastus Lateralis (VL). .....	72
Figure 4-5	Muscles in the shoulder muscle region that were tested and analyzed. Muscles in the group were: Anterior Deltoid (AD), Middle Deltoid (MD), Posterior Deltoid (PD), Upper Trapezius (UT), Middle Trapezius (MT) and Lower Trapezius (LT). .....	72
Figure 4-6	Muscles in the back muscle region that were tested and analyzed. Muscles in the group were: Rectus Abdominus (RA), External Oblique (EO), Internal Oblique (IO), Latissimus Dorsi (LD), Thoracic Erector Spinae (TES) and Lumbar Erector Spinae (LES).....	73
Figure 4-7	Screen capture and CAVE view of the VR scenario for the three-step lift. It was cityscape with a patient on a backboard in the road next to an ambulance. ....	85
Figure 4-8	Mean of adjusting factors at each of the three phases of lifting. ....	87
Figure 4-9	Mean nEMG of left upper trapezius by weight and environment. ....	88
Figure 4-10	Mean NASA-TLX response for physical lift and virtual lift.....	89

Figure 5-1	Experiment setup. (A) Eight boxes in one weight group, the reference box was marked with a black tape. (B) A participant carried the box back to the table. ....	99
Figure 5-2	Polynomial logistics regression models depict the relationship between probability of detection and weight ratio at three different weight levels. The error bars are also $\pm 1S.E$ at the experimental weight ratios. The gray lines represent the $\pm 1S.E.$ of the respective logistics regression model. ....	101
Figure 5-3	Polynomial logistics regression models depict the relationship between probability of detection and weight ratio at two different task conditions. The error bars are also $\pm 1S.E$ at the experimental weight ratios. The gray lines represent the $\pm 1S.E.$ of the respective logistics regression model. ....	101
Figure 5-4	Linear regression model on nRPE across different weight ratios. The error bars are also $\pm 1S.E$ at the experimental weight ratios. the gray lines represent the $\pm 1S.E.$ of the respective logistics regression model. ....	103
Figure 5-5	Mean of NASA-TLX scores for walking and standing condition. ....	104
Figure 5-6	(A) The metal shelf with three levels; (B) The handcart loaded with boxes. ....	109
Figure 5-7	Locations of EMG sensors across the bilateral muscles, figure adapted from (Trigno, Delesys Inc, MA). ....	110
Figure 5-8	Participant performed a series of MMH movements: 1. Push the loaded handcart; 2. Pull the loaded handcart; 3. Squat lift the box; 4. Stoop lift the box. To note, the number/label of the movements were not the actual sequence of the tasks. The participants performed the tasks in the following sequence: 1 - 3 - 4 - 2. ....	111
Figure 5-9	Locations of EMG sensors across the bilateral muscles, figure adapted from (Trigno, Delesys Inc, MA). ....	121
Figure 5-10	One participant performing a squat lifting task. 1) physical lifting tasks and 2) virtual lifting tasks; The participant saw a virtual box, shelf and text through the HMD, the virtual scene is presented in Figure 5-12. ....	122
Figure 5-11	The process of finding optimal lambda with lowest mean squared error (MSE). The green circle located the lambda at minimum cross-validation MSE, and the	

blue circle located the lambda with minimum cross-validation error plus one standard error. For this study, the lambda that contributed to minimum cross-validation MSE (the green circle) was employed..... 124

Figure 5-12 Screenshot of the virtual lifting tasks from 1) a third-person view and 2) a first-person view..... 125

Figure 5-13 Workflow of the regression-based virtual exertion task..... 126

## Chapter 1 Introduction

Virtual reality (VR) is a computer-generated environment that can provide highly interactive, simulated, stereoscopic experience of the real world. VR systems afford adaptable environment, provides highly motivational interactions and offers easily accessible communication channels (Burdea, 2003). Because of these benefits , a variety of VR applications have been developed in the area of education (Freina & Ott, 2015), rehabilitation (Schultheis & Rizzo, 2001), and training (Chua et al., 2003), which show promising potential for future success. Particularly in training and instructional applications, VR provides a safe and controllable platform for trainees to perform the training tasks.

VR systems provide enhanced feedback through varied channels of sensory output. Visual feedback is the most deployed sensory output in VR systems. In specific, current technology makes it possible to create 3-D instructors/agents to guide participants through various tasks. Past studies revealed that people tended to trust the instructors that are similar to them (Behrend & Thompson, 2011; Brewer, 1979), and these similarities arise from surface attributes like age, gender or race and deep attributes like behavior and personality (Behrend & Thompson, 2011). However, these studies focused on real instructors or instructors in 2-D videos. Therefore, there is a need to study the use of 3-D humanoid instructors in VR applications. For haptic feedback, the interactions with virtual objects are usually achieved by input devices like controllers in VR systems, which do not require forceful efforts and intense muscle contractions (Chen, Ponto, Tredinnick, & Radwin, 2015; Radwin, Chen, Ponto, & Tredinnick, 2013), therefore users may perceive less physical fidelity and immersion, which could impede the skill transfer from VR training to the real world (Howard, 2017). Therefore, it is worth investigating novel methods of haptic feedback.

To study the use of 3-D instructors, this dissertation evaluated the functionalities of humanoid instructor in two extended reality (XR) applications, which covers all real-virtual combined environments (Chuah, 2019). Two experiments were conducted to study the function of a graphically rendered 3-D model instructor in a virtual reality exercise (VRE) program and a point cloud based 3-D instructor in an augmented reality (AR) posture training system. To accommodate the lack of forceful feedback in VR training program, previous research has examined the concept of “virtual exertions” (K. B. Chen et al., 2015), which incorporated electromyography (EMG) signal into their novel VR program. EMG signals evaluate electrical activity produced by muscle contractions (Reaz et al., 2006). Post-processed EMG amplitude may demonstrate qualitative relation with force generated by the respective muscle groups (Perry & Bekey, 1981). Two experiments were conducted to generalize the concept of “virtual exertions” to gross movements and common physical tasks.

The manuscript is organized as follows. Background and related works are presented in Chapter 2, which cover literature review of studies in VR and EMG. Chapter 3 consists of two experiments that investigated the use of 3-D humanoid instructors in XR applications, in which the first experiment studied the role of graphically rendered 3-D model instructor on a virtual pick-and-place task; the second experiment studied the use of point cloud based 3-D instructor in a posture training scenario achieved through an AR interface. Chapter 4 discusses the use of EMG to simulate haptic feedback in a virtual patient transfer task. Firstly, one experiment was conducted in the physical world to extract major contributing muscles during the simulated transfer task. Next, the same set of transfer task was conducted in a virtual scenario and haptic feedback was implemented through EMG feedback of the major contributing muscles. Chapter 5 comprises three experiments, the first one studied psychophysical measure of box lifting task in standing condition

and walking condition. The second experiment explored the possibility of classifying whole-body manual material handling movements via multi-EMG. The final experiment implemented the multi-EMG regression methods into the new VR interface and evaluated the validity of the new VR interface.

## Chapter 2 Background and literature review

### 2.1 Virtual reality

Virtual reality (VR) is a computer-generated environment that provides simulated experience of the real world. Depending on the degree of overlap between the real environment and the virtual environment, concepts like augmented reality (AR), mixed reality (MR) were also brought up. As illustrated in Figure 2-1, MR is the merging of real world elements and virtual elements; AR shares more similarities with the real world, and enables users to visualize physical world superimposed with computer generated virtual objects (Blade & Padgett, 2002). Overall, these all terms can be referred to as extended reality (XR), which covers all real-virtual combined environments (Chuah, 2019).

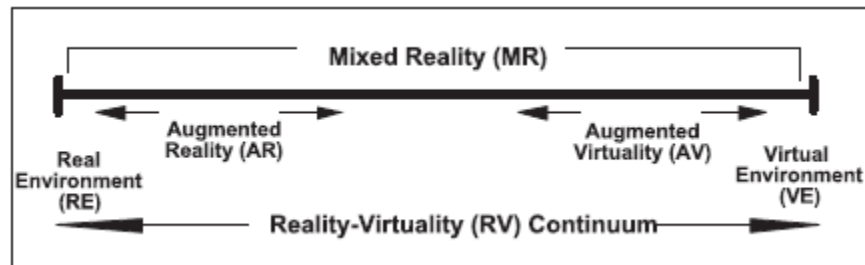


**Figure 2-1** The Reality-Virtuality (RV) Continuum, which consists of the real environment (RE) and the virtual environment (VE) on both ends, and augmented reality (AR) and augmented virtuality (AV) in between. Both AR and AV make up mixed reality (MR). (Milgram & Colquhoun, 1999).

A VR system consists of a processing unit, such as a computer, and user interfaces that include a VR display and a control unit (e.g., controllers). In addition to the software and hardware, some researchers argue the human user is also a component of a VR system (Grady, 2003). A VR display is not limited to visual modality achieved through projectors or monitors, it also includes auditory display and haptic display (Sigrist et al., 2013). Visual effects are created by computers and form the most important sensory feedback in VR system, and they are presented to users

through visual displays that vary in size, cost, and levels of immersion. Table 2-1 and Figure 2-2 below summarize some representative examples of these visual display devices and their characteristics.

**Table 2-1** Different types of VR visual display devices.

Device	Size	Type	Cost	Immersion
TV screen, computer monitor	Medium	Non-immersive	Low	Low
Head-mounter display (HMD)	Small	Fully immersive	Medium	High
CAVE	Large	Fully immersive	High	High



A



B



C

**Figure 2-2** Different VR display systems. A) TV monitor; B) Head-mounter display (HMD); C) Cave automatic virtual environment (CAVE).

Apart from visual effects, VR can also provide auditory feedback and haptic feedback through devices like headphone and tactile gloves. Compared to conventional interactive platforms, VR has abundant advantages. For instance, VR can provide controllable scenarios that allow the users to experience environments and activities that are dangerous in real world (F. D. Rose et al., 2005). The interactions in VR are highly motivational and they facilitate game-like experience (Burdea, 2003; Lohse et al., 2016). In addition, VR is programmable and can be easily adjusted

for different users or needs (Burdea, 2003). For these reasons, VR has various applications and are implemented in the areas of entertainment, education, training, and therapeutic rehabilitation (Burdea, 2003; Naranjo et al., 2020; Parekh et al., 2020; Uppot et al., 2019).

### **2.1.1 Human experiences in Virtual reality**

To study human perception and experience in a virtual environment, there are two concepts that commonly compared: presence and immersion.

#### **2.1.1.1 Presence**

Presence is a subjective feeling of being in an environment (Slater, 2018). For VR systems, it refers to the sense of being present at the location that is displayed to the user in the virtual environment. This psychological feeling can be affected by factors that include VR hardware, sensory feedback, human-computer interactions, etc. (Slater & Usoh, 1993). A “perfect” VR system should convince the users that the virtual world is real and they are truly present at the virtual world (Bates, 1992). Previous studies have shown the feeling of presence had significant effects on users’ performance in VR. For instance, Slater et al. (1996) found that people behaved more naturally in VR when they felt higher degree of presence. However, the sense of presence is highly subjective, thus it has been challenging for researchers to develop a widely accepted way of directly measuring presence (Grassini & Laumann, 2020).

The major methods of measuring presence include: questionnaires and interviews, physiological measures, and user behavior analysis (Grassini & Laumann, 2020; Hein et al., 2018). Questionnaires are the most frequently used methods of measuring presence (Hein et al., 2018) as they are cheap and easy to administer. Various questionnaires have been designed and implemented which include Igroup Presence Questionnaire (IPQ), Slater-Usoh-Steed

Questionnaire (SUS) and Witmer and Singer's Presence Questionnaire (PQ) (Grassini & Laumann, 2020; Slater, 1999; Witmer & Singer, 1998). Among these questionnaires, PQ is the most prevalent tool that is adopted by most of the researchers (Grassini & Laumann, 2020). However, the results from different questionnaires are difficult to compare and are prone to bias (Kober & Neuper, 2013; Szczurowski & Smith, 2018). For the physiological measure, electroencephalography (EEG) that captures human brain activity is the most prevalent measure of presence (Grassini & Laumann, 2020; Terkildsen & Makransky, 2019). Apart from EEG, heart rate (HR) can also be a possible measure of presence (Grassini & Laumann, 2020). While the physiological measures are more objective compared to questionnaires, there is no consensus which one is the best (Grassini & Laumann, 2020). The third method of measuring presence is user behavior analysis. In general, it is achieved through evaluating whether people's performance (e.g. movement pattern like postural sway) in VR is natural as that of real world (Grassini & Laumann, 2020). This method is not easy to control and requires additional feedback in VR.

### **2.1.1.2 Immersion**

Immersion is a metric of VR system that can be mistakenly used for the term presence. While presence depicts the human's subjective experience, immersion is an objective measure of a VR system. Immersive systems are defined as "extensive, surrounding, inclusive, vivid and matching" (Slater et al., 1995). Immersion is a key feature of VR systems and can influence users' subjective presence (T. Rose et al., 2018). Immersion of a VR system depend on the various factors that include VR hardware, sensory feedback and human-computer interactions, etc (Zyda, 2005). For instance, given two systems with all other conditions being the same, a system with a larger field of view is considered more immersive than the one with a smaller field of view; one that generates real-time shadow is more immersive if the other one does not; one allows users to turn

head and still receive visual feedback is more immersive if the other one does not (Slater, 1999). As for the influence of immersion, some researchers argue that human performance improvement in searching task in VR is through increased immersion (Pausch et al., 1997), while some other researchers found no significant relationship between immersion and improvement in VR rehabilitation (T. Rose et al., 2018).

### **2.1.2 Augmented feedback in Virtual reality**

Augmented feedback, also termed as extrinsic feedback, is defined as the information that cannot be present without an external source (Sigrist et al., 2013). For a VR system, various augmented feedback can be manipulated to make the system more immersive.

Visual feedback is the most common augmented feedback in VR systems which is achieved through display devices like TV monitor, HMD and CAVE. These VR displays put up one or two screens in front of the users' eyes and render images in real-time according to the users' activities (Strickland, 2007). Consequently, the position of user's eyes and head need to be tracked. To simulate real life experiences, factors like frame rate and field of view (FOV) need to be properly adjusted (Raaen, 2015; Ragan et al., 2015).

Auditory feedback is another sensory output of the VR system which is usually achieved through headphones. To create realistic experience, the sound in VR needs to be 3-D and its' orientation should shift in a natural way as of the real-world sound (Strickland, 2007). Various studies have been conducted to study the implementation of auditory feedback in VR systems. For instance, Wellner et al. (2008) evaluated visual feedback and auditory feedback in virtual obstacle walking tasks and found that continuous auditory feedback leads to a significantly higher gait speed than visual feedback. Y. Zhang et al. (2005) proposed that integrated feedback (visual and auditory) can lead to increased human performance compared to either feedback alone; for people

with visual impairments, researchers used auditory feedback combined with haptic feedback to navigate them through different virtual scenarios (Zhao et al., 2018).

Haptic feedback is also a key factor in VR systems. In the physical environment, humans interact with objects through body contact by voluntarily contracting the muscles to lift, place, and manipulate physical objects. While in VR, the interactions with virtual objects are usually achieved by input devices like controllers, which do not require natural forceful efforts and intense muscle contractions (K. B. Chen et al., 2015; Radwin et al., 2013), therefore users may perceive less effort and lower workload. To evoke haptic perception, researchers have explored a variety of haptic devices to deliver physical tactile (feedback to sensory receptors in the skin) and kinesthetic (feedback to the sensory receptors in the muscles and joints) experiences in VR. Vibrotactile actuators were integrated with gloves to provide tactile feedback and convey stiffness to users' hands (Bullion & Gurocak, 2009; Perret & Poorten, 2018), but users were not required to exert opposing forces to actively interact with the system. Alternatively, exoskeletons or similar devices were integrated to deliver kinesthetic feedback to users (Chakarov et al., 2017; Frisoli et al., 2009).

Other than sensory feedback, some researchers have utilized bio-signals, such as electromyography (EMG) to create higher immersive VR systems. For instance, Chen et al. (2015) proposed and demonstrated the concept of “virtual exertions” to encode EMG signals and track hand movements for interacting with virtual objects. The experimental task was to reach, grasp, then hold a virtual dumbbell for five seconds, and then return the virtual dumbbell to a virtual table. Specifically, the grasping of virtual objects was achieved in two steps: (1) a user's tracked hand position collided with virtual objects and (2) the user contracted the prime mover muscle group (i.e., biceps brachii) and reached a calibrated EMG threshold. When the two steps were accomplished, the virtual object was considered “grasped” and “moved” with the user's hand.

### **2.1.3 Limitations of VR systems**

Despite of all the advantages and benefits, VR systems also have limitations and challenges. Firstly, from the perspective of hardware, the weight of HMD, interpupillary distance, field of view still need further study and adjustment as they can contribute to users' comfort when wearing the HMD (Mehrfard et al., 2019). Besides, some participants might feel claustrophobic as they feel the pressure on nose when wearing a HMD (Appel et al., 2020). For people wear glasses, HMD can pose additional burdens in terms of fitting HMD to the glasses and focusing on the VR content (Appel et al., 2020).

Secondly, sickness might occur for some VR users and lead to discomfort and symptoms such as headache, stomach awareness, nausea, etc., which are similar to motion sickness (Kolasinski, 1995; J. J. LaViola Jr, 2000). Previous studies have shown that various factors can contribute to VR sickness (Chang et al., 2020). Several studies have even concluded that although HMD can enable more realistic stereoscopic contents, it may also induced more severe VR sickness symptoms (Dennison et al., 2016; K. Kim et al., 2014). This may be due to the discrepancy between expected vestibular inputs induced by stereoscopic contents and actual perceived sensory information (Chang et al., 2020). Some researchers found that latency was closely related with VR sickness (DiZio & Lackner, 1997; Rebenitsch & Owen, 2016). Specifically, the lag time between users' activity and the VR systems' feedback, or latency, needs to be minimized to reduce VR sickness (Chang et al., 2020). Some studies investigated the effects of duration on VR sickness and concluded that longer exposure time could lead to increased VR sickness (So et al., 2001; So & Lo, 1999; Stanney et al., 2003). The severity of VR sickness differs by person, and the factors that can influence VR sickness include age, gender and prior VR experience (Chang et al., 2020). To measure VR sickness, subjective self-reported questionnaires (Kennedy et al., 1993) and

objective physiological measures such as EEG (Y. Y. Kim et al., 2005), postural sway (Lubeck et al., 2015; Palmisano et al., 2018), blood pressure (Farmer et al., 2015) were examined.

Finally, VR is still limited in real applications. For instance, in the area of virtual rehabilitation, despite of the encouraging results from pilot studies, universal clinical acceptance is still underway (Burdea, 2003). In addition, current standard commercial VR equipment cannot accommodate “special needs”, which constrained its’ use for different patients.

## 2.2 Electromyography (EMG)

Electromyography (EMG) is a diagnostic signal that records and evaluates muscle activity (Robertson et al., 2014). EMG can be viewed as a function of time with the unit of voltage (Figure 2-3).

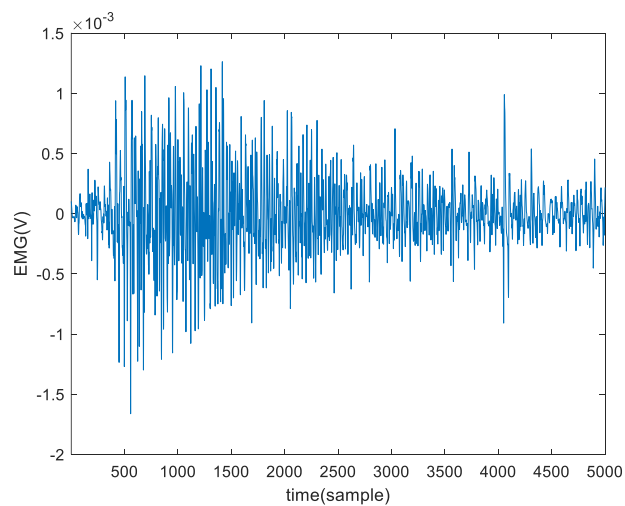


**Figure 2-3** Sample plot of EMG signal.

### **2.2.1 Normalization of EMG**

Raw EMG signals can be affected by various factors, including electrode configuration and placement (Halaki & Gi, 2012), skin preparation (Cram & Rommen, 1989), and perspiration and temperature (Winkel & Jørgensen, 1991). The effect of these factors may vary among individuals, time, and laboratories, which makes direct comparison of EMG signals collected at different instances challenging. To address this challenge, raw EMG signals can be normalized against a reference value. Quantitatively speaking, this means to divide the raw EMG signal by a reference value and the resultant will then be reported as the percentage of the reference. By doing this, normalized EMG (nEMG) values may be used to compare across different experiments as the effects of those influential factors were eliminated (Konard, 2012). Currently there are no standard or unique methods to select the best reference to normalize the raw EMG, but a “good” reference should be reliable, repeatable and meaningful (Halaki & Gi, 2012). Although different tasks and muscles may have preferred methods to choose the normalization reference, the most common normalization methods include the maximum voluntary isometric contractions (MVIC), mean dynamic methods (MDM) and peak dynamic methods (PDM).

#### **2.2.2.1 Maximum voluntary isometric contractions (MVIC)**

Maximum voluntary isometric contraction (MVIC) is a widely used method to normalize raw EMG values. The MVIC is obtained by instructing a participant to perform a series of isometric movements to overcome the opposing static resistance applied on the target muscles. The participants are verbally encouraged to exert maximally to generate maximum muscle contractions for recording. The EMG collected during the MVIC tests are then processed with common signal processing methods (filtering, rectification and smoothing), finally the maximum

value calculated from the processed MVIC EMG can function as the reference to normalize the EMG of the same muscle for the task of interest.

There are many guidelines for obtaining accurate and reliable MVIC results. For instance, each MVIC test needs to be repeated at least three times with reasonable rest provided between each trial (Mathiassen et al., 1995). To be certain of inducing participants' maximum contractions, stabilization and support of the target joints and body segments are also vital (Konard, 2012). For some muscles, there may exist several candidate MVIC tests that can induce maximum contractions. In this case, all the candidate tests need to be performed to determine the one that can truly induce the maximum reference values.

Even though MVIC is the most widely employed method of EMG normalization, it also has many limitations. Firstly, the MVIC method only estimates a muscle's maximum static contractions (Sousa & Tavares, 2012), which makes it unreasonable to normalize a muscle's EMG during dynamic tasks with static MVIC values. Secondly, an ideal MVIC needs to capture an individual's true maximum contractions, but currently there are not universally accepted MVIC tests that can induce maximum contractions. Even for the same muscle, different studies demonstrate varied procedures and MVIC tests (Halaki & Gi, 2012). Thirdly, the MVIC tests are only limited to healthy and young people who are able to exert maximally in the tests, while for patients with physical disabilities or injuries, it is difficult and unsafe to perform MVIC tests on them (Hsu et al., 2006). Finally, the MVIC technique can be time consuming and energy consuming when there are more desired muscles and more MVIC tests are required (Hsu et al., 2006; Korak et al., 2020).

### **2.2.2.2 Peak dynamic methods (PDM) and mean dynamic methods (MDM)**

To avoid obtaining normalized EMG greater than 100%, which may suggest that the MVC tests did not acquire the true maximum activations, some researchers used peak EMG value obtained during the task as the normalization reference (Halaki & Gi, 2012), which is termed as peak dynamic methods (PDM). The advantage of using PDM is that it can be guaranteed that the nEMG is between 0 and 100%, this method has already been used in various studies (Allison et al., 1993; Burden, 2010; Yang & Winter, 1984). Similarly, the mean amplitude during a task can be chosen as the reference to normalize the EMG data, and this is called the mean dynamic methods (MDM). The MDM has been utilized in several studies to be compared with MVIC methods in terms of reliability (Bolgla & Uhl, 2007; Morris et al., 1998). The advantage of MDM and PDM is that they can decrease the variabilities among the individuals compared to the MVIC method (Allison et al., 1993; Winter & Yack, 1987). However, since the MDM and PDM are more related to the specific tasks and do not consider the capacity of different muscles for different individuals, the comparison of muscular activations between tasks or muscles are difficult (Halaki & Gi, 2012).

### **2.2.2 EMG feature extractions**

A feature of an EMG signal quantitatively depicts the EMG signal's specific property in a finite time interval (also called a window) (Toledo-Pérez et al., 2019). An EMG feature can be in the time domain, the frequency domain, and also analyzed using time-frequency analysis.

#### **2.2.2.1 Time domain features**

Common time domain features include integrated EMG (IEMG), mean absolute value (MAV), root mean square (RMS), variance of EMG (VAR), waveform length (WL), simple square integral (SSI), slope sign changes (SSC), zero crossings (ZC), average amplitude change (AAC), and auto-regressive coefficients (AR).

**Table 2-2** EMG features in time domain.

Features	Formula	Descriptions
IEMG	$IEMG = \sum_{n=1}^N  x_n $	Sum of the absolute EMG amplitude
MAV	$MAV = \frac{1}{N} \sum_{n=1}^N  x_n $	Mean of the absolute EMG amplitude
RMS	$RMS = \sqrt{\frac{1}{N} \sum_{n=1}^N x_n^2}$	Root Mean of the squared EMG amplitude
VAR	$VAR = \frac{1}{N-1} \sum_{n=1}^N x_n^2$	Mean of the squared deviations of the EMG amplitude
WL	$WL = \sum_{n=1}^{N-1}  x_{n+1} - x_n $	Accumulated waveform length
SSI	$SSI = \sum_{n=1}^N x_n^2$	Sum of the squared EMG amplitude
SSC	$SSC = \sum_{n=2}^{N-1} f_{SSC}(x_n),$ $f_{SSC}(x_n) = \begin{cases} 1, & \text{if } x_n < x_{n-1} \text{ and } x_n < x_{n+1} \\ & \text{or } x_n > x_{n-1} \text{ and } x_n > x_{n+1} \\ 0, & \text{otherwise} \end{cases}$	Sum of the number of times that EMG signal's slope sign changes
ZC	$ZC = \sum_{n=1}^{N-1} f_{ZC}(x_n),$ $f_{ZC}(x_n) = \begin{cases} 1, & \text{if } x_n x_{n+1} < 0 \text{ and} \\ &  x_{n+1} - x_n  \geq L \\ 0, & \text{otherwise} \end{cases}$	Sum of the number of times that EMG signal crosses zero, a lower bound threshold L is introduced to reduce noise effects (Hudgins et al., 1993; Toledo-Pérez et al., 2019)
AAC	$AAC = \frac{1}{N-1} \sum_{n=1}^{N-1}  x_{n+1} - x_n $	Mean of the accumulated waveform length
AR	$x_n = \sum_{p=1}^P A_p x_{n-p} + \omega_n$	EMG signal is modeled as an autoregressive model, P denotes the number of orders

### 2.2.2.2 Frequency domain features

An EMG signal can be converted into representation of frequency domain through fast Fourier transform (FFT) and analyzed in the frequency domain. Common frequency domain features include mean frequency (MNF), median frequency (MDF), peak frequency (PKF), mean power (MNP), and total power (TTP). In particular, MNF and MDF are commonly utilized as the indicators of muscle fatigue as abundant research has shown muscle fatigue will result in the downward shift EMG frequency spectrum (Phinyomark et al., 2012). The formula and detailed explanations of the time domain features are listed below in Table 2-3.

**Table 2-3** EMG features in frequency domain.

Features	Formula	Descriptions
MNF	$MNF = \frac{\sum_{i=1}^M f_i P_i}{\sum_{i=1}^M P_i}$	Mean power frequency of the EMG signal
MDF	$\sum_{i=1}^{MDF} P_i = \frac{1}{2} \sum_{i=1}^M P_i$	Frequency at which EMG power spectrum is divided into two regions with equal power
PKF	$PKF = \max (P_i)$	Frequency at which maximum EMG power occurs
MNP	$MNP = \frac{\sum_{i=1}^M P_i}{M}$	Mean power of the EMG power spectrum
TTP	$TTP = \sum_{i=1}^M P_i$	Aggregate of EMG power spectrum

### 2.2.2.3 Time-frequency analysis

FFT converts the whole EMG signal in time domain into representations in the frequency domain. However, for the non-stationary signals that are more common in real applications, people are interested in at what times the specific frequency components occur, which leads to the

development of time-frequency analysis. Common time-frequency analysis methods include short time Fourier transform (STFT) and wavelet transform (WT), which comprises of continuous wavelet transform (CWT) and discrete wavelet transform (DWT). EMG features in time-frequency can be extracted after these methods. Compared to time-domain features and frequency-domain features, time-frequency domain features are more computationally complicated (Toledo-Pérez et al., 2019).

### 2.2.3 EMG based movement classification

In recent years, EMG has received increasing attention to build novel human-machine interface (HMI), which develops as a new way of system control (Nazmi et al., 2016; Toledo-Pérez et al., 2019). One of these controls is achieved through EMG based movement/posture classification, which include signal acquisition, signal preprocessing, feature extraction, and classification illustrated in the following flowchart Figure 2-4 (Toledo-Pérez et al., 2019).

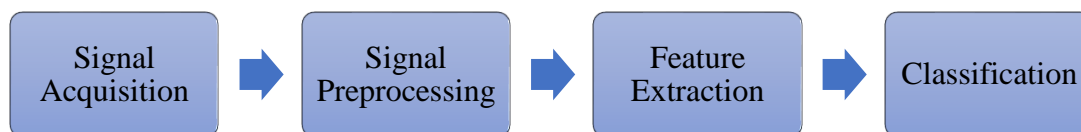


**Figure 2-4** Flowchart of the EMG based movement.

Signal acquisition denotes the early configuration of the EMG system, the type of EMG sensors (invasive or non-invasive), target muscles and type of movements are all confirmed in this early stage. In essence, signal preprocessing is the cleaning of raw EMG data, which includes

segmentation of signal and removal of noise. The purpose of EMG segmentation is to extract the active pattern from the continuous EMG signal, which can be achieved through a threshold technique (Figure 2-5) where the EMG signals below the RMS threshold were discarded (Ahmad & Kim, 2018). To remove noise, EMG signals are usually filtered with a bandpass filter at cutoff frequency of 10-500 Hz (Ahmad & Kim, 2018; Chopp et al., 2010) as the noise produced by skin is normally below 10 Hz and above 500 Hz (Toledo-Pérez et al., 2019). After preprocessing, a windowing technique (Figure 2-6) is applied to the signal and a set of EMG features is calculated on the window, which are then fed into the classifier (Nazmi et al., 2016). The length of window and overlapped window can have an effect on the classification error (Englehart & Hudgins, 2003) and studies have shown the optimal length was between 150 and 250 ms to make a balance between control delay and classification error (Smith et al., 2011).

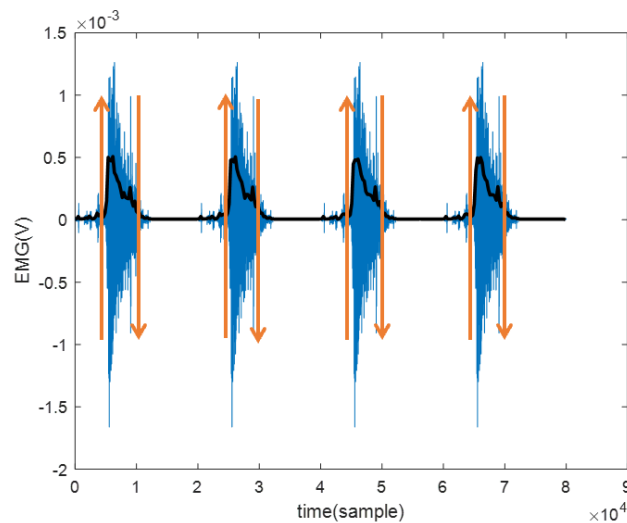


**Figure 2-5** Extract actual EMG pattern through threshold technique. Blue plots denote the raw EMG; black curves denote the RMS plot of the raw EMG; orange arrows denote the extraction threshold (e.g. 0.1\*peak RMS).

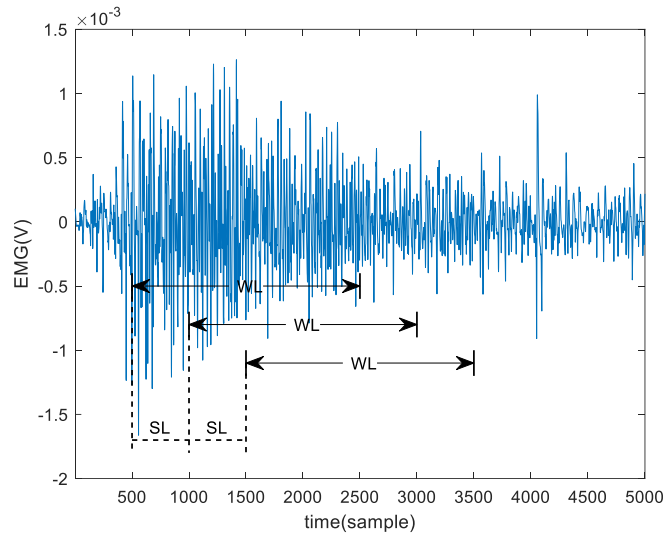


**Figure 2-6** Feature extractions through overlap windowing technique with window length (WL) and step length (SL). In this figure, WL = 2000 samples, and SL = 500 samples.

EMG feature extractions is a critical step in EMG-based movement classification (Shin et al., 2014) as there are quantities of EMG features that lie in the time domain, frequency domain, and time-frequency domain (Toledo-Pérez et al., 2019) which are discussed in the section 2.2.2. Currently, there is no consensus how many EMG features and what EMG features shall be selected for EMG based classification (Toledo-Pérez et al., 2019). Table 2-4 lists some of studies on EMG based classification and their choices of EMG features. Details of these features can be found in Section 2.2.2.

**Table 2-4** EMG classification features and methods.

References	Channels	EMG features	Classifier	Accuracy
(Lucas et al., 2008)	16	MAV, ZC, WFL, SSC, RMS, AR	SVM	95%
(She et al., 2010)	4	MAV, WL, ZC, and SSC	SVM	90%
(Al-Timemy et al., 2013)	11	TD-AR	LDA, SVM	98%
(Miller et al., 2013)	8	MAV, VAR, WL, SSC, and ZC	SVM	95%
(Alomari & Liu, 2015)	4	WL	SVM	99%
(Jarrasse et al., 2017)	24	RMS, AR, WL and SE	LDA	75%
(Paul et al., 2017)	2	MAV, RMS, SSI, WL, AAC, DASDV, LOG	KNN, SVM	60%
(Ishii et al., 2018)	4	IEMG	SVM	90%

To increase the classification efficiency and accuracy, some researchers used dimension reduction methods such as principal component analysis (PCA) on the feature sets prior to the final classification process (D. Zhang et al., 2014). In terms of human movement classifiers, common classifiers like support vector machines (SVM), linear discriminant analysis (LDA), K-nearest neighbor (KNN) are used and compared (Nazmi et al., 2016; Shin et al., 2014; Toledo-Pérez et al., 2019). Overall, these methods could achieve the classification accuracy of 90% to 95%.

#### 2.2.4 EMG based force estimation

For EMG-based muscle force prediction, there are conventional physiological models and data-driven models. For physiological models, various studies proposed models that have incorporated physiological parameters, including muscle cross-sectional area, force-length relationship, and passive elasticity (McGill, 1992; Nussbaum & Chaffin, 1998). For instance, the following equation shows that force in the  $i$ th muscle was determined by: 1) muscle stress  $S$ ; 2) force-nEMG relationship; 3) muscle cross sectional area (CSA); 4) length-tension function  $f_{len}$ ; 5) passive length-tension function  $F_P$ . This model has been used to estimate the trunk loadings and

lumbar muscle force (Nussbaum & Chaffin, 1998). While these studies showed promising modelling accuracy, they also have limitations as the physiological parameters (e.g., muscle cross-sectional area) in the model can be subject-variant and need to be tuned for each individual (Shao et al., 2009).

$$F_i(t) = S_i \times e^{-k_1 n EMG_i(t-k_3)} - e^{-k_1 - 1} \times CSA_i \times f_{len} + k_2 Fp_i \quad (2-1)$$

Another approach to predict muscle force production is through data-driven methods, which included regression and artificial neural network to directly estimate muscle force production from EMG signals (Hoozemans & Van Dieën, 2005; Kamavuako et al., 2012; Martinez et al., 2020; J. L. G. Nielsen et al., 2011). These studies focused on the general output force such as grasping force and lifting force rather than single muscle's exerting force. Table 2-5 summarizes some of these data-driven force prediction studies. EMG-based muscle force prediction can be applied in ergonomics evaluation (S. Chan, 2007), tool design (Hoozemans & Van Dieën, 2005), and myoelectric prostheses control (Martinez et al., 2020). Similar to EMG-based movement classification, most of these data-driven EMG-force models focused on force applied on finger or grasp force and studied forearm and hand muscles (Hoozemans & Van Dieën, 2005; Li et al., 2015; Martinez et al., 2020), while exertions (lifting, pushing, pulling, etc) that involved whole-body muscles were lacking.

**Table 2-5** EMG force prediction methods and performance.

References	muscles	Algorithm	Accuracy
(Hoozemans & Van Dieën, 2005)	6 forearm muscles	Linear regression	0.54-0.86
(J. L. G. Nielsen et al., 2011)	Arm muscles	ANN	0.72-0.93
(P. Liu et al., 2014)	Forearm muscles	Filtering and regression	4.2-10.2%
(Hashemi et al., 2015)	Arm muscles	Parallel cascade identification	8.3-33.3%
(Cao et al., 2017)	Arm muscles	ANN	1.5-2%
(Baldacchino et al., 2018)	12 arm muscles	Bayesian Mixture of Experts	2.6-9.6%
(Martinez et al., 2020)	3 forearm muscles	Regularized regression	2.5%

## Chapter 3 The study of instructional modalities in XR applications

This chapter is adapted from two co-authored papers (K. Chen, Perera, et al., 2020; K. Chen & Chen, 2021b).

### 3.1 Motivation

Modern technology makes the virtual training and virtual education accessible (Halabi, 2020; Pantelidis, 2010). In specific, the use of humanoid character/agent can function as a virtual teacher and provide instructional guidance (Behrend & Thompson, 2011). Previous research has shown the virtual agent can be utilized in a lot of educational and training settings, and they can serve in various activities from hosts, to advisors, to teachers, and to companions (Mohammed & Angell, 2004; Roselyn Lee et al., 2007; Sidner, 2008). In addition, it is common for users to personify the virtual agents and develop emotional bond with them (Nass et al., 1995). Figure 3-1 below depicts the scenario of communication with a 2-D virtual agent.



**Figure 3-1** Example of a conventional humanoid agent (Oertel et al., 2020).

Past studies indicated that people tended to trust the instructors that are similar to them (Behrend & Thompson, 2011; Brewer, 1979). These similarities arise from surface attributes like age, gender or race and deep attributes like behavior and personality (Behrend & Thompson, 2011). For instance, previous studies demonstrated that learners tend to trust advice from agent whose ethnicity is similar to them (Pratt et al., 2007). Thus, it is expected that a more human-like instructor can evoke improved trainee trust and adherence.

Using modern RGB-D cameras, the surface of a human can be captured in the form of point cloud and reconstructed as a complete human model (Z. Liu et al., 2015; Mao et al., 2017). The advantage of point cloud based human model is that it is more similar to a real human compared to 3-D human models. However, since the scan of human is a static posture, it is relatively hard to animate the human point cloud. On the other hand, 3-D human model can be easily animated as they are hierarchically constructed, but they are more like cartoon characters and share fewer similarities with real humans on appearance. Figure 3-2 below presents the use of a 3-D graphic rendered humanoid model and a point cloud scanned humanoid model.

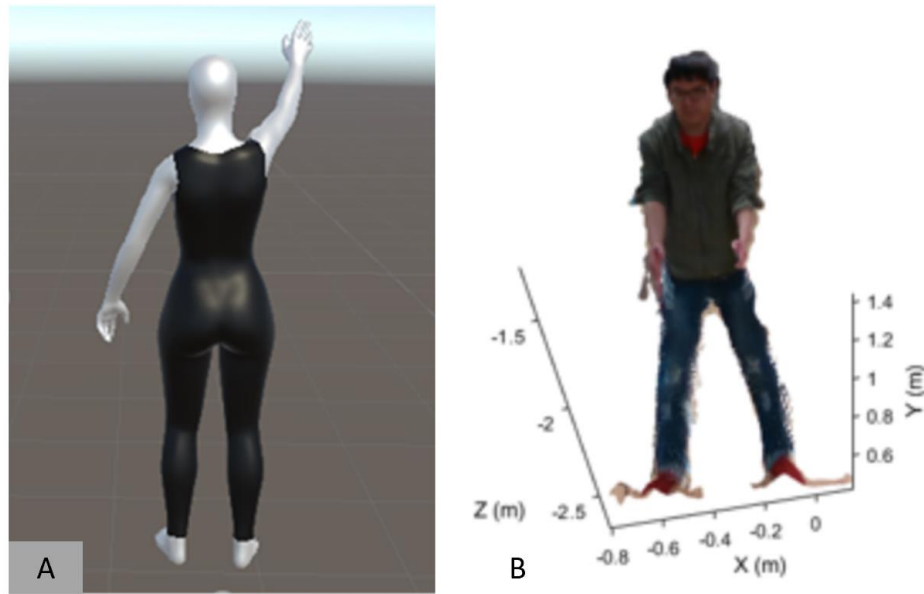


**Figure 3-2** (A) 3-D humanoid model, (B) point cloud reconstructed humanoid model.

In this chapter, the usage of humanoid virtual instructors in two XR systems were evaluated, two experiments were conducted: experiment 1 studied the effect of 3-D humanoid instructor in a VR exercise (VRE) program, experiment 2 studied the implementation of point cloud generated humanoid 1 instructor in an AR posture training platform. The details of these two experiments were presented in Sections 3.2 and 3.3.

## **3.2 Evaluation of an instructor-guided virtual reality exercise (VRE) program**

### **3.2.1 Introduction**

Virtual reality (VR) delivers 3-D spatial-temporal visual information used for virtual reality exercise (VRE) programs in supporting spatial movement learning, such as learning dance moves by imitating a virtual teacher (J. C. P. Chan et al., 2011) and playing immersive VR “exergames”

(exercise games) for full-body exercise (Finkelstein et al., 2011). In the clinical domain, VRE programs have been used for balance training (Duque et al., 2013; J. H. Kim et al., 2009), muscle strength improvement (C.-L. Chen et al., 2012; J. Kim et al., 2013), and fall prevention (Lim et al., 2017). Many VRE programs have shown promising outcomes (Farrow et al., 2019; Mazzone et al., 2013) that led to the increased interest in VR-based exercise and movement learning.

The success of VREs has been reported in studies that primarily compared the outcomes of those who have received VRE intervention to those who received usual care. The positive outcomes of VREs were associated with the hardware and software of virtual environments, including customizable design, multimodal information, and various augmented feedback (Burdea, 2003). Yet, the underlying mechanism and attributes that facilitate VRE outcomes are often overlooked and not specifically examined (Howard, 2017). In other words, aside from the inherent differences between a VRE (e.g., 3-D, “cool factor”) and conventional exercise, it is indispensable to examine contributors to successful VRE design and exercise goal in immersive VR, and thereby support the design of future VRE with appropriate VR features.

To study the constituents of successful VREs, the first step is to understand the positive factors in physical exercises and trainings. Engagement is a key contributing factor in physical exercise and rehabilitation (Schmidt et al., 2019) which is the affective quality or experience of a person when drawn into an activity (Lohse et al., 2016). Interactivity, background sound, and reward are environmental properties of games that contribute to the experience of engagement (Lohse et al., 2016). On the other hand, the motivation is a psychological property that promotes actions toward a goal (Lohse et al., 2016), and attributes such as challenges, sensation, and curiosity can contribute to an individual’s motivation (Pirovano et al., 2016). While engagement and motivation are different, they are in fact related constructs (Lohse et al., 2016).

In a typical physical rehabilitation program, individuals often perceive their experiences as boring and time-consuming, which may lead to decreased effort and engagement (Burdea, 2003; Schuler et al., 2011) and thus compromise rehabilitation outcomes. Promoting motivation is key to ensure continued physical activity and increased muscular activity (Rahman & Rahman, 2010; Schuler et al., 2011). Compared to traditional physical exercise program, VRE provides an enriched and interactive environment that promotes user engagement (Sveistrup, 2004). Even performing similar movements, users naturally consider interactions in VR to be novel and enjoyable (G. N. Lewis & Rosie, 2012). The addition of competition and game feature design (e.g., scoring system, interaction, and feedback) help engage users to exert physical effort during practice (Deutsch et al., 2008). Lohse et al. (2016) studied participants' motor learning outcomes via a goal-oriented computer game, and it was found participants in the engaging condition (game group, abundant game features) demonstrated improved skill retention and transfer when compared to the less engaging condition (sterile group, identical task but fewer game features). Despite of the benefits of game feature design in VRE, few studies explicitly examined increased engagement in VR and overall outcomes (Howard, 2017). Thus, there is a need to study the effect of levels of game features in VR on human physical performance and engagement facilitation.

Practice is also an important factor in successful exercise programs. The amount, intensity, and type of practice are fundamental for therapeutic success (Dobkin, 2004; Kleim & Jones, 2008). There are two modes of practice: imitation-oriented and task-oriented. Imitation-oriented practice (observational learning) is delivered when an instructor demonstrates movements and the learners learn by observing and mimicking (Ferrari, 1996). Pre-recorded videos of an instructor performing the movements can also function as substitutes (Anderson et al., 2013). For instance, a virtual "teacher hand" animation was displayed and users needed to synchronize with the virtual teacher

hand as accurately as possible (Holden & Todorov, 2002). On the other hand, task-oriented practice (task-specific training, goal-directed training) enables participants to practice movements with a goal. Some argued that the outcome of training is optimized when the practice is meaningful and similar to the expected motor skill in physical world (Barnett et al., 1973; Kleim & Jones, 2008). Performing specific task-oriented practices recreate conditions of the physical world and thus increasing physical fidelity of the exercise (Howard, 2017). In conventional gait training, individuals are often guided to perform abstract knee or ankle movements instead of walking (Howard, 2017), which may impede the transfer of skills gained from training. Both engagement and practice mode are important factors for learning in the physical environment, examining these two factors will help glean further insights in VRE and contribute to the understanding of the design of successful VRE.

In this exploratory work, the effects of game features and practice type of a VRE system on human performance were examined, specifically the muscle activity and kinesthetics of the shoulder complex in able-bodied individuals. Three levels of game feature (low, medium, high) and two types of practice (task-oriented, imitated-oriented) in a full factorial experimental design was implemented. A common daily activity of pick-and-place books was implemented in a home-like virtual environment. Thus, enhanced performance was operationalized as greater flexion angle and electromyography (EMG) since rehabilitation exercises aim to increase joint range of motion and muscular activity (Moradi et al., 2020). It was hypothesized that greater shoulder flexion angle and greater muscular efforts are expected in the task-oriented practice compared to the imitation-oriented practice because task-oriented practice has physical meaning and is associated with a real-world task to which people relate. It was also hypothesized that the higher level of game features in VR would produce greater shoulder flexion angle and more intensive muscle activity because

higher game features could promote greater engagement, which may encourage more intensively movements greater muscular efforts (Schuler et al., 2011). In the long-term, the outcomes will be extended to enhance the performance of individuals with different goals, including home-based workout and virtual rehabilitation, and illuminate the design of future VRE.

### **3.2.2 Methods**

#### **3.2.2.1 Participants**

Thirteen participants free of upper extremity disorders (9 males, 4 females) were recruited from North Carolina State University (NCSU) with informed consent. This research complied with the tenets of the Declaration of Helsinki and was approved by the Institutional Review Board at NCSU. The mean age was 25.3 years (SD=3.0, range=11) and all participants were right-handed. Among the participants, three had no experience of using VR through a head-mounted display (HMD) and ten had used HMD before but rarely (0-1 per month). The recruitment criteria were adapted from previous work (K. B. Chen et al., 2015, 2016): participants who self-reported upper-limb injuries in the last 3 months were excluded. Safety related VR exclusion criteria were: individuals who had a history of seizure, motion sickness, and sensitivity to flashing lights. The experiments were conducted in the Biomechanics Laboratory at NCSU and lasted approximated one hour per participant, and each participant was compensated (\$10/hour).

#### **3.2.2.2 Equipment**

The VRE system consisted of virtual scenarios and hardware. Virtual scenarios were rendered by a game engine (Unity, <https://unity3d.com/>) and presented to participants via an HMD (Vive, HTC and Valve Corporation). A controller was used interact with virtual objects in the scenarios. The participants embodied inside an avatar, in which they were able to see their virtual

arms and legs through the HMD. The upper body movements of the avatar were driven by the participants' real-time movements tracked by the HMD and controller positions.

For data collection, participants' whole-body movements were monitored by a set of 14 optical motion tracking cameras (Raptor 4S, Motion Analysis). Twenty motion tracking markers were placed on the participant's major upper body landmarks to collect joint coordinate data (Figure 3-3b). EMG electrodes (Trigno, Delsys) were placed on the muscle belly of the deltoid, supraspinatus, and infraspinatus on the dominant side to monitor shoulder muscle activity (Figure 3-3(a)). The muscles were selected based on the pick-and-place task movements, where the supraspinatus and the deltoid raised the arm and the infraspinatus assists in moving the arm backward (Gray, 2000).

To control for the movements performed in the imitation-oriented practice, an animated virtual instructor was created to deliver a set of standardized movements. The animation of virtual instructor was pre-recorded and generated by mapping upper body joint data of the researcher (179 cm, 78 kg, 26 year old male) to the model of virtual instructor (Jauregui et al., 2014). To create the animation, the researcher picked up a book from the table and placed it on a bookshelf, and the 3-D coordinate was recorded by motion capture system to reconstruct the positions of instructor.

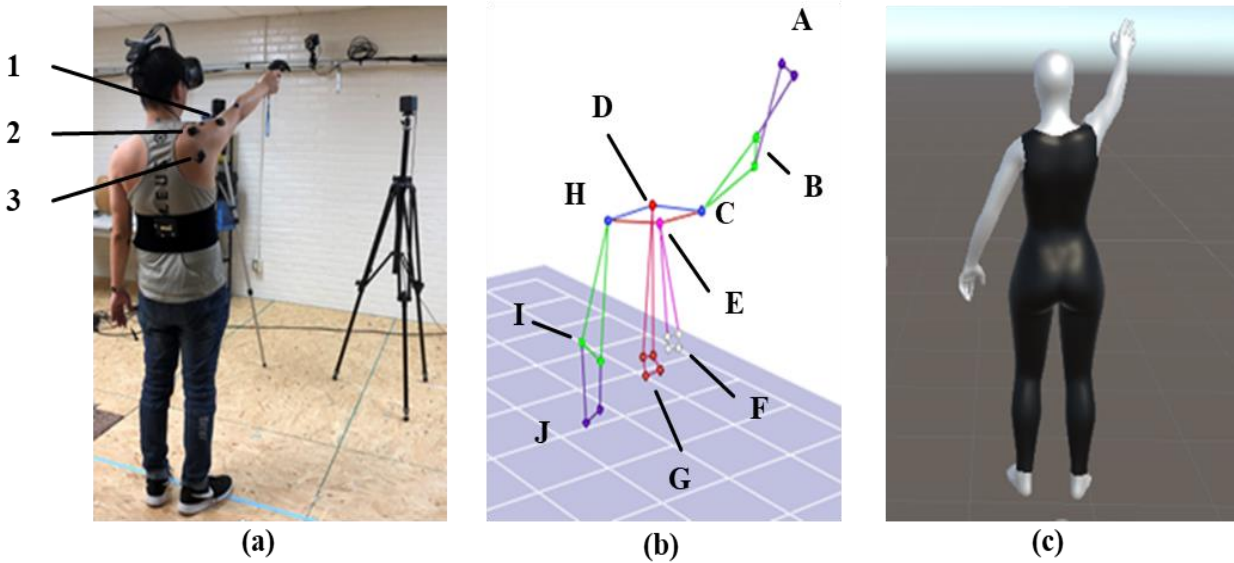


**Figure 3-3** (a) Experimental setup and participant. A participant with EMG sensors and motion-tracking sensors attached on upper body in a fixed standing position holding the controller while looking into a head-mounted display. The EMG sensors are attached to the deltoid (1), the supraspinatus (2), and infraspinatus (3); (b) A snapshot of the real-time joint data captured by the motion capture system at the same posture of (a). The labeled marker regions are as follows: right wrist (A), right elbow (B), right acromion (C), incisura jugularis (D), C7 (E), T8 marker cluster (F), xiphoid process marker cluster (G), left acromion (H), left elbow (I), and left wrist (J); (c) The joint data mapped to humanoid model for generating instructor animations.

joints (Figures 3-3(b), (c)). It was designed to be consistent in all scenarios to guide the participants to perform the movement.

### 3.2.2.3 Experimental design and protocol

A  $2 \times 3$  (practice types  $\times$  game feature levels) full factorial design experiment was conducted, which yielded six scenarios ( $2 \times 3$ ). Within-subjects variables were game feature level (low, medium, high) and practice type (task-oriented, imitation-oriented). The order of the experiment condition was randomized during the experiment: each of the six experimental conditions was numbered and a random sequence of experiment condition was generated for each participant. The experiment ended when participants completed all repetitions in all six scenarios.

Participants were donned with EMG sensors and completed the shoulder muscle maximum voluntary contraction (MVC) test (Boettcher et al., 2008), which was performed by participants maximally exerting against an opposing force. Verbal encouragements were provided to arouse the maximum muscle activation. The EMG measured during the MVC test would be used to normalize participants' shoulder EMG data.

After the MVC test, the motion capture markers were placed on the bony landmarks of participants by following the International Society of Biomechanics recommendations (Wu et al., 2005). Participants wore the HMD and assumed a standing ready position, and they performed a set of practice tasks to become familiar with VR and the use of controller. The practice task was to pick up three virtual boxes using the controller and place them at a specified location in VR, and more practice was provided if needed. The experimental task was to perform a series of shoulder joint flexion movements where the participants would produce a reaching posture involving their dominant hand in two types of guidance conditions: (1) the imitation-oriented practice and (2) the task-oriented practice conditions.

In the imitation-oriented practice condition, the animated virtual instructor demonstrated eight repeated shoulder flexion movements (Figure 3-4a) and the participants were instructed to mimic and follow the instructor's and performed the same pick-and-place movements. The number of repetitions is adopted from a meta-analysis on motor skills training (Behringer et al., 2011), which suggested 8-12 repetitions. 0° orientation (instructor and participants' avatar faced the same direction) was applied to reduce more spatial transformation (Lafortune et al., 2018).

In the task-oriented practice condition (Figure 3-4b), participants were asked to pick up a virtual book from a virtual table using the controller, one at a time, and then place it on the highest level of a virtual bookshelf. The pick-and-place task prompted shoulder flexion and thus produced an

overhead reaching movement that was similar to the movement performed by the virtual instructor. There were eight virtual books and each trial ended when all eight books were picked up and placed.



**Figure 3-4** Exercise scenarios from the virtual environment, where the white camera icon depicts the location of the participant and thus “camera view”. (a) The imitation-oriented practice condition had a virtual instructor standing in front of the participant’s avatar, where the participant controlled the avatar’s movement to mimic the movement of the virtual instructor. (b) The task-oriented practice condition was to perform a pick-and-place task, where the participant controlled an avatar to pick up books and placed them on the shelf.

Both practice conditions had three different levels of game feature (Figure 3-5), which aimed to make the task more interesting by showing varying levels of background richness and reward (Lohse et al., 2016) to elicit greater participant interest and engagement. Game features were based on various visuals and lighting rendering, and a scoring panel that counted the number of books that have been placed on the bookshelf. The VR scene of the lowest game feature had limited environment settings (no grass background), no light rendering and no furniture. The VR scene of the middle game feature had environment settings, no light rendering, and several furniture. The highest game feature scene presented vivid lighting rendering, abundant furniture and a scoring panel that counted the number of books that have been picked up.

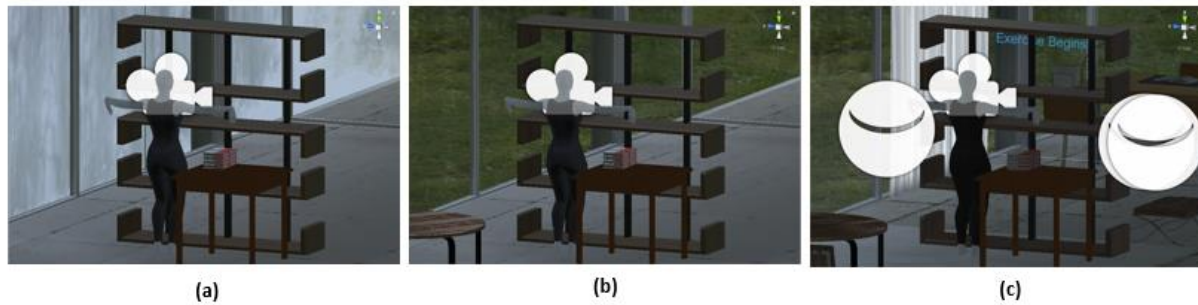


**Figure 3-5** Three levels of game like feature for task-oriented practice condition: (a) low level, (b) middle level, (c) high level. The white camera icon depicts the location of the participant and thus “camera view”. The white circles depict the sophisticated lighting elements in the high game like feature level.

### 3.2.2.4 Variables and analysis

To study the effect of practice types and game feature levels on participant performance, this study examined objective measures: EMG and shoulder joint flexion angle. EMG signals convey valuable information about muscle activity and EMG amplitude can function as an index of muscle strength and muscular effort (Reaz et al., 2006). All EMG signals were filtered with a fourth order band-pass (20 Hz – 350 Hz) Butterworth filter, rectified and smoothed by a time window of 200ms (Schuler et al., 2011). The maximum amplitude in each condition was normalized with respect to the MVC tests, which yielded the normalized EMG (nEMG) values reported in the results. Shoulder joint flexion is a common activity performed during over-head reaching movements. The angle at which shoulder joint flexion reached its maximum was analyzed in this study as an indicator of the extent of shoulder joint flexion. The flexion angles were calculated based on the 3-D coordinates of the motion capture markers that were attached to the upper-body bony landmarks (Lee et al., 2015).

A two-way repeated measure analysis of variance (ANOVA) was used to analyze the effects of game feature level and practice type on participants’ shoulder muscle activity and shoulder joint flexion angle. Statistical significance was set to be  $\alpha=0.05$ .

### 3.2.3 Results

#### 3.2.3.1 Maximum shoulder joint flexion angle

A two-way repeated measure ANOVA indicated a statistically significant main effect of practice type ( $F(1,11) = 9.53, p = 0.01$ ) on maximum shoulder flexion angle, but no statistically significant main effect of game feature level ( $F(2,22) = 1.67, p = 0.21$ ). No statistically significant interaction was found between practice type and game-like feature level ( $F(2,66) = 0.22, p = 0.81$ ). Model residuals' normality is validated as Shapiro-Wilk test showed  $W = 0.975, p\text{-value} = 0.16$ . Data variance homogeneity is validated with Levene's test ( $F(5,66) = 0.83, p = 0.53$ ). Effect size (Olejnik & Algina, 2003) for practice type is  $\eta^2 = 0.16$  and game feature  $\eta^2 = 0.02$ . Table 3-1 presents the overall mean maximum shoulder flexion angles in different VR scenarios.

**Table 3-1** Overall mean ( $\pm 1SD$ ) of maximum shoulder flexion angle for the 3 $\times$ 2 conditions in different VR scenarios.

Measure[degrees]	Imitation-oriented	Task-oriented
Low game features	112.33 (8.52)	119.13 (10.79)
Middle game features	110.97 (6.79)	117.28 (9.93)
High game features	112.85(6.70)	121.38 (8.74)

#### 3.2.3.2 Shoulder muscle activity

The mean nEMG of the deltoid was 26.5% of its MVC (Figure 3-6). A two-way repeated measure ANOVA did not indicate a statistically significant main effect of practice type ( $F(1,9) = 2.90, p = 0.12$ ) nor game feature level ( $F(2,18) = 0.91, p = 0.42$ ) on deltoid nEMG. There was no statistically significant interaction between game feature level and practice type ( $F(2,22) = 0.47, p = 0.64$ ) for deltoid nEMG. Model residuals' normality via Shapiro-Wilk test showed  $W = 0.988$ .

p-value = 0.80. Data variance homogeneity is validated with Levene's test ( $F(5,54) = 0.41, p = 0.84$ ). Effect size for practice type is  $\eta^2 = 0.06$  and game feature  $\eta^2 = 0.005$ .

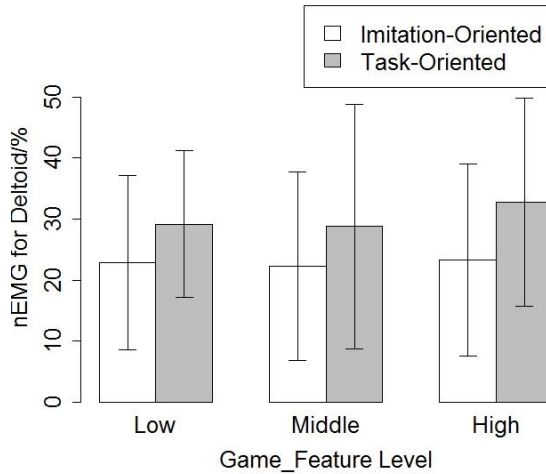


**Figure 3-6** Activity of the deltoid across different game feature levels ( $\pm 1S.E.$ ). The muscle activities were not statistically significantly across different scenarios.

The mean nEMG of supraspinatus was 28.8% of its MVC (Figure 3-7). There was a statistically significant main effect of practice type on supraspinatus nEMG ( $F(1,9) = 12.61, p = 0.006$ ), with the mean nEMG of the task-oriented scenario being 11.2% greater than the nEMG in the imitation-oriented scenario. There was not statistically significant main effect of game feature level ( $F(2,18) = 0.42, p = 0.66$ ) nor a statistically significant interaction between game feature level and practice type ( $F(2,18) = 0.45, p = 0.65$ ). Model residuals' normality via Shapiro-Wilk test showed  $W = 0.983, p\text{-value} = 0.56$ . Data variance homogeneity is validated with Levene's test ( $F(5, 54) = 0.22, p = 0.95$ ). Effect size for practice type is  $\eta^2 = 0.2$  and game feature  $\eta^2 = 0.004$ .

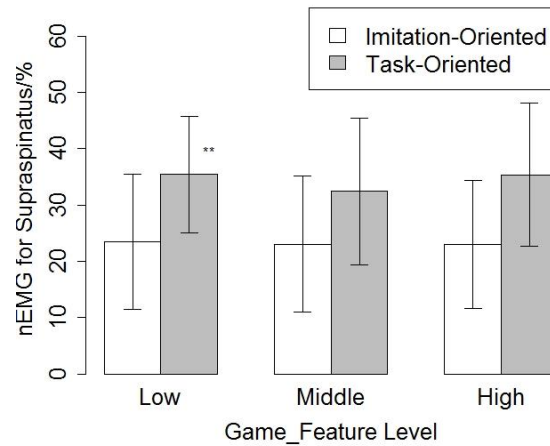


**Figure 3-7** Activity of the supraspinatus across different VR scenarios ( $\pm 1$ S.E.). The muscle activities are statistically different between task-oriented and imitation-oriented scenarios. \*\* $p < 0.001$ .

The nEMG of infraspinatus was 24.6% of its MVC (Figure 3-8). There was a statistically significant main effect of practice type ( $F(1,9) = 12.71, p = 0.006$ ) on nEMG of infraspinatus, with the mean nEMG of the task-oriented scenario being 7.3% higher than the nEMG in the imitation-oriented scenario. There was not statistically significant main effect of game feature level ( $F(2,18) = 0.68, p = 0.52$ ) nor a statistically significant interaction between game feature level and practice type ( $F(2,18) = 0.67, p = 0.52$ ). Model residuals' normality via Shapiro-Wilk test showed  $W = 0.993, p\text{-values} = 0.99$ . Data variance homogeneity is validated with Levene's test ( $F(5, 54) = 0.32, p = 0.90$ ). Effect size for practice type is  $\eta^2 = 0.06$  and game feature  $\eta^2 = 0.002$ .

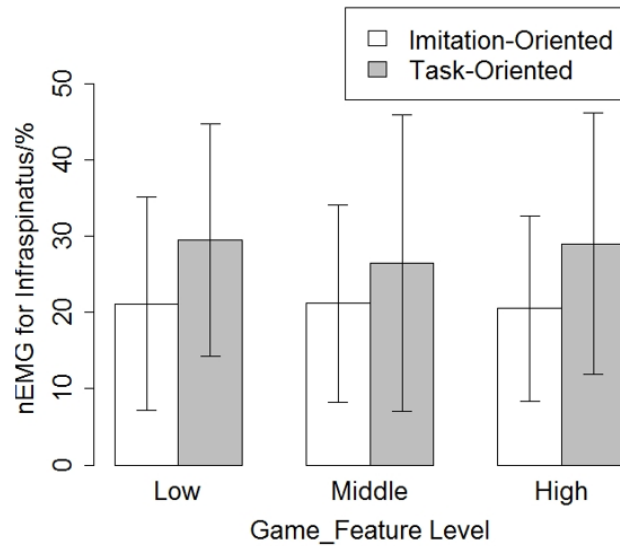


**Figure 3-8** Activity of the infraspinatus across different VR scenarios ( $\pm 1S.E.$ ). The muscle activities were not statistically significantly across different scenarios.

### 3.2.4 Discussion

Understanding the features of VRE that encourage increased user performance is crucial to help advance the designs of VR-based training and exercise. While the long-term goal is to devise VR-based rehabilitation and therapeutic exercises, the purpose of this exploratory study was to investigate the effects of practice types and game feature levels on shoulder muscle activity and kinesthetic performance during VRE. Instructional information was delivered in an immersive VR through an HMD. The nEMG of three shoulder muscles (the deltoid, supraspinatus, and infraspinatus) and the maximum shoulder flexion angle were examined.

#### 3.2.4.1 Effects of guided practice type

The participants performed two types of guided practices in VR: (1) imitation-oriented movements by mimicking the actions of a virtual instructor and (2) task-oriented movements that required them to pick up and place books onto a bookshelf. Since task-oriented movements have physical meaning and end goals (Howard, 2017; Kleim & Jones, 2008), it was anticipated that

participants would demonstrate greater shoulder flexion angle and muscle activity in the task-oriented practice because they aimed to place a book on a bookshelf to accomplish the movement goal. The results revealed confirmed the assumption as it showed a statistically significant main effect ( $F(1,11) = 9.53, p = 0.01$ ) of guided practice type on maximum shoulder flexion angle, in which participants exhibited greater shoulder flexion angles during the task-oriented practice. While the task-oriented practice was designed to be repeated pick-and-place movements, this type of movement can be applied to other tasks such as reaching for a mug in a cupboard or restocking an empty grocery shelf. The physical meaning inherent to the movement could have promoted more engagement and exertions (Howard, 2017; Kleim & Jones, 2008). On the other hand, it was observed that participants did not consistently flex their shoulder joint to the extent that was demonstrated by the virtual instructor when performing the imitation-oriented movements despite the instruction was to copy the exact movement of the virtual instructor. It was also possible that participants became familiar with the shoulder flexion movement and did not adhere to the exact movement demonstrated by the virtual instructor. These observations have implications for designing therapeutic exercises: it may be advantageous to package intended, monotonous exercises within task-oriented movements to encourage individuals who may need continued practices.

The contractile activity of the deltoid, supraspinatus, and infraspinatus were studied because these muscles are related to the raising movements of the shoulder (Gray, 2000). The nEMG of the supraspinatus had the greatest mean nEMG value (28.8% of MVC) and it was statistically significant different between the two types of guided exercise ( $p = 0.006$ ). Specifically, the mean nEMG of the supraspinatus during the task-oriented practice was 11.2% greater than the nEMG during imitation-oriented practice, which may be explained by the characteristic of the

pick-and-place task. The pick-and-place task can be decomposed into shoulder flexion (primary) and slight abduction movements. Both the deltoid and the supraspinatus can contribute to shoulder abduction, but the deltoid primarily supported abduction to the side of the body (Hughes et al., 1997), thus the supraspinatus was more involved for this experimental task. For the infraspinatus, guided practice type had a significant effect on its' nEMG ( $p = 0.006$ ), which was plausible. Compared to imitating the virtual instructor, practice-oriented condition required more external rotation action to place the virtual books in order, thus infraspinatus was more involved.

The primary goal of each exercise can have different measures, including amplitude, accuracy, and speed of the motions (Pirovano et al., 2016). The participants exhibited greater shoulder flexion angle and higher nEMG of the supraspinatus in the task-oriented practice, which could be associated with higher exercise intensity/amplitude. Exercises and tasks that helped increase engagement are important for attaining positive outcomes in therapeutic exercises and rehabilitation (Schuler et al., 2011). On the other hand, the maximum shoulder flexion angle in the imitation-oriented practices had lower variance relative to task-oriented practices (Table 3-1), which indicated that the participants' movements were more consistent when following an instructor. Thus, imitation-oriented practices can be more useful when consistent, accurate movements are required, such as learning martial arts and dancing in VR (Anderson et al., 2013; Chua et al., 2003).

#### **3.2.4.2 Effects of game feature levels**

Three levels (low, middle, and high) of game feature design were examined, and it was hypothesized that having more game features would encourage higher shoulder flexion angles and nEMG. Specifically, this study embodied the participants inside an avatar, and levels of game feature were differentiated by environment enrichment, lighting, and a scoring system. However,

the analysis revealed no significant effect of game feature on shoulder flexion angle nor nEMG. This result may be attributed to the small differences between consecutive levels of game-like feature, which may be insufficient to elicit different magnitudes of participant movement and exertions. Nine participants verbally described in post-experiment debrief that they focused on the tasks and did not notice the variations of game features, and they considered all conditions to be engaging. As observed by Lohse et al. (2016) study, where they examined motor skill learning outcomes in an engaging game condition and a sterile condition, participants perceived both conditions to be challenging and remained involved in the learning tasks and had positive learning outcomes. While some VREs lack game features, they could still promote engagement as most of the participants were relatively novel to interactions in VR. To differentiate game feature levels in VR scenarios design, future studies on motivation effects should implement more game elements and interactions and amplify the gap between each level. Currently, researchers developed their VREs based on existing commercial platform (e.g., Wii) or developed their own exergames to implement exclusive game features, but few research explicitly explained their design guidelines and principles to increase motivational affordances (Matallaoui et al., 2017).

In addition to game features, studies have shown that practice quantity could influence human's motor learning outcomes (Lohse et al., 2016). The present work intended to control the amount of practice and focus on the effects of game features and practice type on participants' performance, thus there were eight repetitions per experimental conditions by adopting the number of repetitions in the literature (Behringer et al., 2011). If the number of repetitions were changed, it would be reasonable to anticipate changes in participant performance in terms of shoulder flexion angle and muscle activity. Moreover, if the number of repetitions were to increase, signs of muscle fatigue embedded in EMG signal could be expected, which was not revealed in the current data.

### **3.2.4.3 The use of a standardized virtual instructor**

For this study, the aim was to present a set of standardized movements to each participant. Thus, to control for potential effects of varying a virtual instructor, one animated virtual instructor was created using a fixed set of movements captured using a laboratory-grade motion capture system. However, it may be advantageous to create a personalized virtual instructor for each participant to match their anthropometry and stature, and this may be achieved in a shorter period of time using a marker-less camera such as the Kinect (Shingade & Ghotkar, 2014). Yet, motions created by participants may vary and it would be challenging to deliver standardized movements. Given this study employed a standardized virtual instructor, which did not share the same anthropometry as the individual participants, additional analysis was performed to examine potential effects of participant anthropometry (height) on their performance, and the results did not reveal a statistically significant effect of height on performance when the participants imitated the movements of the virtual instructor ( $p=0.55$ ). This suggested that participants of similar height to the animated instructor (within  $\pm 1$  standard deviation in height) did not exhibit enhanced performance compared to those who were taller or shorter. The adoption of a standardized or a personalized virtual instructor should be driven by the goal of the VRE. If the goal of a VRE was to encourage users to perform a set of standard movements, such as training workers to perform standard lifting movements, a standardized instructor generated from an expert could be more helpful.

### **3.2.4.4 Limitations and future work**

There were some limitations in this study. This was an exploratory study that involved 13 participants, which was a smaller group of sample size. However, the supplementary analysis indicated that the assumptions of ANOVA were valid. While this study had an end-of-experiment

debriefing with each participant, during which the participants verbally described their perception of the study, game features, and engagement, this study did not administer an empirically validated engagement survey or quantitative engagement measure. Therefore, direct comparison across perceived engagement was unavailable. If this had been available, it can be used to quantify the differences between perceived the game feature levels, which may help explain the insignificant effect of game features on exercise performance found in the current study. As for designing different levels of game feature scenario, the disparity across different levels was not phenomenal as expected as three participants verbally recalled that they did not notice the change of environments. For future direction, the VRE system can be improved by implementing adjustable environment design (customized virtual object size, lighting and challenges). Finally, the use of standard instructor can be extended to more customized instructor, such as building more realistic humanoid instructor via scanning a real human.

### **3.2.5 Conclusions**

Compared to imitation-oriented practice, task-oriented practice elicited more intensive shoulder movements and muscular efforts during VRE but also induced greater movement variations. It is expected that the imitation-oriented practice could be applied in movement learning where users could perform consistent movements. It is also possible to use combined design for customized goals and investigate the final effect of combined design (Bovonsunthonchai et al., 2020). While game feature levels did not affect participant performance, it was reported by the participants that they were mostly attending to the task rather than the surrounding, which suggests substantial differences across game features levels that stand out from different levels should be further investigated.

## **3.3 Design of an augmented reality (AR) based posture training tool**

### **3.3.1 Introduction**

There are different ways to create humanoid instructors and make them look like VR users. Thus, in this experiment, a systematic process to create point cloud reconstructed humanoid instructors for work safety purposes was proposed and examined, and the usage of new instructors in an AR interface was evaluated.

Work safety is of critical importance for all occupations. Yet, there has been over 3.5 million employer-reported cases of non-fatal injuries and illnesses in both public and private goods producing (manufacturing, construction) and service producing (transportation, nursing homes) industries in the U.S. (U.S. Bureau of Labor Statistics, 2019). Overexertion and musculoskeletal disorders (e.g., herniated disc, sprains, strains, and tears) accounted for the majority of these cases (U.S. Bureau of Labor Statistics, 2019). The conventional approach to prepare workers with work safety knowledge is through training using pamphlets, one-time training orientation, and/or videos. Posture training reduced risks of musculoskeletal disorders in various occupations (Jaromi et al., 2012; Melhorn, 1996; Westgaard & Winkel, 1997). However, it was also reported that workers only minimally change after postural training and the incident rate of MSDs did not lower substantially (Amick III et al., 2003; Hignett, 2003; Lavender et al., 2007; Nelson & Baptiste, 2004; Trinkoff et al., 2003). To foster safer work practice in the future workforce, work safety should be beyond uniform and pamphlet-based training. It is expected that training can be better supported in an interactive environment where workers can use their body acquire safety knowledge and minimize safety risks.

Motivated by the need to create more human-like humanoids for an interactive posture training tool, the point cloud technology that could capture the surface features of a real human using **Red Green Blue-Depth (RGB-D)** cameras was utilized (Mao et al., 2017). The RGB-D data were stored in the form of point clouds, which contained the coordinates (x,y,z) and color information (RGB). This 3D reconstruction approach helped retain some human life-like features, as well as joint movement subtleties that were not easily articulated in cartoon-like graphics.

Modern technology such as augmented reality (AR) has become an attractive medium to deliver posture training material and thereby promote work safety. Augmented reality enables users to visualize objects from the physical world and computer-generated virtual entities in the same environment through spatial and temporal registration (Azuma, 1997). Augmented reality has been widely explored for its potential applications in education and training (Klatzky et al., 2008; Vilkoniene, 2009; Yim & Seong, 2010). Moreover, learning using AR has improved learners' motivation and efficiency (Dunleavy et al., 2009; Huang et al., 2010; Yim & Seong, 2010). Augmented reality is also gaining popularity in the logistics industry for the purpose of job training (Ong & Nee, 2013). However, most of these AR training applications only overlaid simple textual information in the users' field of view (Tatić & Tešić, 2017). Displaying posture training information through holistic view of virtual instructors, along with factual information on risks for body joint stresses and strain, is the novelty of this work.

The purpose of this study is to describe and provide developmental information of a user-centered AR posture training tool to promote safety of physical tasks (e.g., lifting, reaching), and to draw implications and identify recommendations for AR posture training tool based on the findings from the user interface (UI) usability evaluation. The AR posture training tool consists of both hardware (AR smart glasses) and UI (virtual instructor and information panel). The usability

evaluation aimed to acquire user feedback regarding three interactive functions on the UI, which are associated with demonstrating safe work postures. Feedback from the usability evaluation will inform the design of the next iteration of the AR posture training tool prior to formative evaluation with actual workers from the industry.

### **3.3.2 Methods**

Three research tasks comprise the methods section: (1) create a humanoid instructor by reconstructing surface features of a live human, (2) build an AR user interface and integrate the virtual instructor into AR, and (3) conduct usability evaluation.

#### **3.3.2.1 Create point cloud humanoid instructor**

The interactive posture training tool includes a vivid, human-like virtual instructor who demonstrates how to lift or bend safely. The general steps include point cloud capture, denoising, registration and stitching.

*Point cloud capture.* Four RGB-D cameras (Intel RealSense D415, Intel, Santa Clara, CA) were oriented 90° relative to each other and then calibrated. An individual assumed ready position (standing upright) at the center of the four cameras and faced one of the four cameras (Figure 3-9). The individual performed a lifting task by lifting a box from the floor using a stoop lifting posture (Occupational Safety & Health Administration, retrieved 2020). The four cameras captured unique views of the individual who demonstrated the listing task (Figure 3-9). Each camera generated one set of point cloud data, which was stored as a pcd (“point cloud data”) file.

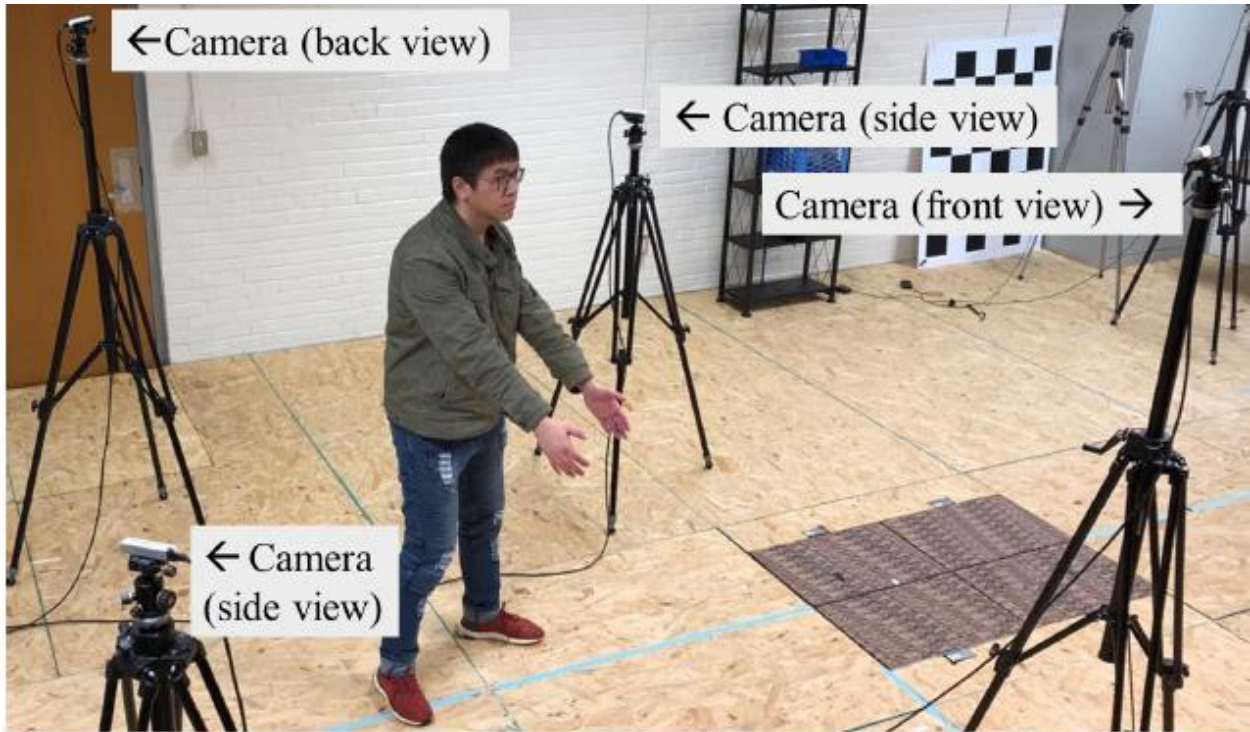


**Figure 3-9** Placement of RGB-D cameras.

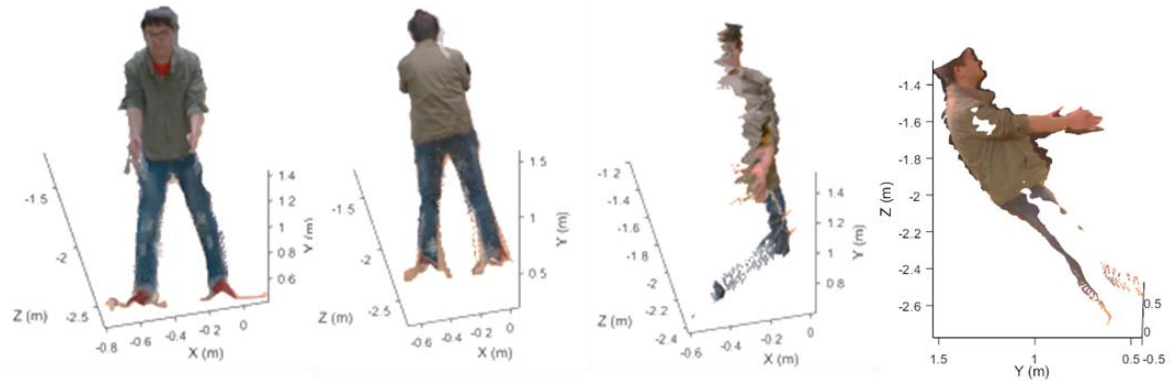


**Figure 3-10** The front, back, left-side, and right-side views, capture by the four RGB-D cameras (starting from the leftmost one).

*Noise removal.* The next step was to remove environmental information (floor, wall, lab furniture) and noise (unclear regions of the human) using MATLAB (MathWorks, Natick, MA). A native MATLAB filter function, *pcdenoise*, was applied to improve the quality of virtual

instructor (Figure 3-11). There were two critical parameters in the *pcdenoise* function: (1) the number of neighboring points  $n$ , and (2) the cut-off threshold  $t$ . In other words, a point is considered noise if the average distance to its  $n$  nearest points is above threshold  $t$ . By adjusting these two parameters, a balance between accuracy and computation time could be achieved.

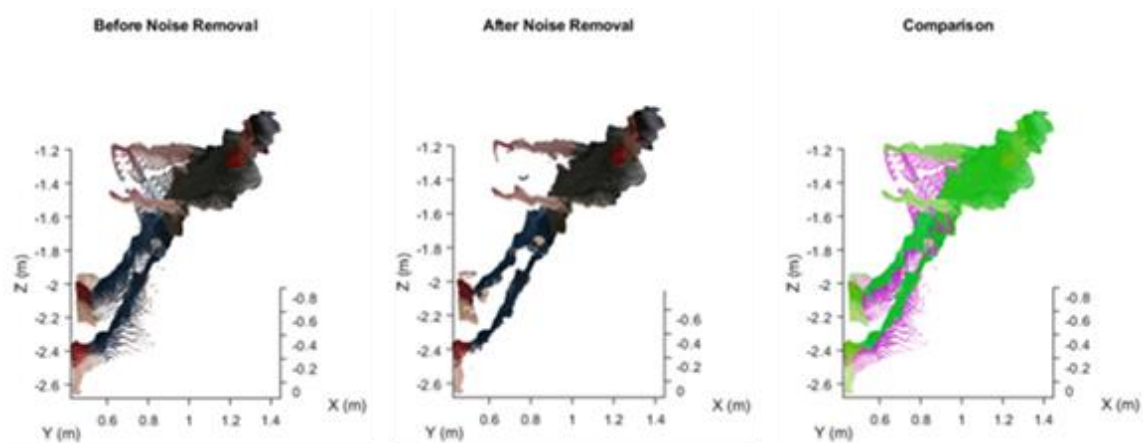


**Figure 3-11** Point cloud before noise removal (left) and after noise removal (middle), and the pink/purple regions depict the noise removed (right).

*Registration and stitching.* The four separate pcd files (Figure 3-10) needed to be reconstructed (“merged”) into a single pcd file to produce a complete, 3D virtual instructor (Sinko et al., 2018). The pcd files shared common overlapping points, which enabled the four pcd files to be reconstructed. Prior to reconstruction, a downsampling process (function *pcdownsample* in MATLAB) was applied to support computational efficiency. Next, all point clouds were verified (or “registered”) to be in the same coordinate system. The quality of registration depends on the quality (e.g., resolution) of point clouds and the quantity of overlapping sections. Point cloud registration algorithm was *iterative closest point* (ICP) algorithm, which is commonly employed in point cloud registration (Besl & McKay, 1992; Y. Chen & Medioni, 1992). The goal of ICP is to minimize the difference or distance between two matching point clouds. As an example for

registering point cloud data, the side view pcd file was selected and a transformation matrix was applied to convert it into the same coordinate system as the front view pcd file, and then they were merged into a new pcd file using function *GridAverage*. This process was repeated until all four pcd files were merged into one, which was then denoised (Figure 3-12).

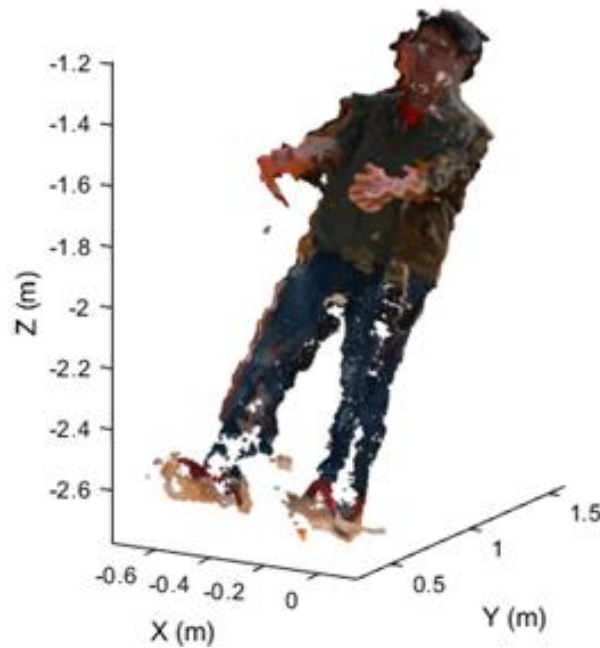


**Figure 3-12** The registered and reconstructed point cloud human from a different view to depict the merged point clouds.

### 3.3.2.2 Build AR user interface to visualize work posture

*UI design specifications.* The essential content of posture training material includes virtual instructors (stationary and animated) and an information panel that presents factual information on risks for unsafe postures. In addition, a user should be able to switch to a different virtual instructor who demonstrates another posture (e.g., from a lifting to a bending task). A user should have the freedom to practice the tasks by following the movements of the virtual instructor, and therefore it is important to free up the hands of the user so he/she could practice lifting a real box

simultaneously. A mixed reality smart-glasses (Microsoft HoloLens 1<sup>st</sup> generation, Microsoft, Redmond, WA) was selected as the hardware for the AR posture training tool because it could be worn over the head. It has approximately 30×17° field of view.

*UI design framework.* A user-centered approach was employed by first considering the target user population, which are workers performing manual material handling tasks, who may not have had sufficient opportunity to practice the lifting task. Technical and scientific jargon were eliminated from the UI so that workers could better understand the information about risks in unsafe postures.

Leveraging a proposed model of AR design consideration and evaluation (Perez et al., 2019), the users should have the flexibility and adjustable settings. Additional UI designs were based on established and 3D UI development guidelines (J. LaViola Jr. et al., 2017). Specifically, the UI elements were simplified (include only essential text) to promote learnability, minimizing the number of complex interactions and screens for memorability (avoid deep links), while providing an efficient learning environment for understanding how to work safely (includes learnability, memorability, efficiency, errors, and satisfaction) (J. Nielsen, 1993; Perez et al., 2019).

*UI functionality.* The UI information panel was built using a rendering engine (Unity 3D ver. 2018.2, Unity Technologies, San Francisco, CA), and the point cloud virtual instructor was imported into Unity as part of the UI. The safety posture contents are incorporated with three interactive functions on the UI. (1) A dropdown menu that allows users to switch from viewing one posture to another. (2) A series of play/pause icons to suggest the possibility of animating the virtual instructor. (3) A block of checkboxes to toggle factual information on/off (e.g., show stress/strain at the lower back).

One specific UI design challenge stems from the head-gaze cursor of Microsoft HoloLens 1<sup>st</sup> generation, which is controlling the cursor through the user's head movement. The information panel was designed to remain in the user's field of view at all times unless the user selects the power button (Figure 3-13). Locking the information panel with the user's field of view was not a practical design it would be locked into the local coordinate system as the head-gaze cursor. In other words, a user would not be able to move the head-gaze cursor independent of the information panel. To overcome this challenge, a "floating information panel" was implemented to enable the users to move the head-gaze cursor to select items on the information panel. In case a user turns the head completely away (i.e., turn to the right 90°), the floating panel would gradually catch up and appear in the user's field of view. Parameters of the floating information panel, such as the catch-up speed, were explicitly examined during usability evaluation.

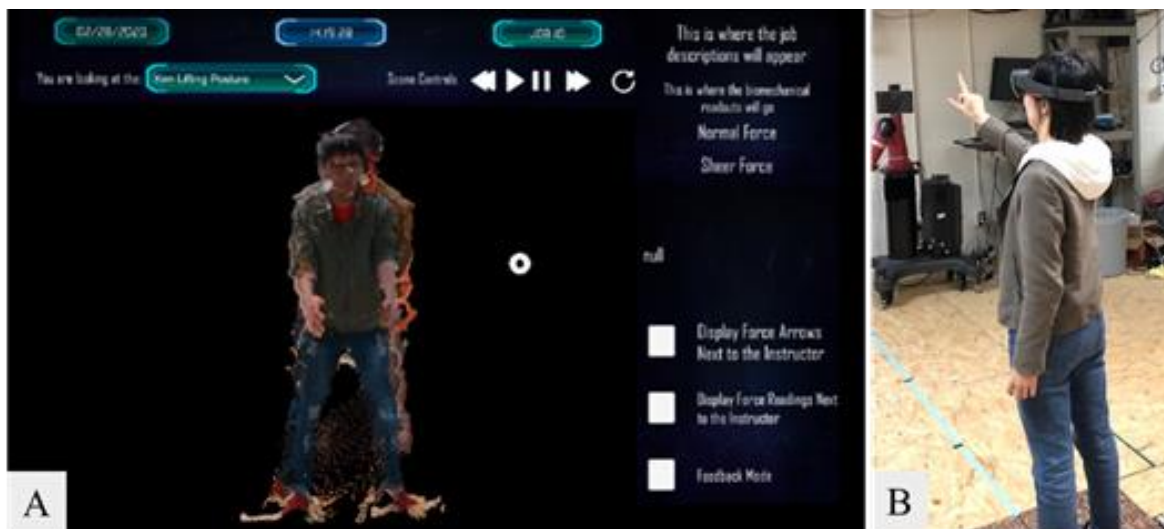


**Figure 3-13** (A) The UI (virtual instructor at the center and information panel). The top center area has the dropdown menu and the series of play/pause icons, as well as date and time elements. The upper right section shows factual information and the description of the task being performed. The lower right has toggle checkboxes to hide/unhide task description. (B) Participant using HoloLens.

### 3.3.2.3 Conduct usability evaluation of the user interface

*Participants.* Ten users (6 males, 4 females) of mean age 28.6 years (range=23-38) were recruited from local community with approval by the Institutional Review Board. Participants were at least 18 years of age and had normal or corrected-to-normal vision. Individuals were excluded from participation if they had tendency of motion sickness or inability to use hand gesture to control UI elements. Four users have had experiences using some type of AR technology (ranged from 0.5 to 5 years since their first use of AR), and all reported the current usage frequency as rarely (from rarely, occasionally, or frequently).

*Usability evaluation procedure.* Upon informed consent, general demographic information was obtained from the participants and then they received simple training on how to use gesture control in AR. Next, they were primed with the description of a persona, which described an average individual that represented our target audience. “You are a 45-year old warehouse worker. The work you do on a daily basis involves putting the boxes onto shelves. You perform a lot of bending, lifting, and reaching tasks, and sometimes your back is sore. You want to know how to safely perform your daily tasks.”

The facilitator assisted the participants to put on HoloLens, and then briefly described the UI elements presented in HoloLens (Figure 3-13). The participants were instructed to think aloud, and their verbalized content written in notes by the facilitator. Each participant was given three task scenarios, which corresponded to the three interactive functions of the posture training tool. The task scenarios were: (1) You want the virtual instructor to move and demonstrate the complete motion of a safe lifting posture; (2) You want to see how much stress level in the lower back when performing a lifting task; and (3) You want to see the safe work posture for a reaching task.

After all task scenarios, participants were prompted with four open-ended questions related to the virtual instructor, the general UI, and the interactive functions. It was followed by a comparison task during which the participants compared the catch-up speed of the floating information panel. Participants then completed Post-Study System Usability Questionnaire (PSSUQ) (J. R. Lewis, 2002) to evaluate the system’s usefulness, information quality, and interface quality on a 7-point Likert-like scale (1=strongly agree, 7=strongly disagree).

*Outcome variables and analysis.* Quantitative data were collected from PSSUQ. Qualitative data were collected from think aloud and open-ended response, which were grouped into recurring themes.

### 3.3.3 Results

#### 3.3.3.1 Post-study system usability questionnaire

Six items from the PSSUQ received a rating greater than 4 (1=strongly agree, 7=strongly disagree) from more than two participants (Table 3-2), which indicated usability problems. All other items from the PSSUQ received ratings below 4 or N/A.

**Table 3-2** Items from PSSUQ received ratings greater than 4 (“neutral”) from more than two participants. Frequency refers to the number of participants gave a rating greater than 4.

<b>Item description summary</b>	<b>Frequency</b>
Has all functions and capabilities expected.	4
Overall satisfied with the system.	5
Satisfied with how easy to use the system.	4
Able to efficiently complete task scenarios.	4
Felt comfortable using the system.	4
Liked using the UI of the system.	4

### 3.3.3.2 Think aloud

Usability comments and recurring themes (Table 3-3) from participants' verbalized thought process were identified.

**Table 3-3** Post-task responses related to four general open-ended questions (count of recurring comments listed as frequency).

<b>Themes from UI usability comments</b>	<b>Frequency</b>
Not sure what to expect from checkboxes.	2
Problems with appearance of virtual instructor (did not seem to be scaled properly / was floating)	4
Text, button, and dropdown menus were small (hard to read and hover over).	10
UI blocked the virtual instructor, did not know how to hide/unhide UI elements.	3
UI drifted while navigating / walking around.	2
Unclear about the meaning of factual information.	1
Unclear about the meaning of force/stress vectors.	4

### 3.3.3.2 Open-ended responses

General feedback and its recurring themes were identified from the post-task open-ended responses. Comments from open-ended responses that were not mentioned during think aloud are identified in Table 3-4.

**Table 3-4** Post-task responses related to four general open-ended questions (count of recurring comments listed as frequency).

<b>General feedback</b>	<b>Frequency</b>
AR smart glasses too heavy / interfered with glasses.	5
Small field of view.	2
Felt eye strain / sickness.	1
<b>Virtual instructor feedback</b>	<b>Frequency</b>
Would like to see more motions / examples of incorrect postures from virtual instructor.	6
Prefer to see mesh as opposed to 3D point cloud.	1
<b>Interactive function feedback</b>	<b>Frequency</b>
Would like additional input methods (complex gestures, voice control).	2
Would like additional, sophisticated functions.	2
<b>Display / UI feedback</b>	<b>Frequency</b>
Would like different colors for different functions.	1
Would like customizable job / information for user.	1
Prefer faster catch-up speed of the floating panel.	4

### 3.3.4 Discussion

This work followed DMAIC (Define, Measure, Analyze, Improve and Control) process during which the design specifications were first defined. The team established the essential postural training material and content that were translated into the AR environment for usability evaluation (measure and analyze), which generated results for the next step: iterative refinement (improve and control) of the AR posture training tool.

The virtual instructor reconstruction process demonstrated the feasibility of creating posture training material using 3D point cloud reconstruction, which was initially applied in computer science or medical research (Mao et al., 2017; Sinko et al., 2018). Three main takeaways will feed into the next iteration. First, there were some missing areas on the virtual instructor that

may be due to camera configuration and occlusion, which will be the immediate subject of improve in the next iteration. Next, the ICP method employed for registration is the most basic and the simplest ICP algorithm, which may have contributed to slight misalignment between two pcd files. More sophisticated ICP algorithm that leverages color and geometric features can be employed. Finally, the noise removal parameter was preliminarily tested for this iteration of the virtual instructor, but the optimal smoothness-accuracy tradeoff will be examined.

The UI building process uncovered a consideration in display compatibility, which refers to the UI elements that appeared to be visually acceptable (complied with general heuristics) in developer mode on a computer monitor may not necessarily be acceptable for users in AR. While the research team has verified and tested the UI elements in the AR environment, the team has become accustomed to the sizes and interactive functions throughout the development process, hence the size issue was not immediately apparent until it was evaluated by the participants who have not seen the UI previously. Usability findings suggested that the size of text and interactive functions (checkbox, dropdown menu) should be designed larger than they needed to be, not only accommodate the potential size difference in AR but also to support new AR users who may have jittery controls of the head-gaze cursor.

Usability evaluation procedure adopted from the conventional interface usability evaluation (e.g., webpage) helped identify six usability problems (Table 3-2). This suggested that the usability framework for conventional interfaces was a practical method to assess usability of AR interface / system. Moreover, comments obtained from think aloud (Table 3-3) were consistent across multiple participants, which suggested that issues identified by participants were not by chance (systematic issues) and highlighted the effectiveness of the adoption of usability evaluation from conventional interfaces.

Quantitative and qualitative data revealed source of usability issues. The PSSUQ revealed two primary types of usability problems: interface quality and system usefulness. For interface quality, four of ten participants indicated that the systems did not have all functions and capabilities as expected, and they did not like using the interface of the system (Table 3-2). More specifically, verbalized responses revealed that the participants were unclear about the meaning of factual information and force/stress vectors, and the UI drifted while navigating which resulted in occlusion of the virtual instructor (Table 3-3). For system usefulness, some participants did not know what to expect from the checkbox toggle functions (Table 3-3). Digging into verbalized responses helped identify UI and system usability problems that were reported by participants during their actual usage, which explained the data from the PSSUQ.

Feedback from the open-ended responses offered insightful features that are valuable for the next iteration of the UI. While some comments may not be addressed directly, particularly with AR hardware being unfriendly to users with eyeglasses (Table 3-4), the opportunity to leverage built-in hardware such as motion sensor and microphone to support additional input methods such as complex gestures and voice activation can be expected (Table 3-4). Feedback specific to the floating information panel helped us to conclude that a faster catch-up speed seemed preferable as users may not want to lose UI information for too long. Finally, it was important for the team to separate comments associated “usefulness” from “user preference” because a participant had preference for a graphic virtual instructor (as opposed to point cloud) but it may be a specific future usability evaluation question as opposed to immediate implementation.

The limitations of this study included: The usability evaluation results did not include time to task completion, which may have been an indicator of system ease of use. However, given the

floating panel on the UI interface, it was difficult to determine an objective starting time because some users did not have the user interface at the center of the screen.

### **3.3.5 Conclusions**

Using surface features and point cloud data to reconstruct a holistic, 3D virtual instructor enabled users to visualize safer work postures of a whole body in AR. Furthermore, by first establishing design specifications made the implementation of interactive functions clearer. Leveraging user-centered framework and 3D UI design provided the heuristics for UI design. Usability evaluation method for conventional interfaces could be adopted to the evaluation of UI in AR. Finally, performing cross-validation by comparing quantitative data against qualitative data helped pinpoint the source of usability issue since numerical ratings from questionnaires provided minimal clues to the specific issue of the UI feature. The AR posture training tool provided great promise in establishing a novel training tool in which a virtual instructor can deliver holistic work movement information to workers.

## **3.4 Summary**

Two humanoid instructors were examined in two XR systems. In specific, a 3-D humanoid model was developed and implemented in a virtual reality exercise (VRE) program to guide participants to perform pick and place movements, and a point-cloud reconstructed humanoid model was built in an AR posture training platform to demonstrate different postures that were commonly seen in manual material handling tasks.

Compared to point cloud reconstructed virtual instructor, 3-D model based virtual instructor was more flexible and could be easily animated to convey movement information to the

participants by altering the joint location of the virtual instructor. While for the point cloud generated virtual instructor, it shared more similarities with real humans on appearances, but it was difficult to edit and animate the point cloud as it was a complete mesh. For future XR ergonomics training platform, 3-D model based virtual instructor might be a better option as it is easier to manipulate and control, and more biomechanics related information could be mapped onto the 3-D virtual instructor, such as EMG signals and joint torque.

## **Chapter 4 Effects of EMG feedback for simulated patient transfer task in VR system**

This chapter is adapted from one co-authored paper (K. Chen, Widmayer, et al., 2020).

### **4.1 Motivation**

As reviewed in Chapter 2, an ideal VR system would include five types sensory feedback to promote real life experiences. Apart from visual feedback in the form of humanoid instructors, other types of feedback can be implemented into the VR system. In specific, haptic interactions are lacking in the VR system as the most interactions with virtual objects are achieved through controllers: people can pick up, touch and throw virtual objects by clicking the respective buttons on the controllers, which doesn't require forceful exertions. To evoke forceful exertions in the VR system, some researchers proposed and demonstrated the concept of "virtual exertions" to encode electromyography (EMG) signals and track hand movements for interacting with virtual objects (K. B. Chen et al., 2015; Radwin et al., 2013). This novel concept proposed that the grasping of virtual objects was achieved in two steps: (1) a user's tracked hand position collided with virtual objects and (2) the user contracted the prime mover muscle group (i.e., biceps brachii) and reached a calibrated EMG threshold. However, these studies only evaluated simple tasks (i.e., lifting a dumbbell) which involved few muscles, thus it is worth investigation when more complicated movements are involved and multi-EMG signals from more muscles are related.

This chapter discusses a specific physical task (patient transfer task) that involved muscles across the whole body. To select appropriate muscles for virtual exertions, the first step is to conduct the simulated task in the physical environment and extract the major contributing muscles through statistical analysis on the EMG, the second step is to set up EMG criteria or models for

selected major muscles to implement the virtual exertions, and finally, the same patient transfer task was repeated examined in a virtual environment through the established virtual exertions criteria. Section 4.2 studied the process of extracting major contributing muscles using principal component analysis (PCA), Section 4.3 examined the concept of virtual exertions for muscles extracted in 4.2 using binary threshold technique.

## **4.2 Identify major contributing muscles in a simulated patient transfer task**

### **4.2.1 Introduction**

Work-related musculoskeletal disorders (WMSDs) are common threats among healthcare personnel (Callison & Nussbaum, 2012; Goswami et al., 2017). In particular, healthcare personnel constantly suffer from back pain, neck pain, and shoulder pain as a result of nursing activities (Yasobant & Rajkumar, 2014). Patient handling, including patient lifting and transferring, accounted for most reported sources of WMSDs among nursing activities, and previous studies showed that patient handling accounted for 33-72% of musculoskeletal disorder injuries and 53% of compensation costs among patient care staff in a hospital setting (H. Kim et al., 2012; Lipscomb et al., 2018; Pompeii et al., 2009). Therefore, considerable efforts have been invested in enhancing the safety and improve patient handling techniques and strategies (Makhoul et al., 2017; Nelson & Baptiste, 2004; Pompeii et al., 2009).

Electromyography (EMG) is an electrodiagnostic signal that commonly used to reveal muscle dysfunction and fatigue during lifting tasks (Andersson et al., 1977; Ekholm et al., 1982; Granata & Marras, 1995; Yates & Karwowski, 1992). The analysis EMG signals can help reveal muscle activity information and fatigue in patient handling tasks (Makhoul et al., 2017;

Nagavarapu et al., 2017). While patient handling is a whole-body movement that involves muscles across the body, current studies focused on separate body sections. For instance, Some studies that examined muscle activities during patient transfer predominantly focused on the low back muscles, particularly the shear/compression forces exerted against the lumbar joint were evaluated and quantified (Andersson et al., 1977; Ekholm et al., 1982; Kang et al., 2013; Nagavarapu et al., 2017). Some researchers considered the shoulder muscular activity and proposed a load transfer strategy from the lumbar to the shoulder region, which helped to lighten the burden on back region (Gagnon et al., 1987; Keir & MacDonell, 2004). Since patient transfer is a complex task that involves multiple actions and steps to complete the transfer (i.e., transfer a patient from ground to a backboard, lift the backboard onto a stretch, and load the into an ambulance), it is clear that muscle groups other than the shoulders and the lumbar are involved in a patient transfer task (Makhoul et al., 2017). The involvement of muscles in the extremities, such as the biceps and the triceps, have been overlooked (Hwang et al., 2019, 2020). It is important to understand which muscles are most extensively engaged during different lifting actions and thereby address the WMSDs specific to different regions of the body.

Principal component analysis (PCA) is an established dimension reduction method and it has been applied in surface EMG analysis for different purposes (Naik et al., 2016). Using time domain features of EMG, PCA has been utilized to differentiate major recruiting muscles between ordinary persons and professional volleyball players when performing a vertical jump, and the results demonstrated that PCA was more sensitive to detect these differences compared to the “area under curve” method (Charoenpanich et al., 2013). With frequency domain features, some researchers used mean power frequency components of muscle EMG as the PCA input and identified the major body sections that led to whole body fatigue during a box lifting task (Ahmad

& Kim, 2018). Moreover, the power spectra of EMG have been used as the input of PCA and the results revealed new parameters for muscle fatigue assessment during cycle ergometer task (Jesus et al., 2016). The utility of PCA has value in discerning activities and contributions of different muscle groups, which renders it a valuable technique in identifying major contributors to a patient transfer task. However, few of these studies clarified the rationales to select their specific EMG features. This work will help contribute to the identification of EMG signal features that are present during a simulated patient transfer task to expand the understanding of In other words, it's worth investigating what EMG signals features may be more appropriate for PCA of a patient transfer task to produce higher explained variances.

The purpose of this study was to objectively quantify and identify the major contributors in a patient transfer task, which involved muscles located in the low back, the shoulder region, the upper extremities, and the lower extremities. Specifically, PCA was applied to identify the major contributing muscles through the analysis of EMG signal features, including RMS in the time domain and MDF in the frequency domain. A mock-up patient lifting task was established in a laboratory setting to simulate the two-step patient lifting task. Muscle activity of participants were monitored using surface EMG sensors. The major contributing muscles are operationally defined as the principal variables in the PCA. The selected major contributing muscles could facilitate further EMG based movement classification or exoskeleton control without losing too much information (Dhindsa et al., 2017) and give insights on muscular training for manual patient transfer tasks.

## **4.2.2 Methods**

### **4.2.2.1 Participants**

Fifteen participants (8 females and 7 males) between the ages 18-35 years (mean = 22.7, SD = 4.9) participated in the study. Informed consent was obtained from all participants with approval from North Carolina State University Institutional Review Board. The inclusion criteria were absence of physical disabilities, no musculoskeletal injuries in the past three months, and willingness to lift/move heavy objects at the time of experiment participation. Each participant was compensated at a rate of \$10 per hour. The experiment lasted approximately two hours for each participant.

### **4.2.2.2 Equipment**

The following equipment were employed during the experiment. A set of 16-channel wireless EMG sensors (Trigno, Delesys Inc, Natick, MA) was used to monitor and record muscle activity during the transfer tasks. A body-length backboard loaded with distributed weights was to simulate a “patient” on the backboard, which was approximately 150 lbs.

### **4.2.2.3 Experimental procedures**

Upon informed consent, participants completed a basic demographic questionnaire that included questions on their age, gender, weight, height, and musculoskeletal injuries in the past three months. To avoid prolonged experiment time and fatigue (e.g., performed maximum voluntary contraction for all muscles of interest, and then performed the simulated patient transfer tasks), the participants were evenly and randomly allocated into three groups. Each group had an emphasis on specific body regions, of which were the shoulders, the lower back, or the extremities

(Table 5). The group assignment was randomized and counterbalanced and each group included five participants.

Next, the experimenter placed the surface EMG sensors bilaterally (i.e., on both the left and right sides) on the muscles and the sensors were secured using medical or athletic tape if necessary. The list and locations of all 19 muscle pairs are shown in Table 4-1 and Figure 4-1. Participants performed maximum voluntary contraction (MVC) against a whole body dynamometer following standard MVC procedures (Gatti et al., 2008; Vera-Garcia et al., 2010)

**Table 4-1** The three regions of muscles and the muscles of interest within each group.

Extremities Region	Shoulder Region	Back Region
Extensor Carpi Radialis (ECR)	Anterior Deltoid (AD)	Rectus Abdominus (RA)
Flexor Carpi Radialis (FCR)	Middle Deltoid (MD)	External Oblique (EO)
Triceps (TRI)	Posterior Deltoid (PD)	Internal Oblique (IO)
Biceps Brachium (BI)	Upper Trapezius (UT)	Latissimus Dorsi (LD)
Hamstring (HAM)	Middle Trapezius (MT)	Thoracic Erector Spinae (TES)
Vastus Lateralis (VL)	Lower Trapezius (LT)	Lumbar Erector Spinae (LES)
Biceps Femoris (BF)		

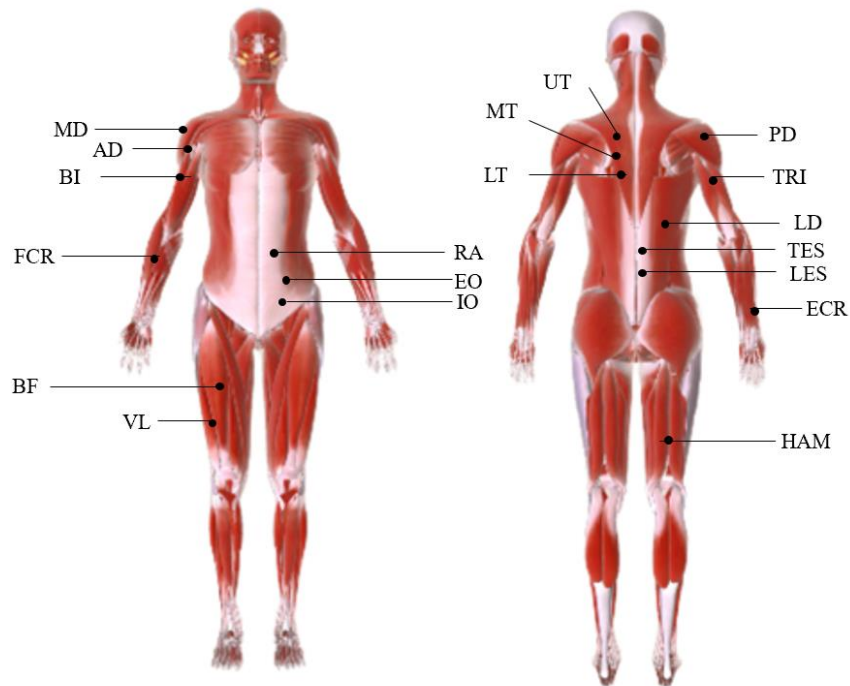


**Figure 4-1** Locations of EMG sensors across three muscle groups, adapted from <https://www.healthline.com/human-body-maps/muscular-system#1>.

After surface EMG sensor placement, participants were instructed to warm up by stretching their legs and arms prior to the experiment. For each experiment session, the participant completed a two-step, two-person lift with the researcher. The participant completed a discomfort survey (ErgoSystems Consulting, Waconia, MN) after the completion of the simulated patient transfer task. The survey used a 0-10 scale to acquire participants' perceived discomforts on different body sections, as "0" referred to no discomfort and "10" corresponded to maximum discomfort.

#### **4.2.2.4 Experimental task**

The experimental task involves a two-step transport lift task, which was adapted from a lifting task performed by emergency medical technicians during patient transport, as used by

(Makhoul et al., 2017). These lifts are often identified as the most demanding lifts (Coffey et al., 2016). The transfer task had two defined steps. Step 1 was to transfer the weighted backboard from the ground laterally to an adjacent location. Step 2 was to lift the weighted to a higher surface similar to an ambulance loading height.

The participant was reminded that he/she should immediately notify the experimenter and stop performing the lift if he/she feels unable to continue the task at any time of the study. In each trial, the participant lifted a weighted backboard (to simulate a stretcher with a patient) in two motions as illustrated in the Figure 4-2. First, the participant transported the weighted backboard from the ground laterally and then lifted the weighted backboard to standing height (**a** → **b** → **c** → **d**), as if loading a “patient” laterally onto a backboard. Next, the participant lifted the weighted backboard onto a higher surface similar to an ambulance loading height (**d** → **e**). After the participant completed the practice trials with lighter loads, the patient transport task was performed by the participant three times with the same weight (150 lb), with two-minute breaks between each trial.

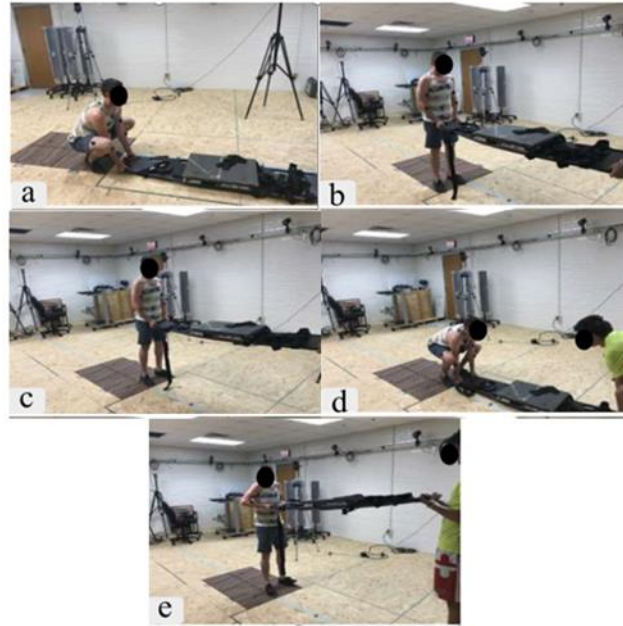


**Figure 4-2** Participants performed the two-step patient transfer task with the researcher. (a) Begin to lift patient. (b) Lift Patient to backboard height. (c) Move patient laterally. (d) Place patient on the backboard. (e) Lift the weighed backboard to ambulance loading height.

#### 4.2.2.5 Variables and data analysis

The independent variables were the steps of lifting (two steps) and the muscles (19 muscles in total). The dependent variables were EMG signals of the muscles and body discomfort survey. For each muscle, the EMG signals were filtered with a 4<sup>th</sup> order Butterworth filter, a 200ms moving window with no overlap was employed. EMG amplitude was normalized to the peak value captured during the MVC tests for each muscle, normalized EMG (nEMG) was then averaged across all experiment trials. Two common EMG features (Chowdhury et al., 2013; Nazmi et al., 2016) were selected as the input of PCA analysis: root mean square (RMS) of EMG amplitude over time in the time domain, and median frequency (MDF) in the frequency domain. RMS and MDF were calculated for each window, and RMS was normalized by dividing the peak RMS value during the tasks (Halaki & Gi, 2012). Principal components analysis was performed for each

muscle group at each trial at Step 1 and Step 2 separately, which enabled the further identification of major contributing muscles during different steps of a task. For each participant, an input data matrix of PCA was created for every single trial. The matrix was organized into  $m$  rows, where  $m$  was equal to the number of muscles for his/her muscle set, and  $n$  columns where  $n$  was equal to the number of time windows. The output of PCA analysis consisted of several principal components (PCs) that were linear combinations of the EMG features, at each component the major contributing muscles were considered to have highest absolute coefficients between zero and one (Ahmad & Kim, 2018; Charoenpanich et al., 2013). The number of PCs from each analysis was the number of muscles. In this study, only the principal component (PC1) and the second principal component (PC2), which covered most of the variances, were reported. A paired t-test was conducted to compare cumulative variances (PC1 + PC2) between the two signal features, which were the RMS and the MDF. The selection of major contributing muscles was based on the EMG signal feature that produced higher explained variances.

The major contributing muscles was selected by proportion of variances (PRV), which considered both the variances of major components  $\lambda_i$  and each muscle's loading coefficients  $R_i$  (Dhindsa et al., 2017). Finally, the calculated PRVs were averaged for the bilaterally muscle pairs (e.g., the left and right upper trapezius). For each trial, the first two muscle pairs that showed highest PRV values were counted as the major contributing muscles in that single trial.

$$PRV = \sum_{i=1}^k \lambda_i R_i^2 \quad (4-1)$$

### 4.2.3 Results

#### 4.2.3.1 Cumulative variances of PC1 and PC2

Mean and standard deviation of the cumulative variances (i.e., sum of PC1 and PC2) of the three main muscle regions are presented in Figure 4-4. For the extremities muscle region, the PCA that used RMS as the input had a cumulative variance of 70.2%, which was statistically significant greater ( $t(29) = 16.3, p < 0.001$ ) than the cumulative variance explained using MDF (43.7%). For the shoulder muscle region, the PCA analysis that used RMS as the input had a cumulative variance of 71.9%, which was statistically significant greater ( $t(29) = 15.3, p < 0.001$ ) than the cumulative variance explained using MDF (40.8%). For the back muscle region, the PCA analysis that used RMS as the input had a cumulative variance of 63.2%, which was statistically significant greater ( $t(29) = 14.9, p < 0.001$ ) than the cumulative variance explained using MDF 42.5%. For all muscle regions, the abovementioned results revealed that using RMS as the input helped explained more variance for this specific patient lifting task than with MDF, and therefore the subsequent analyses were conducted using RMS as the input for PCA.

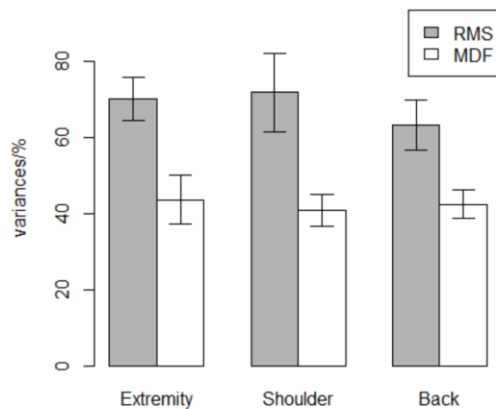


**Figure 4-3** Cumulative variances of PC1 and PC2. PCA with RMS input demonstrated significant higher cumulative variances compared to PCA with MDF input.

#### 4.2.3.2 Selection of major contributing muscles

Figures 4-4, 4-5, and 4-6 present the total frequency of major contributing muscles for the three muscle regions after counting the first two muscle pairs that have highest PRV in each trial.

In the extremity muscle group, the biceps brachium, extensor carpi radialis, flexor carpi radialis and vastus lateralis stood out as major contributing muscles. In specific, PCA revealed differences in major muscles between Step 1 and Step 2, where the extensor carpi radialis showed greater contributions in Step 2 and the vastus lateralis showed greater contributions in Step 1. In the shoulder muscle region, the lower trapezius and upper trapezius showed higher contributions. The middle deltoid showed higher importance in Step 2 while middle trapezius showed higher importance in Step 1. In the back muscle region, latissimus dorsi, thoracic erector spinae and lumbar erector spinae stood out as major contributing muscles.

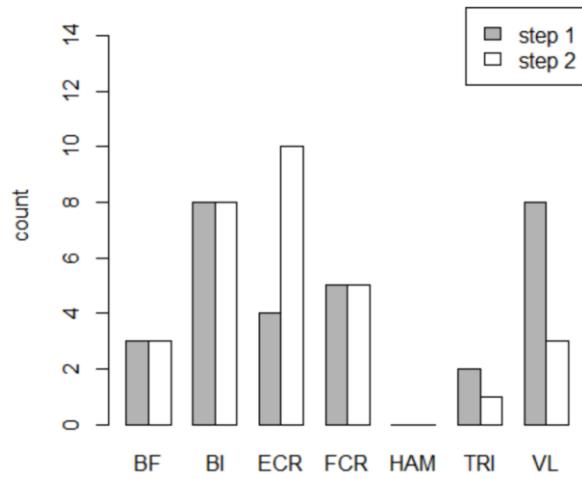


**Figure 4-4** Muscles in the extremities muscle region that were tested and analyzed. The y-axis (count) is the total count of major muscles across all trials. Muscles in this group were: Biceps Femoris (BF), Biceps Brachium (BI), Extensor Carpi Radialis (ECR), Flexor Carpi Radialis (FCR), Hamstring (HAM), Triceps (TRI), Vastus Lateralis (VL).

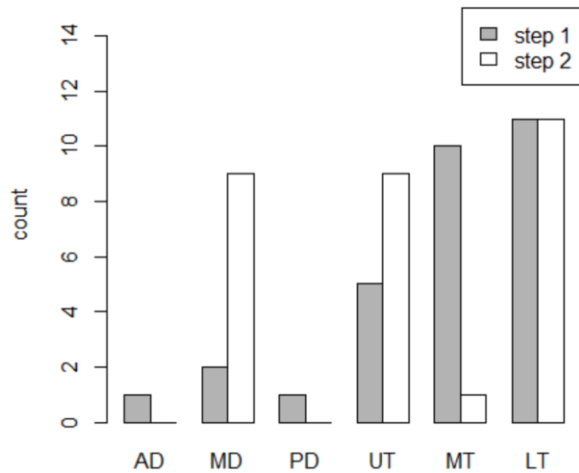


**Figure 4-5** Muscles in the shoulder muscle region that were tested and analyzed. Muscles in the group were: Anterior Deltoid (AD), Middle Deltoid (MD), Posterior Deltoid (PD), Upper Trapezius (UT), Middle Trapezius (MT) and Lower Trapezius (LT).

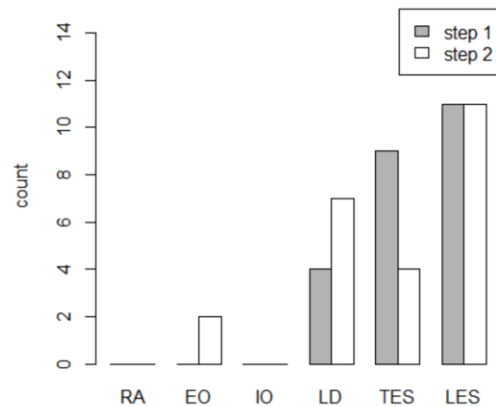


**Figure 4-6** Muscles in the back muscle region that were tested and analyzed. Muscles in the group were: Rectus Abdominus (RA), External Oblique (EO), Internal Oblique (IO), Latissimus Dorsi (LD), Thoracic Erector Spinae (TES) and Lumbar Erector Spinae (LES).

#### 4.2.3.3 Body discomfort survey

Shapiro-Wilk normality test indicated that body discomfort score was not normally distributed for the ten body sections. Therefore, Friedman test was used instead of one-way repeated measure ANOVA to assess if there are any statistically significant differences between the discomfort score of each body section. Friedman test indicated that there was statistically significant across the discomfort scores ( $\chi^2(9) = 19.2, p = 0.02$ ). The mean and standard deviation of discomfort score was presented below in Table 4-2.

**Table 4-2** Mean and standard deviation of body discomfort score of the different body sections.

	Body section	Discomfort Score
Upper body	Head/ Neck/Eyes	0.07 (0.26)
	Upper/ Mid Back	0.8 (1.32)
	Low Back/ Pelvis	0.73 (1.28)
Upper Extremity	Shoulder/ Upper Arm	1.13 (1.68)
	Elbow/ Mid Arm	0.8 (1.47)
	Forearm/ Wrist	1 (1.41)
	Hand	0.73 (1.53)
Lower Extremity	Upper Leg/ Hip	0.6 (1.35)
	Mid Leg/ Knee	1.2 (1.70)
	Lower Leg/ Foot	0.27 (0.70)

#### 4.2.4 Discussion

Since load transfer utilizes various muscles throughout the entire body, this study aimed to contribute to the field by quantitatively identifying the major contributing muscles in a patient transfer task by considering muscles groups across the body. Muscle activity in terms of EMG was analyzed using PCA, which quantitatively identified the major contributing muscles during the different steps of simulated patient transfer task. First, the implications of selecting RMS of nEMG as the input metric for PCA is discussed, followed by the discussion on the selection of major contributing muscles via PCA, and finally the applicability of subjective body discomfort survey in supporting PCA results.

#### **4.2.4.1 Selection of EMG feature and principal components**

In this study, the RMS and the MDF were initially selected as input metrics for PCA as they are commonly analyzed EMG features in the time domain and frequency domain (Chowdhury et al., 2013; Nazmi et al., 2016). The results of PCA produced the cumulative variances explained (e.g., sum of PC1 and PC2) by the RMS and the MDF inputs, which enabled the comparison of cumulative variance explain by the two inputs using a paired t-test. The result of the paired t-test revealed that the RMS input for PCA explained greater cumulative variances when considering the first two principal components, which provided the basis of for selecting the input metric for identification of the major contributing muscles. The selection of the RMS, which is a feature in the time domain, is aligned with other studies. For instance, EMG amplitude, which is a time domain feature, was used extract major contributing muscles during the movement of vertical jump (Charoenpanich et al., 2013), which was a short burst of muscle activity that happened over the course of less than 2 seconds. Frequency domain features can be utilized to identify major muscles that contribute to fatigue and exertions (Ahmad & Kim, 2018). Frequency domain features, such as median frequency is a good indicator of muscle fatigue as research has shown median frequency decrease as muscle fatigue appears (Phinyomark et al., 2012). While the studies adopted frequency domain features involved tasks that were associated with prolonged repetitive movements, which could lead to fatigue. Yet, each single trial in the present study lasted approximately 15 seconds and participants reported low body discomfort score, thus it was plausible to infer that the participants did not experience enough muscle fatigue and RMS could induce higher explained variances. It was expected MDF would be a suitable input for PCA analysis for tasks that are prolonged and repetitive that induce greater fatigue.

With the RMS input metric for PCA, the present study considered the first two principal components (PC1 and PC2), which explained approximately 70% variance. The number of principal components included was dictated by the percent of variance explained rather than based on a fixed rule. In fact, some proposed to retain the components that have eigenvalues greater than 1 (Kaiser, 1961), and some proposed to plot the explained variances in descending order as a scree plot and major components were extracted where abrupt transition appears, which was highly subjective (Naik et al., 2016). Some studies using PCA for EMG analysis only considered the first principal component (Ahmad & Kim, 2018; Charoenpanich et al., 2013), which covered 55% variance and the authors extracted major contributing muscles via each muscle's loadings on the first major component. The PCA results achieved higher explained variances by selecting the first two major components, and thereby identified the major contributing muscles via PRV calculation that considered both principal component's variances and each muscle's loading coefficients on the principal components.

#### **4.2.4.2 Selection of major muscles or variables**

The results from PCA revealed that the biceps, extensor carpi radialis, flexor carpi radialis, and vastus lateralis were the muscles that had the greatest counts and contributed the most among those in the extremities muscle region. During the simulated lifting task, the biceps brachium flexed the forearm at elbow joint and work together with the forearm muscles (extensor carpi radialis and flexor carpi radialis) to produce the hand/wrist movements. Given that the vastus lateralis was the largest and most powerful muscle among the quadriceps (Bordoni & Varacallo, 2018), it promoted stability and strength of knee and hip during the lifts (Bohm et al., 2018). In particular, the extensor carpi radialis had greater contribution in Step 2, and it was involved in lifting the simulated patient to the height of an ambulance. In general, increasing the height of

lifting destination could result in higher muscular activity (Habes et al., 1985; P. K. Nielsen et al., 1998). One direct influence of height on lifting activity is the joint angle (Oliveira et al., 2011), as can be seen in Figure 4-2e, where lifting to ambulance height increased elbow flexion angle and decreased shoulder flexion angle compared to lifting to the standing posture (Figure 4-2(b)). The PCA result suggested extensor carpi radialis bore increasing loadings with such alteration.

In the shoulder muscle group, trapezius (lower trapezius, middle trapezius and upper trapezius) stood out as major muscles. Trapezius contributed to movement and stability of scapula during the lift task (Johnson et al., 1994). Similar to the extensor carpi radialis, the middle deltoid also showed increasing contribution in the Step 2, which could be associated with its' function. Previous box-lifting study indicated that the most significant effect of height was shoulder abduction angle (Oliveira et al., 2011), lifting to ambulance height resulted in increasing shoulder abduction angle, and the middle deltoid assisted in the abduction of the shoulder joint (Lam & Bordoni, 2019).

In the low back muscle group, the lumbar erector spinae, thoracic erector spinae, and latissimus dorsi demonstrated higher count frequencies, and the findings are quite plausible. The lumbar erector spinae and the thoracic erector spinae are part of erector spinae muscles that were exposed to high compressive force during the lifting task (Dolan & Adams, 1998; Makhoul et al., 2017). Some researchers studied the lifting activity on trained paramedics and found that they generated more work from the lower body rather than trunk to avoid high L4 and L5 spine moments (Makhoul et al., 2017). As can be seen in Figure 4-7, the latissimus dorsi showed increasing contributions in Step 2, and it is one of the largest muscle in the back that contribute to shoulder and trunk movements (Bogduk et al., 1998; Hall et al., 1999). The PCA results revealed

that the participants shifted load from the erector spine to latissimus dorsi to overcome the increasing task difficulty in Step 2.

The PCA revealed that the biceps brachium, extensor carpi radialis, flexor carpi radialis, and vastus lateralis from extremity muscle group, the lower trapezius and upper trapezius from shoulder muscle group, the latissimus dorsi, thoracic erector spinae and lumbar erector spinae from back muscle group stood out as major contributing muscles in the simulated patient transfer task. It could be inferred that muscle pairs with greater EMG amplitude contained more information, which can be extracted via PCA. Using PCA to extract major muscles could facilitate further EMG based movement classification and prosthesis control as it removed some irrelevant muscles and EMG features and achieved higher efficiency (Caesarendra et al., 2017; Zhai et al., 2016).

#### **4.2.4.3 Body discomfort survey**

The body discomfort survey had the whole body into ten body sections, which was not a direct one-to-one mapping with the 19 muscle groups. Broadly speaking, the shoulder/upper arm sections included the major contributions in the deltoid and biceps, the forearm/wrist sections included the major contributions in extensor carpi radialis and flexor carpi radialis, and the mid leg/knee sections included the major contributions in the vastus lateralis. While the 19 muscle groups could be broadly categorized into each of the ten body sections, the mean of body discomfort scores reported by the participant was relatively small (mostly 0 and 1 on a scale of 10). This was likely since experimental lifting task is a one-time lifting action that did not require repetitive, prolonged lifting. The Friedman test indicated that the mean of discomfort score was different for these body parts. Considering the shoulder/upper arm, forearm/wrist, and mid leg/knee sections, they demonstrated higher discomfort scores (greater than 1) and it may suggest some relationship between major contributors identified by PCA and muscle discomfort. It was

worth investigation why discomfort score in low back (0.73) was relatively small as nEMG and PCA revealed high exertions on the back muscles.

#### **4.2.4.4 Limitations**

The limited number of EMG sensors made it impossible to study all muscles in a single person, so grouping was necessary. As a result, the extract major muscles were dominant in the respective muscle group, the relationship between muscles in different group remained unclear. Another limitation was the body discomfort survey, the average score was relatively small in a tenth scale, which might be due to lack of instructions and training before the participants took the survey. In the future study, more common movements/ tasks would be investigated and other subject surveys such as Borg scale on rated perceived exertions shall be adopted (Dawes et al., 2005).

#### **4.2.5 Conclusions**

Principal component analysis (PCA) can be utilized to extract major contributing muscles in simulated patient transfer tasks. In short-term movement like one-time lifting, time-domain feature such as RMS showed higher explained variance compared to frequency-domain feature such as MDF as the PCA input. In different step of the simulated transfer task, major contributing muscles might shift as participants demonstrated varying joint angles. The biceps brachium, extensor carpi radialis, flexor carpi radialis and vastus lateralis from extremity muscle group, the lower trapezius and upper trapezius from shoulder muscle group, the latissimus dorsi, thoracic erector spinae and lumbar erector spinae from back muscle group stood out as major contributing muscles in the simulated patient transfer task. In specific, extensor carpi radialis, middle deltoid and latissimus dorsi showed increasing contributions in action that induced increasing lifting height.

## **4.3 Simulate forceful exertions during virtual patient transfer tasks**

### **4.3.1 Introduction**

Virtual reality has shown promising potential for in training and instructional applications as it provides a controllable platform for trainees to perform the training tasks. However, previous research suggested some variability in human behaviors between virtual and physical environments (Hoareau et al., 2017; Riccio, 1995). Specifically, in the physical environment, humans interact with objects with body contact, and they voluntarily contract their muscles to lift, place, and manipulate physical objects. While in VR, the interactions with virtual objects are usually achieved by input devices like controllers, which do not require forceful efforts and intense muscle contractions (K. B. Chen et al., 2015; Radwin et al., 2013), therefore users may perceive less effort and lower workload.

Chen et al. (2015) proposed and demonstrated the concept of virtual exertions to encode electromyography (EMG) signals and track hand movements for interacting with virtual objects. The experimental task was to reach, grasp, then hold a virtual dumbbell for five seconds, and then return the virtual dumbbell to a virtual table. Specifically, the grasping of virtual objects was achieved in two steps: (1) a user's controller (wand) collided with virtual objects and (2) the user contracted the prime mover muscle group (i.e., biceps brachii) and reached a calibrated EMG threshold. When the two steps were accomplished, the virtual object was considered "grasped" and "moved" with the user's hand. While the research evoked the sense of exerting force in virtual environments, it was a relatively simple biceps curl task that involved only one muscle group in the upper arm. When simulating more complex tasks like lifting, which involve whole body movement, more EMG signals from multiple muscle groups are needed and encoding EMG can get more complicated.

In this work, the concept of virtual exertions to monitor and encourage muscle activation in a whole-body virtual lifting task was explored and extended. The complete experiment consisted of two tasks. The first task was conducted in the physical environment to examine and quantify the activity of 12 muscle groups (EMG signals) during a three-step patient lifting task. The second task was conducted in a virtual environment, during which participants performed the same three-step patient lifting task and the same muscles' activations were quantified.

### **4.3.2 Methods**

#### **4.3.2.1 Participants**

Nine participants with ages 18-32 (mean = 23.4, SD = 4.0) were recruited for the exploratory study with informed consent and IRB approval. This sample represented a younger and relatively active population because the simulated patient transfer task was physical demanding. Upon applying the exclusion criteria, all participants had no physical disabilities, no musculoskeletal injuries in the past 3 months, no history of epileptic seizure or blackout, no self-reported tendency for motion sickness, no sensitivity to flashing lights, and no history of Lasik or similar eye surgery. They were eligible if indicated willingness to lift/move heavy objects at the time of experiment participation. Each session lasted approximately 2.5 hours.

#### **4.3.2.2 Equipment**

The virtual environment scenario was developed in a game engine (Unity 3D ver. 2018.2, Unity Technologies, San Francisco, CA). The VR experience was delivered via a Cave Automatic Virtual Environment (CAVE), which was a 4-sided 10×9×12 ft space with one projector for each wall (VisCube C4, Visbox, Inc., St. Joseph, IL). Each projector had a maximum brightness of 4,500 lumens with a total of 1,920×1,200 pixels. User head position tracking was accomplished

using a 4-camera optical tracking system (TRACKPACK 4, Advanced Realtime Tracking, Weilheim i.OB, Germany). Position trackers were mounted on the top rim of the active shutter glasses. A wand was utilized for hand position tracking

Muscle activity was tracked using wireless surface EMG sensors with a sampling rate of 1926 Hz (Trigno, Delsys Inc, Natick, MA). These sensors measured and wirelessly transmitted surface EMG signals to the Delsys EMGworks software (Delsys Incorporated, Natick, MA). A dynamometer (System 4 MVPTM, Biodex Medical Systems, Shirley, NY) was used to isolate specific muscle exertion directions using anatomy-specific attachments, and thereby collect maximum voluntary contraction (MVC) of specific muscle groups.

#### **4.3.2.3 Experimental Design**

The experimental session consisted of a MVC test, a physical lifting task (also the calibration task), and a virtual lifting task. The EMG sensors were affixed to 12 muscle groups prior to the MVC task. The MVC values were necessary for EMG signal normalization and inter-subject comparisons.

The 12 muscles were selected based on the preliminary study that aimed to identify the muscle groups, throughout the entire body, that are major contributors to a lifting task. The results from the preliminary study suggested the following muscle groups (six on the right and six on the left): in the shoulders (upper trapezius), the low back (thoracic erector spinae and lumbar erector spinae), and the extremities (extensor carpi radialis, biceps brachii, and vastus lateralis).

The purpose of the physical lifting task was to determine the muscle activity signals (EMG) during a three-step lifting task in the physical environment. Twelve muscle groups were monitored. The EMG signals of the 12 muscle groups from the physical lifting task also served as threshold values of which the participants needed to reach and maintain in order to “move” the virtual patient

during the virtual lifting task. The virtual lifting task was the same three-step lifting task but performed in the CAVE against a virtual patient, which represented a standard three-part emergency lift performed during patient transport (Makhoul et al., 2017).

#### **4.3.2.4 Procedure**

*MVC test.* Participants warmed up by stretching their legs and arms, similar to the movements performed before physical exercises. After donned with EMG sensors, participants were guided to complete the MVC test for all 12 muscles. For each of the 12 muscles, participants performed muscle contractions maximally by exerting against an opposing force produced by the dynamometer that constrained the exertion movements and thereby isolated the MVC to the specific muscle group. Verbal encouragements such as “keep going, go, go, go” were consistently provided to arouse the maximum muscle activation. Each MVC test was performed for three seconds, three times per muscle, with a one-minute rest between each MVC test.

*Physical lifting task (Calibration task).* After MVC tests were completed, the experimenter demonstrated the appropriate, two-person lifting method for the patient which can be referred to section 4.2.2.4. For this experiment, there were three phases in a standard patient lifting task (Figure 4-2). (1) Transport the weighted backboard from the ground laterally to where a stretcher would be at (**a** → **b** → **c** → **d**). (2) Lift the weighted backboard to standing height (**d** → **c**). (3) Lift the weighted backboard onto a higher surface similar to an ambulance loading height (**c** → **e**). These were exactly the same set of movements that were employed in the previous experiment. But the whole experiments were further decomposed into three steps. There were three different weights of simulated patients, which were 100, 150, and 200 lb. The loads were spread out across and secured to the backboard that corresponded to the relative distribution of a human body.

Participants practiced lifting the backboard of the three different weights with the research experimenter. With the actual calibration trials, participants performed the three-step lift three times for each of the three weighted backboards. They were provided with one-minute breaks between each trial per weight, and three-minute rest periods between each weight. Subjective discomfort ratings were verbally asked to determine whether the participants should be provided a longer break to prevent potential injury. This resulted in a total of nine lifting trials (3 repetitions per weight). After the nine lifts, participants completed the NASA Task Load Index (Hart & Staveland, 1988) to assess the workload of physical lifts.

The recorded EMG signals from all 12 muscle groups during the physical lifting task were processed to be used as the lifting threshold of the virtual lifting task. For each muscle group, the EMG signals were filtered with a 4<sup>th</sup> order Butterworth filter, and then a root mean square (RMS) value was calculated from each phase of the three-step lift. Since there were three repetitions, the final threshold value for each phase of the lift was the average RMS across the three repetitions.

*Virtual lifting task.* Participants wore the tracked, active shutter glasses and held a wand for the virtual lifting task. The VR scenario (Figure 4-7) had a patient lying on a backboard in a cityscape scene next to an ambulance, which depicted a typical scenario where an emergency medical technician may be required to perform a patient lift and transport task.



**Figure 4-7** Screen capture (left) and CAVE view (right) of the VR scenario for the three-step lift. It was cityscape with a patient on a backboard in the road next to an ambulance.

The participants were instructed to position themselves at one end of the backboard and attempt to perform the patient lift the same way they did for the physical lifts. The virtual lift consisted of the same phases in the three-step lift: (1) Transport the patient on the backboard laterally onto a stretcher, (2) Lift the stretcher to standing height, and (3) Lift the stretcher higher to ambulance loading height.

The virtual patient would not move unless two requirements were met: (1) The participant's all 12 muscles reached the lifting thresholds, which were the RMS of EMG from the physical task (calibration task), and (2) The wand's position intersected with the handles on the virtual backboard or stretcher, depending on the phase of the lift.

To check whether a participant's EMG has reached the lifting threshold, the RMS of a 200ms moving window was computed in real time. This checking loop output a binary check; for each of the 12 muscle groups, it either reached the lifting threshold (true) or did not reach the lifting threshold (false). The virtual patient would only move when all 12 muscle groups reached the threshold. The research experimenter was able to visualize on the data collection workstation which muscle group did not reach the threshold and provided verbal feedback to the participant.

There was also the option for the research experimenter to scale down the threshold using an adjustment factor (AF), which was written in the data collection program in case the participant was unable to reach the lifting threshold by voluntarily contracting and stiffening the muscle groups (i.e., no physical counterweight). The AF was applied after ten unsuccessful attempts, which started at 0.95 for the 11th attempt and decreased in increments of 0.05 for the subsequent attempts. For example, if the AF was changed to 0.5, the participant's EMG signal output would only need to be 50% of the calibration threshold for the virtual patient to be movable. There were nine trials of the virtual lifting task (3 repetitions per weight). After the experiment, the participant completed another NASA-TLX to assess their workload based on the virtual lifts.

#### **4.3.2.5 Variable and analysis**

The independent variables for the experiment were task type (physical lift against virtual lift) and object weight (100 lb, 150 lb, and 200 lb). This was a 2×3 (task type × weight) experiment design. The dependent variables for both the physical and virtual lifts were the muscle exertion normalized EMG (nEMG) values and NASA-TLX questionnaire responses. All raw EMG signals were filtered with a fourth order band-pass (20–350 Hz) Butterworth filter, rectified and smoothed by a time window of 200ms. This included EMG signals from the MVC test and EMG from the physical and virtual lifting tasks.

### **4.3.3 Results**

#### **4.3.3.1 Adjusting factors**

No participants could reach the threshold for virtual lifting without adjusting the threshold, Figure 4-8 shows the average of AF under different virtual lifting scenarios (weight × action).

The average AF decreased as the virtual weight increased (Figure 4-8). In other words, as the virtual lifting weight increased, the EMG threshold for a successful virtual lift also increased, which was likely more difficult for participants to complete a successful lift and therefore the thresholds were scaled down with a smaller AF value.

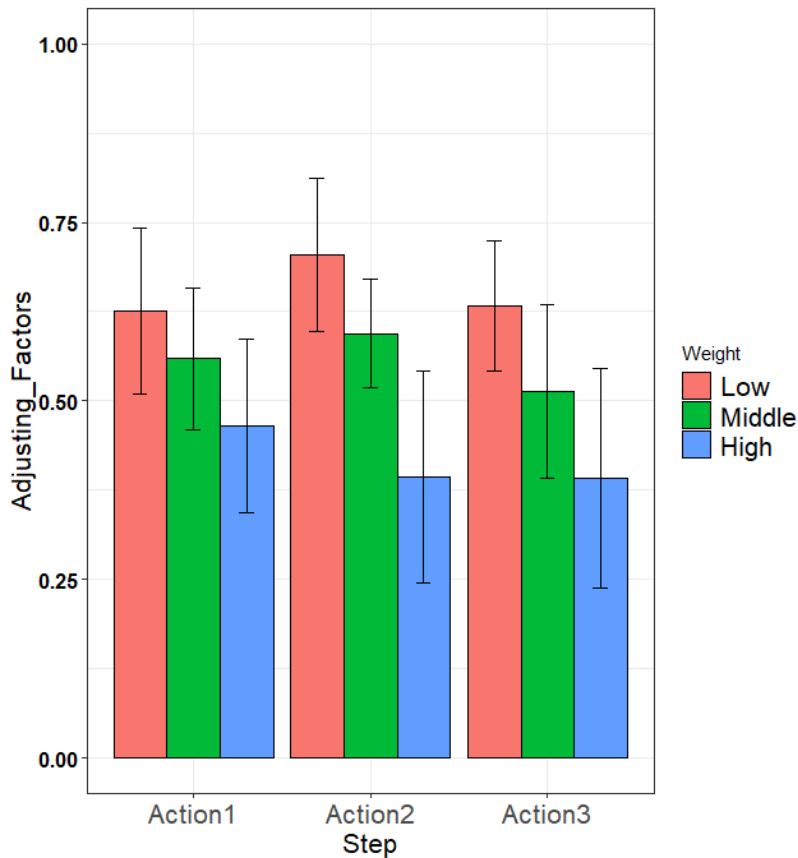


**Figure 4-8** Mean of adjusting factors at each of the three phases of lifting.

#### 4.3.3.2 Mean of Normalized EMG (nEMG)

The maximum amplitude (peak value) in each trial was normalized with respect to the MVC tests, which yielded the normalized EMG (nEMG) values reported in the results. Figure 4-9 shows the nEMG of the left upper trapezius in different scenarios. A nEMG value greater than

1 indicated that the muscle activity acquired during the lifting tasks were greater than those collected during the MVC test.

Since AFs were applied to enable successful virtual lifts, conducting a  $2 \times 3$  ANOVA on nEMG would be comparing a scaled-down nEMG in VR to the original nEMG in the physical environment. Thus, objective comparisons were performed instead: (1) In a physical lift, nEMG increased as weight increased, while in virtual lift, there was no such trend; (2) in most cases, nEMG in physical lift was greater than the respective virtual lift.

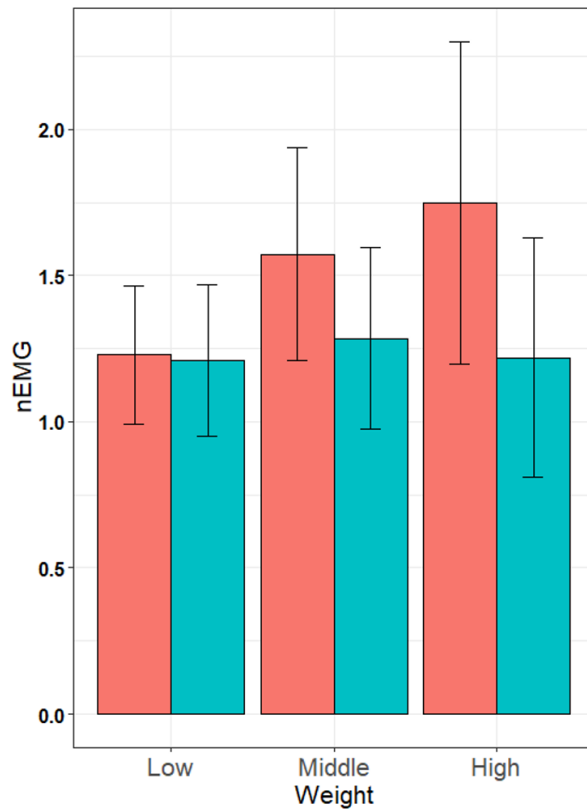


**Figure 4-9** Mean nEMG of left upper trapezius by weight and environment.

### 4.3.3.3 NASA-TLX

A one-way repeated ANOVA was conducted to compare the workload between virtual and physical lifting tasks. The mental demand ( $F(1,8)=24.33$ ,  $p=0.001$ ) was significant and the physical demand ( $F(1,8)=4.30$ ,  $p=0.07$ ) was marginally significant (Figure 4-10). All other domains were not significantly different.

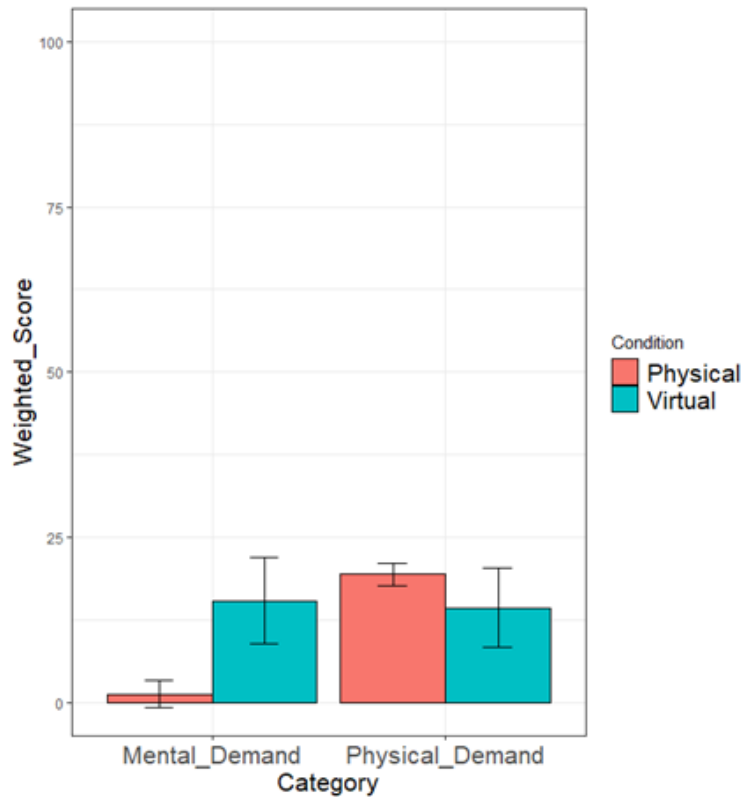


**Figure 4-10** Mean NASA-TLX response for physical lift and virtual lift.

### 4.3.4 Discussion and conclusions

The aim of this study was to assess human muscle activity in terms of EMG in physical and virtual whole-body lifting tasks when virtual exertion method was applied. Participant muscle activity (nEMG) and workload in physical and virtual simulated patient lifting tasks were measured.

Compared to common VR applications where users interact with virtual objects with input device like tactile gloves and controllers, this study used forceful exertion as a requirement for interacting with virtual objects to encourage users to actively contract their muscles, which is required in the physical environment.

The threshold for lifting was scaled down via AF for all participants in the CAVE. The AF was introduced to modify the virtual weights because (1) the weights in the physical calibration were very high (100 lb to 200 lb) and (2) the passive contractile element in the muscles might not be recruited and thus the level of exertion in the virtual environment may be lower than the physical environment. Comparing to Chen et al., they examined weights at or below 10 lb and did not use AF to facilitate participants to “lift” the virtual dumbbell (K. B. Chen et al., 2015). As suggested in Figure 4-8, the mean of AF decreased as the virtual weights increased (ultimately lowering the lifting threshold), which explained the need for AF to accommodate the higher EMG threshold and thereby enable participants to ‘lift’ heavier virtual patients.

In physical lifting task, nEMG increased as the weight of load increased, which was consistent with the literature (K. B. Chen et al., 2015; Radwin et al., 2013). As the load increased, participants needed to exhibit greater muscle contraction to yield higher EMG values. However, in the virtual lifting task, nEMG stayed nearly constant. A plausible explanation was due to the levels of the weight that were employed in this experiment being very high. In the physical environment, a person contracts several muscle groups to overcome a resistive load in the hand. This physical resistive load not only stabilizes a joint by balancing the agonist-antagonist muscle pair (e.g., biceps and triceps work together to flex and extend the arm), the resistive load also works as a counterweight to yield more passive contraction in the muscles. Thus, to lift an object that was more than 100 lb, participants’ muscles needed to produce greater passive contractile

forces. However, in a virtual scenario it was difficult for the participants to contract their muscles to reach the same EMG level through passive contraction (participants only actively contracted as the passive contractile elements were not as involved since there were no resistive loads). In addition, the use of AF lowered the EMG threshold and participants did not contract muscles to the same level as in the physical lift.

The MVC test employed in this study was a possible source of limitation. The mean nEMG of the left upper trapezius during all lifts was greater than 1, which suggested that participants experienced greater muscle contraction during the lifts than the MVC test. Since the MVC test was performed statically on the dynamometer, it may be more appropriate to consider dynamic lifting tasks to obtain the MVC or identify other approach to normalize EMG values.

The NASA-TLX revealed that participants perceived the physical lifts to be more physical demanding. This was expected because lifting a heavy object of 100 lb (co-lifted with the experimenter for calibration) was physical demanding. As of the virtual lifting task, the introduction of AF lowered the virtual lifting EMG threshold and therefore participants were not required to exert the same physical efforts. While in the virtual lift, participants perceived it to be more mentally demanding because they needed to see and carefully maneuver the virtual patient, and at the same time they were consciously exerting to intentionally increase EMG.

This research utilized the method of virtual exertions to successfully guide participants to perform a whole-body physical task in VR as they performed in physical world. It was found that after scaling down the EMG threshold, participants successfully lifted the virtual patients. While participants felt more physical demand for the physical lift, they experienced more mental demand during the virtual lift. Currently, the lifting EMG threshold checking algorithm was simple: *all* muscles need to reach the threshold, which did not accurately reflect the muscles' contributions

and coordination in the whole-body lifting task. The proposed future effort is to build a model that can estimate the exertion output (object weight or force) based on muscle EMG values. Some researchers used linear regression to predict the hand grip force based on forearm muscles (Hoozemans & Van Dieën, 2005), it was based on a static grip and limited to forearm muscles' contributions. It would be more complex to predict whole-body movement and exertion solely with EMG. In addition, the weight of the physical lift is too high, and AFs are needed for all trials, which may affect the comparisons between physical lift and virtual lift.

#### **4.4 Summary**

This study extended the concept of virtual exertions to a more complex task that involved muscles across the whole body. Principal component analysis (PCA) was firstly used to extract major contributing muscles during the task, the selected muscles were then studied in the virtual task. For this study, the criteria of virtual exertions for multi-EMG were relatively simple: all muscles need to reach their respective calibration threshold, the controller needs to collide with the virtual objects. The multi-binary criterion extends the single-binary criterion to more complicated muscles that integrate more muscles.

However, there were several limitations for this study: 1) multi-binary criterion did not reflect the real relationship between each muscle and did not consider the coordination between muscles, more accurate multi-EMG-force modelling is required to set up new criterion; 2) The weight/load for this task is too high, and it is hard for the participants to virtually contract their muscles to the calibration threshold, common physical tasks that involve less weight need to be further studied; 3) There lacked evidence to verify that the movements in VR are the same as that of physical world and participants experience the same level of exertions; 4) From the perspective

of psychophysics, there should be a tolerable interval for the new proposed multi-EMG-force model, as there is a threshold for people to perceive the different of weights or force. For instance, people might perceive the load of 5 N and 4.9 N to be same exertions, so if the predicted force from multi-EMG-force modelling is 4.9 N while the real force is 5 N, it is in the range of tolerable interval. To address these limitations, the methods of EMG based movement classification and force prediction to set up new criteria for virtual exertions is explored in Chapter 5.

## **Chapter 5 Effects of EMG feedback for generalized gross movements in VR system**

### **5.1 Motivation**

To accommodate the limitations summarized in the previous study, this chapter discusses several extended experiments to improve the concept of virtual exertions. Firstly, one experiment was conducted to examine human's just noticeable difference (JND) for weight perception, which provided psychophysical measure to evaluate EMG-force modelling. Secondly, four common manual material handling (MMH) movements (pulling, pushing, and squat lifting and stoop lifting) that involved muscles across the whole body were studied in a physical environment, the EMG data could be utilized to classify the MMH movements. Finally, a virtual lifting task was designed in VR, and the concept of virtual exertions were further evaluated and examined with new criteria.

### **5.2 Examine human's just noticeable differences (JND) for weight perception**

This section is adapted from one co-authored paper (K. Chen & Chen, 2021a).

#### **5.2.1 Introduction**

Manual material handling (MMH) of loads and carrying of loads is common in the workplace and even in everyday life (Ramadan et al., 2018). While objective measures, such as trunk load, muscle electromyography (EMG) have been analyzed to evaluate the risks of MMH, some studies utilized subjective methods such as rated perceived exertions, perceived weight to evaluate the workload and fatigue (Ahmad & Kim, 2018). However, human's perception of weight is not always accurate, which can influence people's decisions on lifting heavy objects and lead to potential risks (Amazeen, 2014). On the other hand, this inaccuracy can also have positive

prospects, as the therapists can increase the load and effort needed for therapeutic exercises and rehabilitation tasks without being noticed by the patients (Allin et al., 2002).

There are two general types of errors when estimating the weight of an object. The first one arises when an object is perceived to be heavier or lighter than an object of the same weight, which is termed “weight illusion” (Buckingham, 2014a). The most commonly studied factor associated with weight illusion is the object size: smaller objects are perceived to be heavier than larger objects of the same weight (Flanagan & Beltzner, 2000; Plaisier & Smeets, 2012). This size weight illusion phenomenon can be generalized for studying other related factors, such as material weight illusion (Buckingham et al., 2011; Flanagan & Beltzner, 2000) and temperature weight illusion (Kuhnz-Buschbeck & Hagenkamp, 2020). Material weight illusion is induced by the surface material of the objects, objects that demonstrate heavy material appearances, such as metal, will feel lighter than objects having light material appearances even though they are actually the same (Buckingham et al., 2009). Temperature weight illusion happens when the temperature of the objects affect people’s perception of the object weights, where people perceived the same item to be heavier at cold temperature than room temperature (Buckingham, 2014b). Another type of perceptual error occurs when two objects of different weights are perceived to be the same weight as there is a threshold, or just noticeable difference (JND), for people to discriminate two weights (Brodie & Ross, 1984; Jones, 1986). In this case, the appearances of the objects are identical while the weights are different. Weber proposed that the JND was proportional to the original weight, (e.g., JND is 0.1g for weight of 10 g, then JND is 0.5 g for weight of 50 g) while Fechner assumed the JND was fixed across all weights and a logarithmic relationship was proposed (Ekman, 1959). Both of these two assumptions were later questioned and new models were proposed (Masin et al., 2009).

While many studies have been conducted to investigate weight illusions and JND for hand haptic perceptions, most of them restrained the participants to a fixed position, either by instructing the participants to lift weighted boxes in situ (Amazeen, 2014) or tied the forearm of participants to a dynamometer (Allin et al., 2002). There has been little literature in studying weight perceptions during dynamic daily movements, which may have greater practical meaning.

Walking while holding weighted objects is a common daily task that can be seen in activities like moving boxes, carrying shopping bags (Ramadan et al., 2018). Some studies found that daily walking with hand held loads could pose increasing load on low back and cause spinal disorders (Fowler et al., 2006; Park et al., 2014). Other studies investigated the influence of carrying shopping bag on walking and proposed techniques including bags' holder or two-hands carrying (Ramadan et al., 2018). While these studies analyzed trunk loadings and subjective discomfort ratings, few of them evaluated the influence of walking on perception of weighted objects. As weight perception is a subjective measure that is influenced by many factors (size, material, temperature, etc.), it was hypothesized that being in motion can affect the perception of object weight.

The purpose of this study was to investigate the influence of standing and walking on weight perception. In addition to the traditional stationary weight perception task, a task of walking while carrying a box was introduced. In specific, this study focused on the second type of perceptual errors, so the appearances of all boxes were controlled to be the same. The JND for weight perception between standing position and walking condition was compared. Weber-Fechner law for weight perception was evaluated.

## **5.2.2 Methods**

### **5.2.2.1 Participants**

A total of ten participants (8 males, 2 females) with ages 24 - 38 years (mean = 27.7, SD = 3.9) were recruited for the study with informed consent approved by North Carolina State University's Institutional Review Board approval. All participants reported no physical injuries or surgeries within last three months.

### **5.2.2.2 Apparatus**

A total of 24 identical cardboard boxes were employed to deliver the weight stimuli to the participants. All boxes were of the same size (length = 15 inches, width = 10 inches, height = 12 inches) with three weight groups: 4 lb, 8 lb, and 12 lb. An earlier pilot experimental session revealed that 20 lb load would result in participant fatigue, and therefore the three weights groups were selected to prevent fatigue. Each group had one reference box and seven experimental boxes. Weight ratio (calculated by dividing each box's weight by the reference box weight) was set from 0.85 to 1.15 with incremental = 0.05. The range of weight ratio was also informed by the lab's earlier pilot session. Specifically, for the 4 lb weight group, seven boxes were used to create an array of weights that ranged from 3.4 lb to 4.6 lb in 0.2 lb increments. For the 8 lb group, seven boxes were used to create an array of weights that ranged from 6.8 lb to 9.2 lb in 0.4 lb increments. For the 12 lb group, seven boxes were used to create an array of weights that ranged from 10.2 lb to 13.8 lb in 0.6 lb increments. The boxes were placed on a table and had no identifying markers except for the three reference boxes (4lb, 8 lb, and 12 lb).

### 5.2.2.3 Procedure

Upon arrival at lab, participants were instructed with proper manual material handling techniques, including: maintain a good grip and keep the boxes close to body (Amazeen, 2014). Next, participants were given practice trials to walk and carry a box until they became confident about the experimental task. Afterwards, participants were familiarized with rated perceived exertion (RPE) survey in Borg-10 scale (Borg, 1998).

Firstly, the participants were instructed to stand in front of the table and lift the boxes to their waist height and place them back onto the table. Each trial comprised of two lifts, the participant first lifted the reference box and gave a RPE score for the reference lift. The participant randomly lifted the other box in the same weight group and place it back, and next the participant was asked whether these two boxes were of the same weight. A response of “yes” indicated that they perceived the weight difference and a response of “no” indicated that they did not perceive the weight difference, and finally the participant verbally gave a RPE score for the second lift. Each run consisted of 21 comparisons (3 weight groups  $\times$  7 comparisons per group) and 42 lifts. Short breaks were provided to ensure the participants did not feel fatigue and could be extended if required. Then the participants completed the NASA-TLX (NASA, 1986) and had a rest.

Secondly, the participant was instructed to carry a box from the table and walk along the metal plates of the lab. Participant was guided to walk to the end of the metal plates and turned back, walk towards the table, and place the box back onto the table. Afterwards, participants were verbally asked to perform the same weight discrimination task and gave RPE scores, respectively. The positions of boxes in each group were reset before the walk-carrying task. Longer breaks were provided between two consecutive comparison tasks. In the end, the participants completed the

NASA-TLX and had a rest. The total experiment tool about 1.5 hours. Figure 5-1 below depicts the experiment configuration.

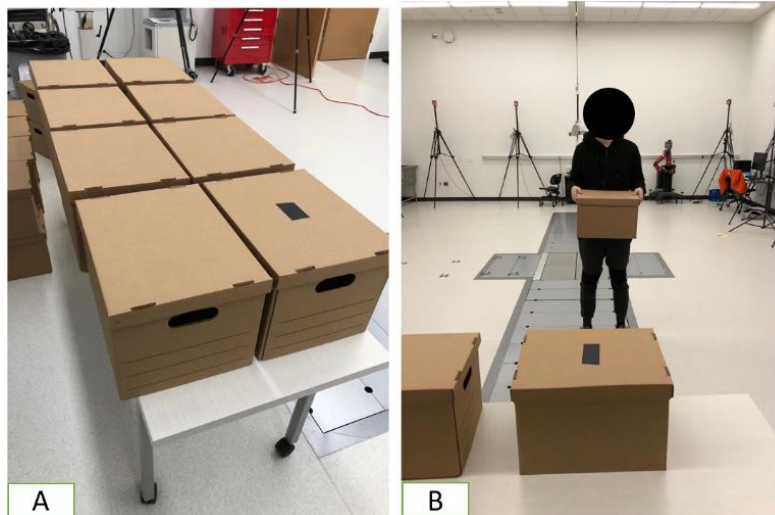


**Figure 5-1** Experiment setup. (A) Eight boxes in one weight group, the reference box was marked with a black tape. (B) A participant carried the box back to the table.

#### 5.2.2.4 Variables and Analysis

The independent variables in this experiment included task type (standing and walking), weight ratio (from 0.85 to 1.15), and box weight groups (4 lb, 8 lb, and 12 lb). The dependent variables were probability of detecting the difference, just noticeable differences (JND), RPE scores and NASA-TLX scores.

For this study, probability of detecting the difference was calculated by taking the number of yes responses divided by total number of responses. JND was calculated at 50% level as it is a common level used in psychophysics (Booth & Freeman, 1993), which means the weight ratio difference at which people had a 50% chance of detecting the weight differences. RPE score was normalized to the RPE score captured when lifting the reference weights, thus normalized RPE (nRPE) was calculated.

A polynomial logistic regression model was built to relate the probability of detection and weight ratio. A linear regression model was built to study the effects of weight ratio on nRPE. A two-sample t-test was used to evaluate participants' workload under different conditions by NASA-TLX. Significance level was set at  $\alpha = 0.05$  for all the analysis.

### **5.2.3 Results**

#### **5.2.3.1 Probability of detection**

The polynomial logistics regression (Figure 5-2 and Figure 5-3) revealed there was a statistically significant effect of weight ratio on probability of perceiving the differences, quadratic coefficient  $b_2 = 121.89$  ( $\chi^2(1) = 67.28, p < 0.001$ ) and  $b_1 = -0.83$  ( $\chi^2(1) = 0.38, p = 0.54$ ). Weight group also showed a significant effect on probability of difference detection ( $\chi^2(1) = 6.23, p = 0.013$ ). Task type did not induce a statistically significant effect on probability of detection ( $\chi^2(1) = 2.23, p = 0.14$ ).

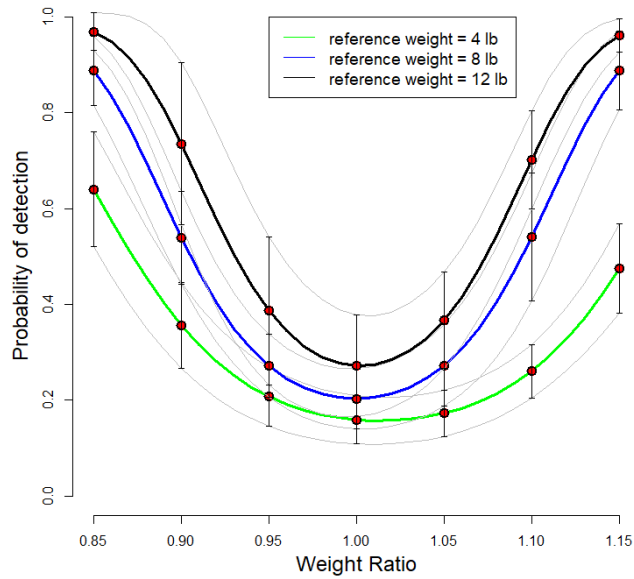


**Figure 5-2** Polynomial logistics regression models depict the relationship between probability of detection and weight ratio at three different weight levels. The error bars are also  $\pm 1$ S.E. at the experimental weight ratios. The gray lines represent the  $\pm 1$ S.E. of the respective logistics regression model.

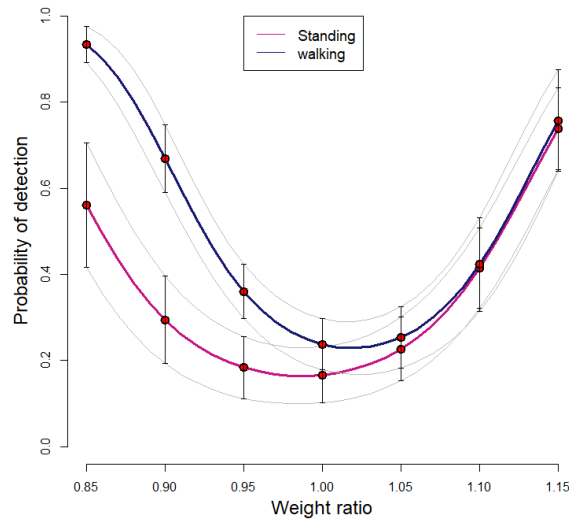


**Figure 5-3** Polynomial logistics regression models depict the relationship between probability of detection and weight ratio at two different task conditions. The error bars are also  $\pm 1$ S.E. at the experimental weight ratios. The gray lines represent the  $\pm 1$ S.E. of the respective logistics regression model.

### **5.2.3.2 Just Noticeable differences**

Polynomial logistics regression revealed that 50% JND for 4 lb weight group was at weight ratio = 0.873 and weight ratio = 1.154; 50% JND for 8 lb weight group was at weight ratio = 0.905 and weight ratio = 1.094; 50% JND for 12 lb group is at weight ratio = 0.931 and weight ratio = 1.073. The model also revealed that 50% JND for standing condition was at weight ratio = 0.872 and weight ratio = 1.106; 50% JND for walking condition is at weight ratio = 0.929 and weight ratio = 1.109.

Accordingly, 50% JND by weight was at 3.49 lb and 4.62 lb for 4 lb group; 50% JND was at 7.24 lb and 8.75 lb for 8 lb group; 50% JND was at 11.17 lb and 12.88 lb for 12 lb group.

### **5.2.3.3 nRPE**

The linear regression model (Figure 5-4) revealed that weight ratio is a significant indicator of nRPE ( $F(1,418) = 357.8, p < 0.001$ ).

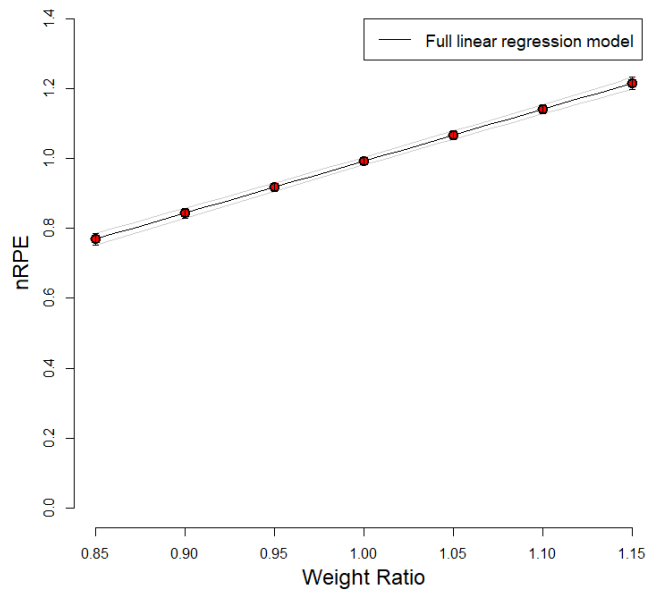


**Figure 5-4** Linear regression model on nRPE across different weight ratios. The error bars are also  $\pm 1$ S.E at the experimental weight ratios. the gray lines represent the  $\pm 1$ S.E. of the respective logistics regression model.

### 5.2.3.4 NASA-TLX

Two-sample t-test indicated that participants' physical demand ( $t(18) = 3.67, p = 0.001$ ) and efforts ( $t(18) = 3.34, p = 0.002$ ) were significantly higher during walking condition as illustrated in Figure 5-5.

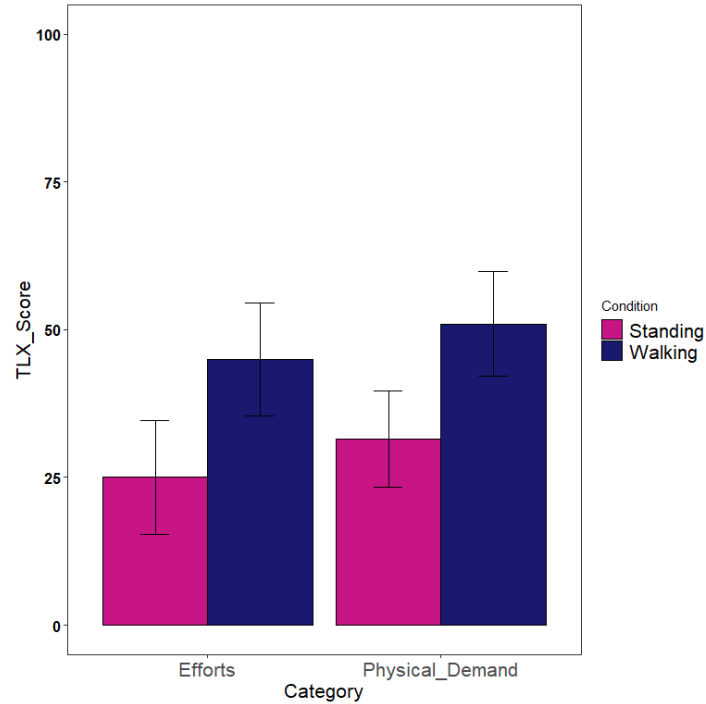


**Figure 5-5** Mean of NASA-TLX scores for walking and standing condition.

## 5.2.4 Discussion

This study evaluated human weight perceptions during different conditions. Earlier studies have examined the perception of weight in stationary postures, yet various jobs actually require moving and carrying of loads. In specific, effects of weight ratio, weight level and walking were studied on human probability of detecting weight differences. The results demonstrated that weight ratio and weight level had significant influences on probability of detection, normalized rated perceived exertion was significantly related with weight ratio, participants' physical demand and efforts were significantly higher during walking condition.

Weight ratio had a statistically significant effect on probability of detection, which is plausible, as the weight ratio deviates more from the unity weight ratio = 1, the difference between reference box weight and task box weight increased, and it was easier for participants to perceive

the discrepancy (K. B. Chen et al., 2016). Given that participants showed lower detection probability at weight ratio near to the unity weight ratio, it was possible that the therapist could increase the loads of rehabilitation task slightly while without being noticed by the patients (Allin et al., 2002).

Weight group indicated a statistically significant effect on participants' probability of weight differences detection ( $\chi^2(1) = 6.23, p = 0.013$ ), with 12 lb weight group showed highest detection probability and 4 lb weight group showed lowest detection probability. Weber's law stated that JND is proportional to the initial stimuli and relative discrimination sensitivity is constant across different stimuli intensity (Ekman, 1959), such that JND is 1 g for 100 g object and 2 g for 200 g object. According to Weber's law, at the same weight ratio, participants should have the same probability of detecting a difference across three weight levels, which did not hold for this study, as participants had higher detection probability at higher weight levels. JND by weight was at 3.49 lb and 4.62 lb for 4 lb group; JND was at 7.24 lb and 8.75 lb for 8 lb group; JND was at 11.17 lb and 12.88 lb for 12 lb group, which revealed that JND is approximately between 0.6 lb and 0.8 lb across three weight levels, and thus this finding was more aligned with Fechner's assumptions that all JNDs were equal ("Weber-Fechner Law," 2005).

Walking did not induce a significant higher detection probability compared to standing and lifting ( $\chi^2(1) = 2.23, p = 0.14$ ). However, it can be seen from Figure 5-3 that walking and carrying showed higher detection probability when weight ratio  $< 1$ , which could be due to the fact that walking and carrying a box is a physically demanding task (can be seen from the NASA-TLX results), thus it was easier for participants to detect the alleviated differences when the second boxes were lighter compared to the reference box.

To accommodate perception discrepancies of different participants, the term nRPE was utilized, which showed relative exertions compared to the exertions caused by lifting the reference box, the results showed that nRPE was linearly related with weight ratio, in addition, using nRPE centered the RPE scores and lowered original RPE variances. NASA-TLX revealed that participants experienced significant higher physical demand and exerted more efforts during walking and carrying task, and more attention need to be paid to walking and carrying tasks.

One limitation of this study is the number of participants was relatively small ( $n = 10$ ) due to recruitment challenges. The study can be further expanded with other postures and weight ranges to validate the JND in weight perception. Another limitation was the weight ratio gap between boxes, to avoid participants getting fatigue during the experiment, the design of weight ratio incremental = 0.05 was adopted, more closely compacted weight incremental shall be used to accurately depict the detection probability – weight ratio curve.

This experiment showed that RPE was a good indicator of lifting load, and it could be a proper criterion to evaluate participants' perceived exertions from the perspective of psychophysics. When informing participants to perform virtual tasks, RPE can be utilized to determine whether the participants underwent same level of exertions.

## **5.3 Examine EMG based classification for manual material handling tasks**

### **5.3.1 Introduction**

EMG has been widely utilized in human movement classification and force prediction, which can facilitate prosthesis control and ergonomics evaluation (Hoozemans & Van Dieën, 2005; Sapsanis et al., 2013). By attaching EMG sensors to the skin of individuals, researchers

acquire abundant muscular activation information from the EMG signal to which various machine learning methods could be applied for gesture recognition (Khokhar et al., 2010; Martinez et al., 2020).

The details of EMG based movement classification and regression have been summarized in Chapter 2. Previous studies on EMG classification focused on hand gesture recognition using different classifiers where the target muscles were usually forearm muscles. However, little attention was paid to the classification of full-body, gross motor movements that involves muscles across the whole body, which is a generalization of conventional localized hand gesture classification. Manual material handling (MMH) tasks involve muscles from upper limb, trunk and lower body, which make them suitable for this study. Besides, conventional research on EMG-based hand gesture classification usually studied static hand posture with no external loads on hand or constant loads (Atzori et al., 2015), while classifiers' performance under varied conditions (load, position) has not been commonly studied.

The purpose of this study was to explore the potential of classifying MMH movements using EMG signal from muscles across the entire body. In specific, four common MMH posture/movements were selected: squat lifting, stoop lifting, push and pull. Two experiments were conducted in the lab: Experiment I focused on classification of static MMH posture and Experiment II focused on classification of dynamic MMH movements with varied load and position. This study had practical meanings: (1) MMH professionals and novices can be differentiated via EMG classification, which could give insights on training program for MMH practitioners, even if the two groups of population performed the same MMH movement visually, their muscle activation patterns might be different; (2) Full-body movement classification can be

integrated into EMG-driven human-machine interface, which may be implemented in virtual reality guided MMH training program.

### **5.3.2 Methods**

#### **5.3.2.1 Participants**

Female was less involved in the MMH tasks and only 21.6% of material moving jobs were occupied by women in 2021 (Firouzabadi et al., 2021; U.S. Bureau of Labor Statistics, 2021), thus only male participants were recruited for this study. Three participants (26 - 31 years old, mean = 28) were recruited for Experiment I and 12 participants (20 – 31 years old, mean = 25.3) were recruited for Experiment II. Informed consent, approved by North Carolina State University's Institutional Review Board, was obtained from each participant. All participants reported no physical injuries or surgeries within last three months.

#### **5.3.2.2 Apparatus**

Nine cardboard boxes of identical appearance were used to deliver different loads to the participants. All boxes were of the same size (length = 15 inches, width = 10 inches, height = 12 inches) with three weight groups: Group A included three boxes that weighed 7 lb., 8lb., and 9 lb.; Group B included three boxes that weighed 11lb., 12lb., and 13 lb.; Group C included boxes that weighed 15 lb, 16 lb, and 17lb. A steel shelf consisting of three heights (20 inches, 35 inches, and 50 inches above the floor) was used to produce different lifting weights, which corresponded to knee height, waist height and shoulder height, respectively. A handcart (handle bar at 35 inches above the floor) was used for pushing and pulling tasks. A set of 14-channel wireless EMG sensors (Trigno, Delesys Inc, Natick, MA) were used to record participants' muscle activity during the MMH tasks.

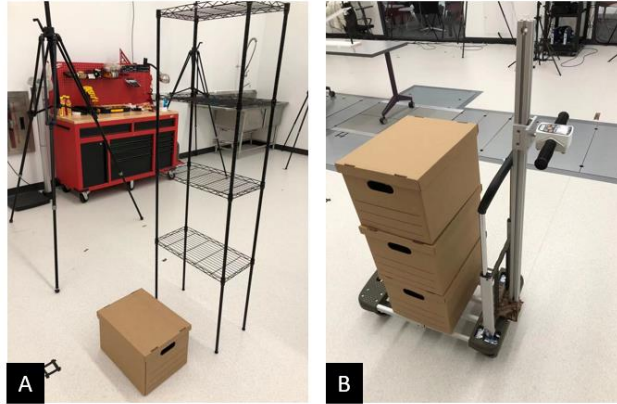


**Figure 5-6** (A) The metal shelf with three levels; (B) The handcart loaded with boxes.

### 5.3.2.3 Procedures

Upon arrival at lab, participants were instructed with proper manual material handling techniques, which included: get a secure grip; avoid jerking by performing smooth, even motions, keep the loads close to the body, etc. (NIOSH & CDC, 2007). Next, participants were given two practice trials to do squat lifting and stoop lifting, pull, and push the loaded handcart to make them familiar with the experimental task, the number of practice trials were increased if the participants did not perform the movements correctly.

Next, the participants were prepped for attaching EMG sensors. A set of 14 EMG sensors (Trigno, Delsys Inc, Natick, MA) were placed on the bilateral muscles across the body (Figure 5-7), which included middle deltoid (MD), biceps (BI), flexor carpi radialis (FCR), latissimus dorsi (LD), lumbar erector spinae (LES), biceps femoris (BF), and gastrocnemius (GA).

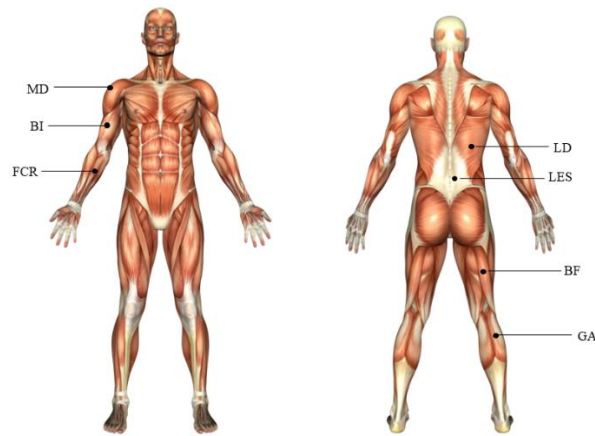


**Figure 5-7** Locations of EMG sensors across the bilateral muscles, figure adapted from (Trigno, Delesys Inc, MA).

For Experiment I, the three participants were guided to perform eight rounds of MMH tasks. In each round, the participant would first push the handcart loaded with boxes from the Group A (7 lb, 8 lb, and 9 lb) and walk 15 ft, which aimed to acquire abundant EMG data for pushing and pulling. The participant then squat-lifted the 8 lb box slightly above the floor (about 2 inches) and maintained the squat posture for 5 s, afterwards he was informed by the experimenter to relax. Next, the participant stoop-lifted the 8 lb. box slightly above the floor and maintained the stoop posture for 5 s. Finally, the participant would pull the handcart (loaded with all boxes from the Group A) backwards and returned to the starting location. A 30-second rest was provided between each posture and a 2-minute break was provided between each round. The rest time could be extended upon request of the participants. The whole experiment took about one hour.

While Experiment I consisted of static lifting postures and constant loads, Experiment II involved dynamic lifting movements with varied loads and lifting heights. Experiment II consisted of six rounds, which were two lifting movements  $\times$  three box groups. In each round, the twelve participants were instructed to use only one lifting technique (either squat or stoop). The participant would first push the handcart (loaded with boxes from one group) for 15 ft and then completed

nine (three heights  $\times$  three boxes) lifting movements (squat or stoop, from floor to the shelf) and nine lowering movements (squat or stoop, from the shelf to the floor). Finally, the participants would pull the handcart (loaded with boxes from the same group) back to the start position. The participants were instructed to keep a constant speed when performing the tasks. The protocol for resting was the same with Experiment I. The whole experiment took about two hours.

To avoid inducing muscle fatigue to the participants, the experimenter helped place the boxes and handcart in the ready positions and kept asking the participants about their status throughout the experiments.



**Figure 5-8** Participant performed a series of MMH movements: 1. Push the loaded handcart; 2. Pull the loaded handcart; 3. Squat lift the box; 4. Stoop lift the box. To note, the number/label of the movements were not the actual sequence of the tasks. The participants performed the tasks in the following sequence: 1 - 3 - 4 - 2.

#### 5.3.2.4 Data Processing and Analysis

Raw EMG data were collected in the EMGworks software (Delsys Incorporated, Natick, MA) and exported into MATLAB (MATLAB 2021a, MathWorks, Natick, MA) for analysis. For each EMG recording, only the middle 80% of the data were extracted: (1) The early stage and final stage were less informative limited to system delay and participant's reaction time (Saeed et al., 2021; Too et al., 2019); (2) The data at the initial and final stages were in a transition stage as the

participants switched between MMH movements and resting status, which posed increasing risks of classification errors. For each muscle, the EMG signal was filtered with a 4<sup>th</sup> order Butterworth filter at cutoff frequencies 10-500 Hz (Chopp et al., 2010). An overlapping window technique (Sapsanis et al., 2013) was applied on the filtered EMG with time window of 200ms and incremental length of 100 ms (Smith et al., 2011; Spiewak, 2018), and the EMG features were calculated for the sliding windows. Currently there are no golden rules as how many EMG features and what EMG features could facilitate best classification performance, this study selected five common EMG features that had been frequently used in previous studies: Mean Absolute Value (MAV), Waveform Length (WL), Zero Crossings (ZC) , Mean Frequency (MNF) and Median Frequency (MDF) (Toledo-Pérez et al., 2019). As such, a seventy-dimensional (14 muscles  $\times$  5 features) feature matrix was built for each movement/posture. In contrast to the raw EMG feature sets, normalized EMG feature sets were built with time domain features (MAV, WL and ZC) normalized to the respective peak value during the task and frequency features (MNF and MDF) normalized to the sampling frequency. The movement/posture was then labeled for each EMG recording as can be seen in Table 5-1.

**Table 5-1** Movement/posture decoding number.

Movement/Posture	Label number
Push	1
Pull	2
Squat	3
Stoop	4

For movement classification, three common classifiers were selected: Support Vector Machines (SVM), linear discriminant analysis (LDA) and k-Nearest Neighbor (kNN). A polynomial kernel was chosen for the SVM as it showed higher accuracies in the preliminary study. Classification accuracy (CA) is a widely used metric in EMG classification studies (Gu et al., 2018; Krasoulis et al., 2017), and there CA is adopted to evaluate classification performance in this study. The classification performance was evaluated in two ways. For intra-participant evaluation, the training data and testing data were from the same participant and a 10-fold cross-validation was applied for all participants. For inter-participant evaluation, the training data and the testing data were from different participants, and the leave-one-participant-out cross-validation was used to evaluate the classification performance.

$$CA = \frac{\text{Number of correct predictions}}{\text{Number of all predictions}} \times 100\%$$

### 5.3.3 Results

#### 5.3.3.1 Results from Experiment I

The results for intra-participant and inter-participant posture classifications are presented in Table 5-2 and Table 5-3, respectively.

**Table 5-2** Results of intra-participant classification from Experiment I (static lifting postures). LDA = linear discriminant analysis; kNN = k-nearest neighbor; SVM = support vector machine.

Participant	Classification accuracy					
	Raw feature sets			Normalized feature sets		
	LDA	kNN	SVM	LDA	kNN	SVM
P1	0.884	0.947	0.873	0.967	0.983	0.994
P2	0.937	0.982	0.98	0.989	0.996	0.996
P3	0.949	0.966	0.974	0.993	0.997	0.996
Mean	0.923	0.965	0.942	0.983	0.992	0.995

**Table 5-3** Results of inter-participant classification from Experiment I (static lifting postures). LDA = linear discriminant analysis; kNN = k-nearest neighbor; SVM = support vector machine.

Participant	Classification accuracy					
	Raw feature sets			Normalized feature sets		
	LDA	kNN	SVM	LDA	kNN	SVM
P1	0.603	0.566	0.485	0.356	0.564	0.613
P2	0.707	0.653	0.589	0.668	0.577	0.569
P3	0.4	0.318	0.562	0.498	0.535	0.517
Mean	0.57	0.512	0.545	0.507	0.559	0.566

### 5.3.3.2 Results from Experiment II

The results for intra-participant movement classification are presented in Table 5-4, it shows that SVM with normalized feature sets produces highest average classification accuracy. Thus, confusion matrix for SVM classifier with normalized feature sets is presented in Table 5-5. The results for inter-participant condition are presented in Table 5-6.

**Table 5-4** Results of intra-participant classification for Experiment II (dynamic lifting movements).

Participant	Classification accuracy					
	Raw feature sets			Normalized feature sets		
	LDA	kNN	SVM	LDA	kNN	SVM
P4	0.745	0.821	0.84	0.885	0.901	0.924
P5	0.761	0.813	0.835	0.885	0.931	0.933
P6	0.762	0.854	0.848	0.92	0.926	0.951
P7	0.797	0.864	0.847	0.924	0.921	0.947
P8	0.809	0.87	0.867	0.898	0.923	0.949
P9	0.798	0.843	0.862	0.923	0.919	0.948
P10	0.838	0.902	0.936	0.853	0.791	0.779
P11	0.738	0.838	0.851	0.894	0.914	0.922
P12	0.774	0.834	0.802	0.883	0.901	0.925
P13	0.794	0.856	0.879	0.869	0.886	0.93
P14	0.84	0.94	0.95	0.877	0.835	0.844
P15	0.788	0.821	0.87	0.871	0.893	0.904
Mean	0.787	0.855	0.866	0.89	0.895	0.913

**Table 5-5** Confusion matrix for SVM classifier with normalized feature sets.

		Predicted			
		1	2	3	4
True motion	1	99.6%	0.4%	0	0
	2	0.5%	99.5%	0	0
	3	1.0%	1.0%	87.7%	10.3%
	4	4.3%	2.8%	11.3%	81.6%

**Table 5-6** Results of inter-participant classification for Experiment II (dynamic lifting movements).

Participant	Classification accuracy					
	Raw feature sets			Normalized feature sets		
	LDA	kNN	SVM	LDA	kNN	SVM
P4	0.551	0.501	0.499	0.556	0.531	0.565
P5	0.511	0.506	0.554	0.674	0.55	0.617
P6	0.502	0.479	0.485	0.556	0.499	0.545
P7	0.639	0.524	0.561	0.56	0.505	0.543
P8	0.637	0.529	0.578	0.667	0.538	0.622
P9	0.546	0.467	0.495	0.637	0.547	0.632
P10	0.579	0.489	0.442	0.493	0.321	0.367
P11	0.526	0.473	0.467	0.553	0.447	0.518
P12	0.595	0.41	0.469	0.618	0.551	0.635
P13	0.456	0.494	0.433	0.493	0.512	0.573
P14	0.68	0.559	0.472	0.346	0.303	0.374
P15	0.568	0.446	0.384	0.48	0.49	0.482
Mean	0.566	0.49	0.487	0.553	0.483	0.541

### 5.3.4 Discussion

This study aimed to investigate the potential of classifying MMH posture/movement using EMG signal acquired from the muscles across the whole body. Two experiments were conducted in a laboratory setting, with Experiment I focusing on static posture and Experiment II focusing on dynamic movements. EMG features were extracted on sliding windows of the EMG and normalized to the peak value or the sampling frequency, respectively. Three common machine learning methods were selected as the classifiers. The data sets were split in two ways: for intra-

participant condition, classification performance was evaluated using 10-fold cross-validation; for inter-participant condition, leave-one-participant-out cross-validation was used.

For experiment I, the participants kept a static squat lifting posture and a static stoop posture. The intra-participant condition, the mean accuracies of all classifiers were above 90% (Table 5-2). In specific, normalized EMG feature sets achieved comparatively higher classification accuracy compared to the raw EMG feature sets, this might be that some machine learning methods (e.g. SVM) were sensitive to scaling of the data, thus normalizing the raw feature sets induced higher accuracy. Notably, SVM achieved the highest average accuracy of 99.5% with the normalized feature sets. While for the inter-participant condition, the results from the Table 5-3 showed that mean accuracies were slightly above 50%. This was expected as EMG was highly participant-dependent, which made it increasingly difficult to predict the posture or movement of a new participant from the classifiers that trained with other participants (Totah et al., 2018). Other studies combined all participants' EMG data and then split data into training and testing, which were neither intra-participant nor inter-participant (Adewuyi et al., 2016). Another possible explanation for the low accuracy could be the number of participants. In Experiment I, three participants were recruited, thus the inter-participant modelling split the data in the following format: two participants' EMG data formed training data, and the remaining participant's EMG data served as the testing dataset. Thus, it was likely that the trained model from two participants had relatively low generalizability to the third participant. Consequently, Experiment II recruited 12 participants, which could construct trained models from eleven participants that could have more generalizability.

For Experiment II, the participants performed dynamic squat movements and stoop movements to transfer the loaded box from the floor to the shelf. In specific, the loads of boxes

and lifting height varied while still labeled as “3-squat” and “4-stoop”. The results from the Table 5-4 suggested that for the intra-participant condition, mean accuracies of all classifiers were about 80% to 90%, which was lower compared to that of Experiment I. While Experiment I involved static lifting postures, it was reasonable to assume that the participants’ muscle patterns were consistent during the tasks and could be labelled and classified; as for Experiment II, even though the participants were instructed to perform the tasks in a constant pace, it was possible that the participants’ muscle patterns changed during different phase of the movement, which could lead to decreased overall classification accuracy. Totah et al. (2018) found that EMG-driven load classification achieved highest accuracy occurred around load-onset moment. Similar to Experiment I, normalized EMG feature sets induced higher accuracy for the intra-participant condition, and the SVM classifier reached an average accuracy of 91.3%. The results from the confusion matrix (Table 5-5) suggested that most misclassification occurred between 1 and 2 (push and pull), 3 and 4 (squat and stoop), which was plausible due to the nature of these movements. For the inter-participant condition, the results from the Table 5-6 showed that mean accuracies were about 50%, which was comparable to the results from Experiment I. While the reasons explained for low accuracy in Experiment I also applied here, the increased number of participants did not help improve classification performance in Experiment II, which suggested that the training models from 11 participants had lower prediction ability on the remaining participant.

In summary, the analysis and results from this study suggested that full-body MMH posture and movements could be recognized with multi-EMG classification. In specific, for intra-participant condition, the classifiers could reach average accuracy above 90% for the static posture and about 80% - 90% for the dynamic movement. While for the inter-participant, the average classification accuracy was about 50% for both the static posture classification and dynamic

movement classification. Normalization of EMG features helped to increase classification performance for the intra-participant condition while did not work for the inter-participant condition. This study also gave insights on the future design of EMG-based human machine interface, to achieve better performance, a calibration stage was needed for each user to obtain customized EMG data and models, which could be implemented as customized trigger logic for the specific user.

## **5.4 Examine EMG guided virtual exertions for manual lifting task**

### **5.4.1 Introduction**

As revealed by the results in Section 5.3, EMG classification accuracy was high (approximately 90%) in the intra-participant condition while considerably lower (approximately 50%) in the inter-participant condition, which indicated that EMG signal is highly participant-dependent for the MMH tasks. Consequently, a calibration stage that acquired the actual user's EMG data was necessary to build customized EMG-driven model and interface. The application of a calibration stage was reported in Section 4.3 which aimed to collect participants' EMG data during the physical patient transfer task as reference values in the virtual tasks. However, participants still encountered difficulties in performing the patient transfer task in VR because they needed to voluntarily contract all 12 muscles to the threshold value captured during the calibration (physical) task, which was hard to achieve and did not reflect the contribution and coordination between the target muscles. Compared to the multi-binary model employed in Section 4.3, a regression-based EMG-force model might more accurately depict the relationship between output forces and muscle activities. Some researchers had used regression methods to predict finger force (Baldacchino et al., 2018) and hand grasping force (Hoozemans & Van Dieën, 2005; Hou et al.,

2007). Among these studies, some used simple linear regression methods to predict the output force from EMG amplitude (Hoozemans & Van Dieën, 2005), while others used more complicated regularized regression methods (Martinez et al., 2020). The results from Section 5.3 suggested that different participants have different muscle activities and different regression parameters, thus a calibration stage was needed to obtain the customized parameters and build customized regression models.

The purpose of this study was to design a regression-based multi-EMG program for virtual lifting tasks and validate the practicality of the program through experiments with two healthy participants. The process of design and validation for EMG-assisted system followed a previous study (Meng et al., 2014) where one participant was recruited. This study focused on one common manual material handling task, squat lifting, and comparable squat lifting tasks were designed in the physical world and VR. It was expected that the regression-based multi-EMG interface could evoke similar perceived exertions between the physical lifting tasks and virtual lifting tasks. Findings from this study could give insight on future design of virtual exertion applications.

## **5.4.2 Methods**

### **5.4.2.1 Participants**

Two participants in the lab were recruited for the experiments with Informed consent obtained from the North Carolina State University's Institutional Review Board. The participants reported no physical injuries or surgeries within last three months.

### **5.4.2.2 Apparatus**

Three identical cardboard boxes employed in the previous study (section 5.3) was used to deliver different lifting weights, which weighed 6 lb, 10 lb, and 16 lb. The steel shelf in the

previous study was used to deliver three lifting weights, which were 20 inches, 35 inches and 50 inches that approximately corresponded to knee height, waist height and shoulder height. Ten wireless EMG sensors (Delesys Inc, Natick, MA) were used to record the participants' muscle activity. Trigno Control Utility (Delesys Inc, Natick, MA) was used to acquire the EMG signal in real time, MATLAB (MATLAB 2021b, MathWorks) was used to process the EMG signal in real time. Virtual scenarios were rendered by a game engine (Unity, <https://unity3d.com/>) and presented to the participants via an HMD (Vive, HTC and Valve Corporation). A pair of controllers was used to track the position of virtual hands in VR and interact with virtual objects when participants' muscle activity met the requirements.

#### **5.4.2.3 Experiment design**

The experimental session consisted of a physical lifting task (also the calibration task), and a virtual lifting task. The EMG sensors were affixed to 10 bilateral selected muscle pairs according to Figure 5-9 that covered upper extremity, trunk and lower body. The selected muscles were biceps (BI), flexor carpi radialis (FCR), lumbar erector spinae (LES), biceps femoris (BF), and gastrocnemius (GA).

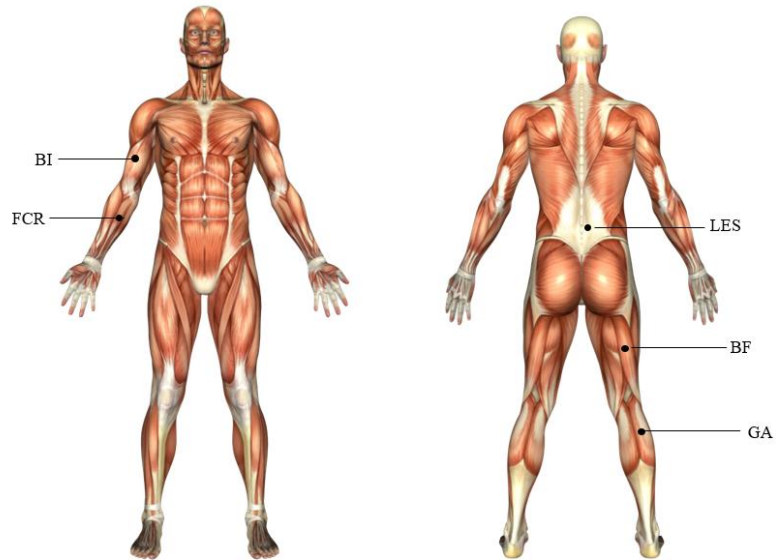


**Figure 5-9** Locations of EMG sensors across the bilateral muscles, figure adapted from (Trigno, Delesys Inc, MA).

The physical lifting task functions as a calibration stage that determines a customized regression model for each participant. The virtual lifting task was the same lifting task but performed in VR against a virtual box and a virtual shelf,

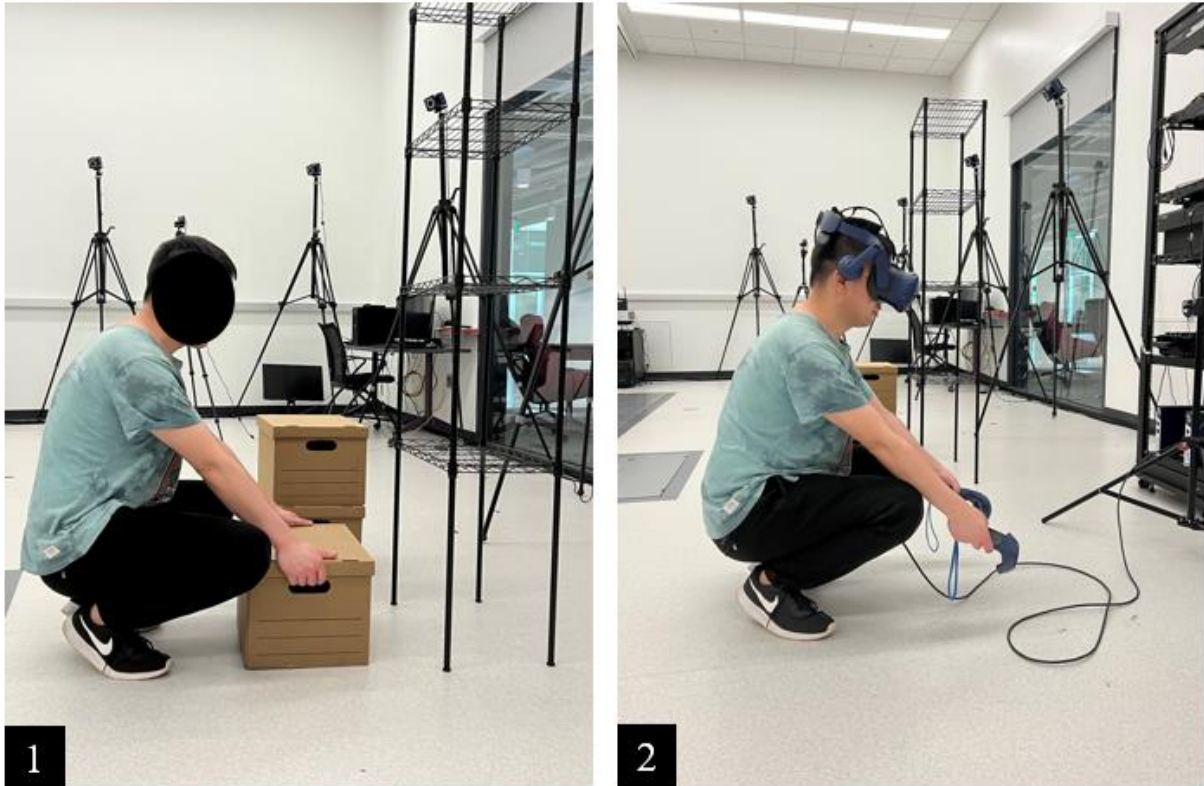


**Figure 5-10** One participant performing a squat lifting task. 1) physical lifting tasks and 2) virtual lifting tasks; The participant saw a virtual box, shelf and text through the HMD, the virtual scene is presented in Figure 5-12.

#### 5.4.2.4 Experiment procedure

*Physical Lifting Task* (calibration task). Participants performed nine squat lifting tasks (three boxes  $\times$  three lifting heights) in the physical world and verbally indicated their rated perceived exertion (RPE) using the Borg-10 scale for each trial. The recorded EMG signal from the 10 muscles were processed to build a multi-EMG based regression model. The EMG processing protocol followed the steps described in Section 5.3, where the raw EMG signal was transformed to EMG features in the moving windows. In this study, only the RMS and the MAV were chosen as these metrics were related with EMG amplitude and muscle force (Jebelli & Lee, 2019). In addition, lifting height was incorporated into the feature matrix, which was an important biomechanical variable for manual lifting tasks (Elfeituri & Taboun, 2002), which formed a

twenty-one-dimensional (ten muscles  $\times$  two EMG features + lifting height) feature matrix. The output of the feature matrix was lifting force, which could be approximately related with the weights of the boxes. For the regression model, lasso (least absolute shrinkage and selection operator) was chosen, which performed both regularization and variable selection to increase the prediction accuracy (Tibshirani, 1997). For simple linear regression, it looks for optimal parameters that minimize the cost function in Equation 5-1. While the cost function of lasso regression in Equation 5-2 adds a penalty term that is sum of the absolute value of the coefficients, which can shrink some coefficients to zero and reduces over-fitting (Ranstam & Cook, 2018). In specific, the parameter lambda denotes the degree of shrinkage and preferred lambda can be obtained through cross-validation.

$$\sum_{i=1}^n (y_i - \sum_j x_{ij}\beta_j)^2 \quad (5-1)$$

$$\sum_{i=1}^n (y_i - \sum_j x_{ij}\beta_j)^2 + \lambda \sum_j |\beta_j| \quad (5-2)$$

After the nine physical squat lifting trials, the participants were guided to have a rest while the researcher processed the participants' EMG data to obtain a customized EMG-lifting weight lasso model. Figure 5-10 shows the process of obtaining optimal lambda for the lasso regression. In this study, lambda at the minimum MSE were chosen as the parameter of lasso regression model for later virtual lifting tasks.

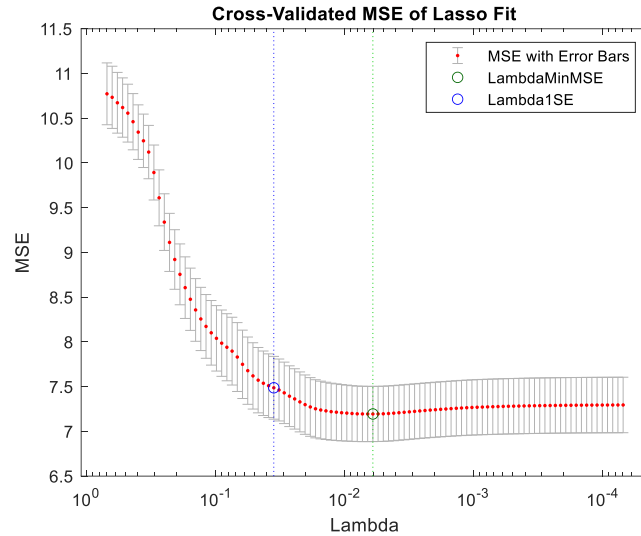


**Figure 5-11** The process of finding optimal lambda with lowest mean squared error (MSE). The green circle located the lambda at minimum cross-validation MSE, and the blue circle located the lambda with minimum cross-validation error plus one standard error. For this study, the lambda that contributed to minimum cross-validation MSE (the green circle) was employed.

*Virtual Lifting Task.* Participants wore the HMD and held two controllers for the virtual lifting task. The VR scenario (Figure 5-12) had a virtual box in front of a virtual shelf, which was comparable to the lifting tasks in physical world. A floating virtual text was placed in front of the user’s view, when the virtual tasks started, the text changed to “Not ready”, indicating that the participants did not reach the threshold to lift the virtual box yet. To reach the lifting threshold, the participants were verbally informed to voluntarily contract their muscles across the whole-body. They gradually increased the exertion and when the predicted exerting force from the lasso model reached the predefined virtual weights of the virtual box, the text changed to “OK to lift”, indicating that the box was ready to be lifted. After that, the participants could use the controllers to lift the virtual box and place it on the shelf. The participants also gave RPE scores for the virtual lifting trials.

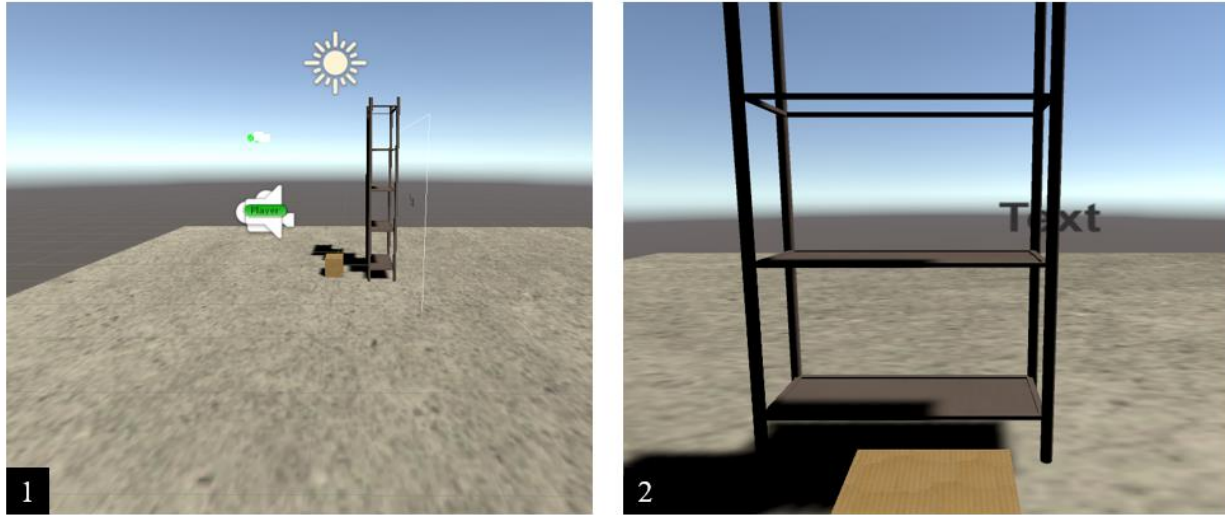


**Figure 5-12** Screenshot of the virtual lifting tasks from 1) a third-person view and 2) a first-person view.

The workflow of regression-based virtual lifting tasks included three steps: multi-EMG acquisition from the Trigno software; real-time EMG processing in the MATLAB; text feedback in the Unity. As can be seen from the flowchart (Figure 5-13), Trigno software acquired real-time EMG signal and sent it to MATLAB, MATLAB processed the real-time EMG signal following the protocols to obtain customized lasso regression model, and then the real-time raw EMG signal was transformed into feature matrix on moving windows. Finally, the lifting force was predicted using the regression model obtained during the physical lifting task. When the lifting force prediction reached or exceeded the predefined virtual weight of the box, MATLAB sent the text of “OK to lift” to the Unity’s virtual interface.

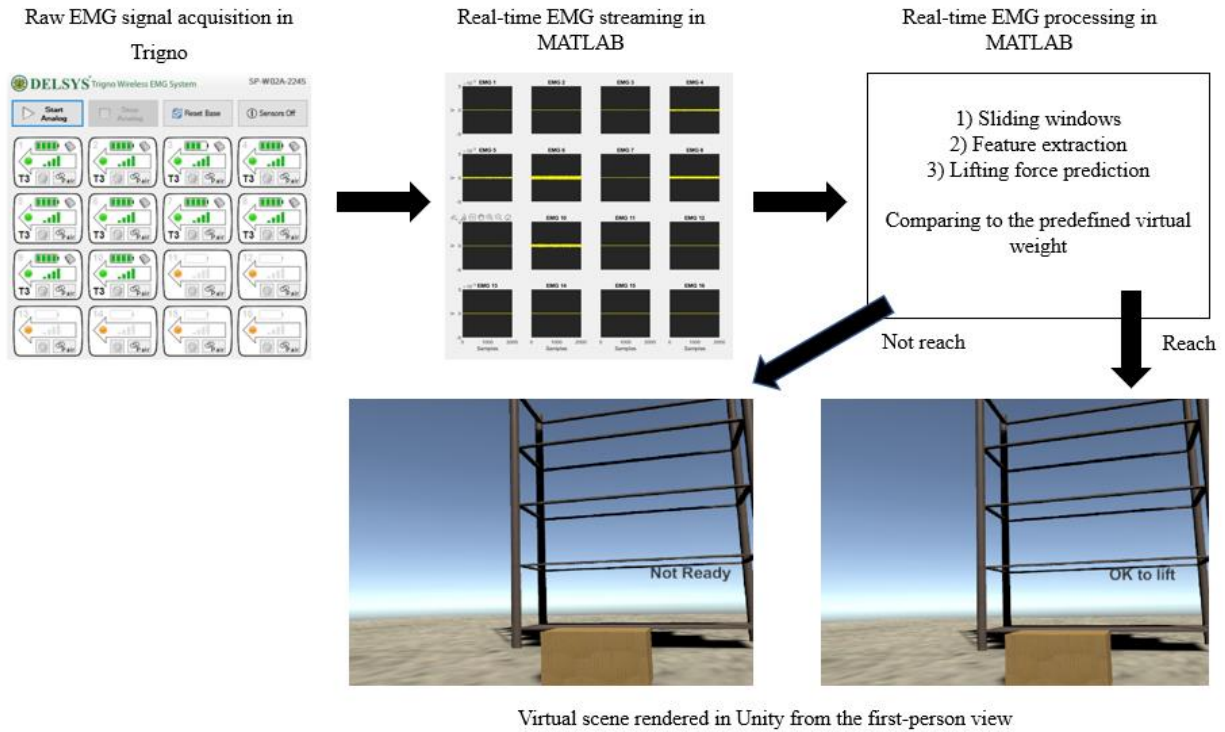


**Figure 5-13** Workflow of the regression-based virtual exertion task.

For each virtual height, the participant was asked to lift a virtual box of 1 lb, 5 lb, 10 lb, and 20 lb. For each weight, if the participant failed to contract their muscles to reach the lifting force, they were given a second chance to try to reach that lifting force. In addition, participants' virtual lifting limit was obtained with the baseline of 20 lb. If the participant could not lift a virtual box of 20 lb, the researcher would decrease the box's virtual weight in increments of 1 lb until the participant could lift the virtual box. Similarly, if the participant could lift the virtual box of 20 lb, the researcher would increase the box's virtual weight in an increment of 1 lb until the participant could not lift the virtual weight. For each virtual lifting task, they were asked to give a RPE score based on their exertion.

### 5.4.2.5 Data analysis

Participants' RPE scores across all the physical lifting trials and virtual lifting tasks were obtained. Participants' trial results were summarized (failure or success). In addition, participants' virtual lifting limit was obtained.

## 5.4.3 Results & Discussion

### 5.4.3.1 Perceived exertion for the physical lifting task

**Table 5-7** Rated perceived exertion (RPE) scores for the physical lifting task. There were three lifting weights and three lifting heights.

Lifting index	Participant 1	Participant 2
6 lb. 20 inches	4	1
6 lb. 35 inches	3	1
6 lb. 50 inches	4	2
10 lb. 20 inches	6	3
10 lb. 35 inches	5	3
10 lb. 50 inches	7	4
16 lb. 20 inches	7	5
16 lb. 35 inches	7	4
16 lb. 50 inches	9	6

As shown in Table 5-7, participants' RPE scores increased with the increase of lifting weight, which is reasonable. Participants needed to exert more to lift the heavier boxes. In addition, participants' RPE scores were lower when lifting to 35 inches than lifting to 20 inches and 50 inches, which indicated that the participants felt less exertions when lifting from floor to waist height compared to lifting from floor to knee height or shoulder height. Notably, participant 1's RPE scores ranged from 4 to 9 and the peak value of 9 occurred when lifting the 16lb. box from floor to the shoulder height; while for participant 2, the RPE scores ranged from 1 to 6 and the peak RPE value was much lower than that of participant 1, indicating that participant 2 had a higher acceptable lifting limit.

### 5.4.3.2 Perceived exertion and trial results for the virtual lifting task

**Table 5-8** Rated perceived exertion (RPE) scores for the virtual lifting task. If the participants failed to reach the threshold in 5 seconds, they were given a second chance to try to exert their muscles to reach the threshold.

Lifting index	Participant 1		Participant 2	
1 lb. 20 inches	Success, 0		Success, 0.5	
1 lb. 35 inches	Success, 0		Success, 0	
6 lb. 20 inches	Success, 2		Success, 3	
6 lb. 35 inches	Success, 2		Success, 2	
6 lb. 50 inches	Success, 3		Success, 4	
10 lb. 20 inches	Success, 4		Success, 6	
10 lb. 35 inches	Success, 3		Success, 5	
10 lb. 50 inches	Success, 3		Failure, 9	Success, 6
16 lb. 20 inches	Failure, 7	Success, 5	Success, 7	
16 lb. 35 inches	Success, 5		Failure, 9	Failure, 9
16 lb. 50 inches	Failure, 8	Failure, 7	Success, 8	
20 lb. 20 inches	Success, 5		Failure, 9	Failure, 9.5
20 lb. 35 inches	Failure, 8	Failure, 8	Failure, 9	Failure, 9
20 lb. 50 inches	Failure, 7	Failure, 8	Failure, 9	Failure, 9

As can be seen from the Table 5-8 above, the participants could successfully lift a virtual box that weighed from 1 lb to 10 lb. In particular, when the virtual box was assigned a weight of 1 lb the virtual text changed to “OK to lift” immediately after the researcher started the VR program, which indicated that the participants did not need to purposely contract their muscles to reach the lifting threshold, and both participants gave RPE scores of 0 for that condition. Consistent with the results in physical lifting tasks, participants’ RPE scores increased while the virtual lifting weights increased. When the lifting weight of the virtual box exceeded 16 lb, it was more difficult for the participants to contract their muscles to the target threshold and the participants failed to lift the virtual box. There existed no trend of lifting height on RPE scores. When comparing the RPE scores between the physical lifting and the virtual lifting (e.g., physically lifting a 6 lb box to 20 inches and virtually lifting a 6 lb box to 20 inches), participant 1 reported lower RPE scores in virtual lifting than physical lifting while participants 2 reported higher RPE scores in virtual lifting.

That could be because the RPE scores were more subjective, and the two participants had different decision criteria when giving the scores. Participant 1 indicated that he did not feel much exertion on his back in the virtual lifting task that could be comparable to the physical lifting trials. While participant 2 verbally indicated that he contracted his biceps maximumly during the virtual lifting trials and felt high exertions, especially during the failed lifting trials. To note, in the two trials (P1, 16 lb 20 inches; P2, 10 lb 50 inches) that participants failed the first trial and succeeded in the second trial, the participants gave a lower RPE scores in the successful lifting trial, which was reasonable as the participants kept increasing muscle contractions during the failed trials.

#### 5.4.3.3 Maximum lifting weight for the virtual lifting task

**Table 5-9** Maximum virtual lifting weight.

Lifting height	Participant 1	Participant 2
20 inches	22 lb.	18 lb.
35 inches	19 lb.	15 lb.
50 inches	15 lb.	17 lb.

Participants' virtual lifting limit was obtained, which ranged from 15 lb to 22 lb. This is plausible as some agonist muscles like biceps are easy to control and contract while some other antagonist muscles like lumbar erector spinae are not easy to voluntarily contract. Thus, it was likely that participants could not voluntarily contract the whole-body muscles to the activation levels obtained in physical lifting. In addition, it also led to over-exertions for the agonist muscles while antagonist muscles remained unactive. One possible solution is to only investigate agonist muscles in future virtual exertion program.

#### 5.4.3.4 Comparison between different virtual exertions studies

**Table 5-10** Comparison between the virtual exertion studies.

Studies	Muscles	Methods	VR medium	Functionality
(K. B. Chen et al., 2015)	Biceps and triceps	Binary	CAVE	good
(K. Chen, Widmayer, et al., 2020)	Twelve muscles across the full body	Multi-Binary	CAVE	Low, needs to be adjusted to finish
This study	Ten muscles across the full body	Lasso regression	HMD	good

From the perspective of system practicality, the virtual lifting program could function as expected and evoked participants' sense of forceful exertions when lifting the virtual box, and both participants agreed that the innovative program had potential functionality of manual material handling training program. Comparing to the two previous virtual exertion studies, this work extended the idea of EMG-driven virtual interface into a fully immersive virtual environment through an HMD, and the participants were able to finish the virtual lifting tasks without using adjusting factors (AFs) employed in the previous virtual patient transfer study. On the other hand, the program had significant delay because of signal transfer from different software and real-time data processing. Consequently, it could happen that participants' current exertion level reached the lifting weight while the text changed to "OK to lift" after a while, which led to over-exertion. To solve the problem, the researcher asked the participants to increase their muscle exertion level in

a constant and smooth pace, which was difficult to manipulate. Future studies should try to decrease the delay from the system level.

In conclusion, the regression based virtual exertion interface functioned as expected and evoked participants' sense of exertions during virtual lifting tasks. Two major limitations remain, the first one is the uneven muscle contraction, as some muscles were over-exerted and while other muscles were under-exerted; the second limitation was the system delay due to data transfer between different software, which resulted in delayed visual text display as the participants continued to contract their muscles. Future study should be conducted to overcome the limitations.

## **5.5 Summary**

This chapter extended the method of binary-based virtual exertion to a broader regression-based virtual exertion. Three experiments were conducted, the first experiment examined the usage of psychophysical methods to evaluate manual material carrying tasks, which indicated that there was a detection threshold for human to perceive a weight difference. The second experiment explored the possibility of classifying common manual material handling posture and movements using EMG signal across whole-body muscles. The results suggested that the classifiers could achieve optimal accuracy for intra-participant condition where the training data and the testing data were from the same participant. The third experiment designed a regression-based virtual exertion program, which involved calibration step in physical world, regression parameters acquisition step and validation step in VR. The results showed that despite of system delay, the program could evoke comparable sense of forceful exertions in the virtual lifting tasks. Future studies can focus on muscle contraction's mechanism and program delay reduction.

## Chapter 6 Conclusion

In this dissertation, two modalities of augmented feedback in VR system were examined: 1) instructional visual feedback using 3-D humanoid virtual instructor; 2) bio-signal based pseudo-haptic feedback through real-time EMG processing. To achieve the research goals, several studies and experiments were designed and conducted.

For the instructional feedback, two humanoid instructors were designed and examined in two XR applications. In particular, a 3-D humanoid model was developed and implemented in a VR exercise program to guide users to perform pick and place movements. The results indicated that the task-oriented practice elicited more intensive shoulder movements and muscular activities compared to the imitation-oriented practice during VRE, which also induced greater movement variations. A point cloud reconstructed humanoid model was built in an AR posture training platform to demonstrate common manual material handling postures, despite of some usability limitations revealed during the user study, the AR-based posture training system provided the users more intuitive perspective to visualize the manual lifting posture in 3-D space. Compared to the point cloud reconstructed virtual instructor, the 3-D model based virtual instructor was more flexible and could be easily animated to convey movement information to the participants by updating the joint position of the virtual instructor. While for the point cloud generated virtual instructor, it shared more similarities with real humans on appearances, but it was difficult to animate the point cloud that was a complete mesh.

For the bio-signal feedback, EMG was utilized as a medium to deliver senses of forceful feedback when interacting with VR objects. Two studies were conducted, both of which focused on physical tasks that involved muscles across the whole body. The first study investigated the task of emergency patient transfer task. A mock-up patient transfer task was set up in the laboratory

setting, EMG sensors were attached to muscles across the whole body. Principal component analysis was utilized to select the major contributing muscles during the task. Next, a virtual patient transfer task was conducted in a virtual environment targeting the selected major muscles, the criteria of virtual transfer were relatively simple: all muscles need to reach their respective calibration threshold obtained during the physical (calibration) tasks, the controller needs to collide with the virtual objects. The results suggested that participants could only finish the tasks with adjusting factors that scaled down the lifting thresholds, and participants reported higher physical workload during physical transfer tasks while higher mental workload during virtual transfer tasks. There were several limitations in this study: 1) multi-binary criterion did not reflect the coordination and contributions between the muscles and more accurate multi-EMG-force modelling is required to set up new criterion for virtual exertion program; 2) The weight/load for this task was too high, which made it difficult for the participants to virtually contract their muscles to the calibration threshold. Thus, common physical tasks that involve less weight need to be further studied.

To solve the problems revealed in the simulated patient transfer task, a second study that investigated manual material handling tasks was conducted. Three sub-studies were conducted, the first sub-study examined the usage of psychophysical methods to evaluate manual material carrying tasks, the results indicated that there was a detection threshold for human to perceive a weight difference, which varied with the reference weight. In addition, Borg perceived exertion survey in CR-10 scale could be used to evaluate participants' perceived exertions, which increased with the increment of weight ratio. The second sub-study explored the possibility of classifying common manual material handling posture and movements using EMG signal across whole-body muscles. The results suggested that the classifiers could achieve optimal accuracy for intra-

participant condition where the training data and the testing data were from the same participant, which indicated that a calibration task that obtained customized EMG data was necessary to build customized regression-based virtual exertion criteria. In the third sub-study, a virtual squat lifting task was designed, which involved calibration step in physical world, regression parameters acquisition step and validation step in VR. The results showed that the program could evoke comparable sense of perceived exertions in the virtual lifting tasks and the perceived exertion increased with the increase of virtual weights.

Some limitations remained for the virtual exertion study, participants often had difficulty contracting some muscles without a physical object on hand, which led to imbalanced exertions during the virtual lifting trials: some muscles were over exerted while others were under exerted. Secondly, system delay existed due to data transfer between different software, thus when the predicted lifting weight from the regression model reached predefined virtual weight, it could take a while for the participants to see the instructional text changed to “OK to lift”. Future studies on virtual exertion should focus on selecting appropriate muscles and reducing system delay.

## REFERENCES

- Adewuyi, A. A., Hargrove, L. J., & Kuiken, T. A. (2016). Evaluating eMg Feature and classifier selection for application to Partial-hand Prosthesis control. *Frontiers in Neurorobotics*, *10*(October), 1–11. <https://doi.org/10.3389/fnbot.2016.00015>
- Ahmad, I., & Kim, J. Y. (2018). Assessment of whole body and local muscle fatigue using electromyography and a perceived exertion scale for squat lifting. *International Journal of Environmental Research and Public Health*, *15*(4), 1–12. <https://doi.org/10.3390/ijerph15040784>
- Al-Timemy, A. H., Bugmann, G., Escudero, J., & Outram, N. (2013). Classification of finger movements for the dexterous hand prosthesis control with surface electromyography. *IEEE Journal of Biomedical and Health Informatics*. <https://doi.org/10.1109/JBHI.2013.2249590>
- Allin, S., Matsuoka, Y., & Klatzky, R. (2002). Measuring just noticeable differences for haptic force feedback: Implications for rehabilitation. *Proceedings - 10th Symposium on Haptic Interfaces for Virtual Environment and Teleoperator Systems, HAPTICS 2002*. <https://doi.org/10.1109/HAPTIC.2002.998972>
- Allison, G. T., Marshall, R. N., & Singer, K. P. (1993). EMG signal amplitude normalization technique in stretch-shortening cycle movements. *Journal of Electromyography and Kinesiology*. [https://doi.org/10.1016/1050-6411\(93\)90013-M](https://doi.org/10.1016/1050-6411(93)90013-M)
- Alomari, F., & Liu, G. (2015). Novel hybrid soft computing pattern recognition system SVM-GAPSO for classification of eight different hand motions. *Optik*. <https://doi.org/10.1016/j.ijleo.2015.08.170>
- Amazeen, E. L. (2014). Box shape influences the size-weight illusion during individual and team

lifting. *Human Factors*. <https://doi.org/10.1177/0018720813497980>

Amick III, B. C., Robertson, M. M., DeRango, K., Bazzani, L., Moore, A., Rooney, T., & Harrist, R. (2003). Effect of office ergonomics intervention on reducing musculoskeletal symptoms. *Spine*, 28(24), 2706–2711.

Anderson, F., Grossman, T., Matejka, J., & Fitzmaurice, G. (2013). YouMove: enhancing movement training with an augmented reality mirror. *Proceedings of the 26th Annual ACM Symposium on User Interface Software and Technology*, 311–320.

Andersson, G. B. J., Ortengren, R., & Herberts, P. (1977). Quantitative electromyographic studies of back muscle activity related to posture and loading. *Orthopedic Clinics of North America*.

Appel, L., Appel, E., Bogler, O., Wiseman, M., Cohen, L., Ein, N., Abrams, H. B., & Campos, J. L. (2020). Older Adults With Cognitive and/or Physical Impairments Can Benefit From Immersive Virtual Reality Experiences: A Feasibility Study. *Frontiers in Medicine*. <https://doi.org/10.3389/fmed.2019.00329>

Atzori, M., Gijssberts, A., Kuzborskij, I., Elsig, S., Mittaz Hager, A. G., Deriaz, O., Castellini, C., Müller, H., & Caputo, B. (2015). Characterization of a benchmark database for myoelectric movement classification. *IEEE Transactions on Neural Systems and Rehabilitation Engineering*, 23(1), 73–83. <https://doi.org/10.1109/TNSRE.2014.2328495>

Azuma, R. (1997). A survey of augmented reality. *Presence: Teleoperators and Virtual Environments*, 6(4), 355–385. <https://doi.org/10.1162/pres.1997.6.4.355>

Baldacchino, T., Jacobs, W. R., Anderson, S. R., Worden, K., & Rowson, J. (2018).

- Simultaneous Force Regression and Movement Classification of Fingers via Surface EMG within a Unified Bayesian Framework. *Frontiers in Bioengineering and Biotechnology*.  
<https://doi.org/10.3389/fbioe.2018.00013>
- Barnett, M. L., Ross, D., Schmidt, R. A., & Todd, B. (1973). Motor Skills Learning and the Specificity of Training Principle. *Research Quarterly. American Association for Health, Physical Education and Recreation*, 44(4), 440–447.  
<https://doi.org/10.1080/10671188.1973.10615224>
- Bates, J. (1992). Virtual Reality, Art and Entertainment. *Presence*, 1(1), 133–138.
- Behrend, T. S., & Thompson, L. F. (2011). Similarity effects in online training: Effects with computerized trainer agents. *Computers in Human Behavior*.  
<https://doi.org/10.1016/j.chb.2010.12.016>
- Behringer, M., vom Heede, A., Matthews, M., & Mester, J. (2011). Effects of strength training on motor performance skills in children and adolescents: a meta-analysis. *Pediatric Exercise Science*, 23(2), 186–206.
- Besl, P. J., & McKay, N. D. (1992). Method for registration of 3-D shapes. In P. S. Schenker (Ed.), *Sensor Fusion IV: Control Paradigms and Data Structures* (Vol. 1611, pp. 586–606). SPIE. <https://doi.org/10.1117/12.57955>
- Blade, R. A., & Padgett, M. Lou. (2002). Virtual environments standards and terminology. *Handbook of Virtual Environments*, 15–27.
- Boettcher, C. E., Ginn, K. A., & Cathers, I. (2008). Standard maximum isometric voluntary contraction tests for normalizing shoulder muscle EMG. *Journal of Orthopaedic Research*,

26(12), 1591–1597. <https://doi.org/10.1002/jor.20675>

Bogduk, N., Johnson, G., & Spalding, D. (1998). The morphology and biomechanics of latissimus dorsi. *Clinical Biomechanics*, 13(6), 377–385. [https://doi.org/10.1016/S0268-0033\(98\)00102-8](https://doi.org/10.1016/S0268-0033(98)00102-8)

Bohm, S., Marzilger, R., Mersmann, F., Santuz, A., & Arampatzis, A. (2018). Operating length and velocity of human vastus lateralis muscle during walking and running. *Scientific Reports*, 8(1), 1–10. <https://doi.org/10.1038/s41598-018-23376-5>

Bolgia, L. A., & Uhl, T. L. (2007). Reliability of electromyographic normalization methods for evaluating the hip musculature. *Journal of Electromyography and Kinesiology*. <https://doi.org/10.1016/j.jelekin.2005.11.007>

Booth, D. A., & Freeman, R. P. J. (1993). Discriminative feature integration by individuals. *Acta Psychologica*. [https://doi.org/10.1016/0001-6918\(93\)90068-3](https://doi.org/10.1016/0001-6918(93)90068-3)

Bordoni, B., & Varacallo, M. (2018). Anatomy, Bony Pelvis and Lower Limb, Thigh Quadriceps Muscle. In *StatPearls*.

Borg, G. (1998). Borg's rating of perceived exertion and pain scales. In *Human Kinetics*.

Bovonsunthonchai, S., Aung, N., Hiengkaew, V., & Tretriluxana, J. (2020). A randomized controlled trial of motor imagery combined with structured progressive circuit class therapy on gait in stroke survivors. *Scientific Reports*. <https://doi.org/10.1038/s41598-020-63914-8>

Brewer, M. B. (1979). In-group bias in the minimal intergroup situation: A cognitive-motivational analysis. *Psychological Bulletin*. <https://doi.org/10.1037/0033-2909.86.2.307>

Brodie, E. E., & Ross, H. E. (1984). Sensorimotor mechanisms in weight discrimination.

*Perception & Psychophysics*. <https://doi.org/10.3758/BF03207502>

Buckingham, G. (2014a). Analyse experimentale: De quelques elements de la sensation de poids.

*Experimental Brain Research*, 232(6), 1623–1629. <https://doi.org/10.1007/s00221-014-3926-9>

Buckingham, G. (2014b). Getting a grip on heaviness perception: A review of weight illusions and their probable causes. In *Experimental Brain Research*. <https://doi.org/10.1007/s00221-014-3926-9>

Buckingham, G., Cant, J. S., & Goodale, M. A. (2009). Living in a material world: How visual cues to material properties affect the way that we lift objects and perceive their weight.

*Journal of Neurophysiology*. <https://doi.org/10.1152/jn.00515.2009>

Buckingham, G., Ranger, N. S., & Goodale, M. A. (2011). The material-weight illusion induced by expectations alone. *Attention, Perception, and Psychophysics*.

<https://doi.org/10.3758/s13414-010-0007-4>

Bullion, C., & Gurocak, H. (2009). Haptic glove with MR brakes for distributed finger force feedback. *Presence*, 18(6), 421–433. <https://doi.org/10.1162/pres.18.6.421>

Burdea, G. (2003). *Virtual Rehabilitation - Benefits and Challenges*. February 2003.

<https://doi.org/10.1267/METH03050519>

Burden, A. (2010). How should we normalize electromyograms obtained from healthy participants? What we have learned from over 25 years of research. In *Journal of Electromyography and Kinesiology*.

<https://doi.org/10.1016/j.jelekin.2010.07.004>

Caesarendra, W., Lekson, S. U., Mustaqim, K. A., Winoto, A. R., & Widyotriatmo, A. (2017). A

classification method of hand EMG signals based on principal component analysis and artificial neural network. *Proceedings of the 2016 International Conference on Instrumentation, Control, and Automation, ICA 2016*.

<https://doi.org/10.1109/ICA.2016.7811469>

Callison, M. C., & Nussbaum, M. A. (2012). Identification of physically demanding patient-handling tasks in an acute care hospital. *International Journal of Industrial Ergonomics*, 42(3), 261–267. <https://doi.org/10.1016/j.ergon.2012.02.001>

Cao, H., Sun, S., & Zhang, K. (2017). Modified EMG-based handgrip force prediction using extreme learning machine. *Soft Computing*. <https://doi.org/10.1007/s00500-015-1800-8>

Chakarov, D., Veneva, I., Tsveov, M., & Zlatanov, E. (2017). Adjusting the natural stiffness of a pneumatic powered exoskeleton designed as a virtual reality haptic device. *International Journal of Advanced Robotic Systems*. <https://doi.org/10.1177/1729881417739432>

Chan, J. C. P., Leung, H., Tang, J. K. T., & Komura, T. (2011). A virtual reality dance training system using motion capture technology. *IEEE Transactions on Learning Technologies*, 4(2), 187–195. <https://doi.org/10.1109/TLT.2010.27>

Chan, S. (2007). *the Use of Emg for Load Prediction During Manual Lifting*.

Chang, E., Kim, H. T., & Yoo, B. (2020). Virtual Reality Sickness: A Review of Causes and Measurements. *International Journal of Human-Computer Interaction*.

<https://doi.org/10.1080/10447318.2020.1778351>

Charoenpanich, N., Boonsinsukh, R., Sirisup, S., & Saengsirisuwan, V. (2013). Principal component analysis identifies major muscles recruited during elite vertical jump.

*ScienceAsia*, 39(3), 257–264. <https://doi.org/10.2306/scienceasia1513-1874.2013.39.257>

Chen, C.-L., Hong, W.-H., Cheng, H.-Y. K., Liaw, M.-Y., Chung, C.-Y., & Chen, C.-Y. (2012). Muscle strength enhancement following home-based virtual cycling training in ambulatory children with cerebral palsy. *Research in Developmental Disabilities*, 33(4), 1087–1094. <https://doi.org/10.1016/j.ridd.2012.01.017>

Chen, K. B., Ponto, K., Tredinnick, R. D., & Radwin, R. G. (2015). Virtual exertions: Evoking the sense of exerting forces in virtual reality using gestures and muscle activity. *Human Factors*, 57(4), 658–673. <https://doi.org/10.1177/0018720814562231>

Chen, K. B., Sesto, M. E., Ponto, K., Leonard, J., Mason, A., Vanderheiden, G., Williams, J., & Radwin, R. G. (2016). Use of Virtual Reality Feedback for Patients with Chronic Neck Pain and Kinesiophobia. *IEEE Transactions on Neural Systems and Rehabilitation Engineering*, 25(8), 1240–1248. <https://doi.org/10.1109/TNSRE.2016.2621886>

Chen, K., & Chen, K. B. (2021a). Examining human perception of weight during loaded standing and walking. *Proceedings of the 2021 HFES 65th International Annual Meeting*.

Chen, K., & Chen, K. B. (2021b). Task-Oriented and Imitation-Oriented Movements in Virtual Reality Exercise Performance and Design. *Human Factors*. <https://doi.org/10.1177/00187208211010100>

Chen, K., Perera, G., Li, L., Xu, X., & Chen, K. B. (2020). Develop and evaluate an augmented reality posture training tool to promote work safety. *Proceedings of the Human Factors and Ergonomics Society Annual Meeting*, 64(1), 2051–2055. <https://doi.org/10.1177/1071181320641496>

- Chen, K., Widmayer, R., & Chen, K. B. (2020). Simulate and sense force exertions during virtual patient transfer tasks. *Human Factors and Ergonomics Society 2020 Annual Meeting*, 2092–2096. <https://doi.org/10.1177/1071181320641507>
- Chen, Y., & Medioni, G. (1992). Object modelling by registration of multiple range images. *Image and Vision Computing*, *10*(3), 145–155. [https://doi.org/10.1016/0262-8856\(92\)90066-C](https://doi.org/10.1016/0262-8856(92)90066-C)
- Chopp, J. N., Fischer, S. L., & Dickerson, C. R. (2010). The impact of work configuration, target angle and hand force direction on upper extremity muscle activity during sub-maximal overhead work. *Ergonomics*, *53*(1), 83–91. <https://doi.org/10.1080/00140130903323232>
- Chowdhury, R. H., Reaz, M. B. I., Bin Mohd Ali, M. A., Bakar, A. A. A., Chellappan, K., & Chang, T. G. (2013). Surface electromyography signal processing and classification techniques. *Sensors (Switzerland)*, *13*(9), 12431–12466. <https://doi.org/10.3390/s130912431>
- Chua, P. T., Crivella, R., Daly, B., Hu, N., Schaaf, R., Ventura, D., Camill, T., Hodgins, J., & Pausch, R. (2003). Training for physical tasks in virtual environments: Tai Chi. *IEEE Virtual Reality, 2003-Janua*, 87–94. <https://doi.org/10.1109/VR.2003.1191125>
- Chuah, S. H.-W. (2019). Why and Who Will Adopt Extended Reality Technology? Literature Review, Synthesis, and Future Research Agenda. *SSRN Electronic Journal*. <https://doi.org/10.2139/ssrn.3300469>
- Coffey, B., MacPhee, R., Socha, D., & Fischer, S. L. (2016). A physical demands description of paramedic work in Canada. *International Journal of Industrial Ergonomics*. <https://doi.org/10.1016/j.ergon.2016.04.005>

Cram, J. R., & Rommen, D. (1989). Effects of skin preparation on data collected using an EMG muscle-scanning procedure. *Biofeedback and Self-Regulation*.

<https://doi.org/10.1007/BF00999342>

Dawes, H. N., Barker, K. L., Cockburn, J., Roach, N., Scott, O., & Wade, D. (2005). Borg's rating of perceived exertion scales: Do the verbal anchors mean the same for different clinical groups? *Archives of Physical Medicine and Rehabilitation*.

<https://doi.org/10.1016/j.apmr.2004.10.043>

Dennison, M. S., Wisti, A. Z., & D'Zmura, M. (2016). Use of physiological signals to predict cybersickness. *Displays*. <https://doi.org/10.1016/j.displa.2016.07.002>

Deutsch, J. E., Borbely, M., Filler, J., Huhn, K., & Guarrera-Bowlby, P. (2008). Use of a Low-Cost, Commercially Available Gaming Console (Wii) for Rehabilitation of an Adolescent With Cerebral Palsy. *Physical Therapy*, 88(10), 1196–1207.

<https://doi.org/10.2519/jospt.2010.3332>

Dhindsa, I. S., Agarwal, R., & Ryait, H. S. (2017). Principal component analysis-based muscle identification for myoelectric-controlled exoskeleton knee. *Journal of Applied Statistics*, 44(10), 1707–1720. <https://doi.org/10.1080/02664763.2016.1221907>

DiZio, P., & Lackner, J. R. (1997). Circumventing side effects of immersive virtual environments. *Advances in Human Factors/Ergonomics*.

Dobkin, B. H. (2004). Strategies for stroke rehabilitation. *Lancet Neurology*, 3(9), 528–536.

[https://doi.org/10.1016/S1474-4422\(04\)00851-8](https://doi.org/10.1016/S1474-4422(04)00851-8)

Dolan, P., & Adams, M. A. (1998). Repetitive lifting tasks fatigue the back muscles and increase

the bending moment acting on the lumbar spine. *Journal of Biomechanics*.

[https://doi.org/10.1016/S0021-9290\(98\)00086-4](https://doi.org/10.1016/S0021-9290(98)00086-4)

Dunleavy, M., Dede, C., & Mitchell, R. (2009). Affordances and limitations of immersive participatory augmented reality simulations for teaching and learning [JOUR]. *Journal of Science Education and Technology*, 18(1), 7–22.

Duque, D., B., G., L.-D., S., H., H., S., D., G., P., S., A., S., & O., D. (2013). Effects of balance training using a virtual-reality system in older fallers. *Clinical Interventions in Aging*, 8, 257–263. <https://doi.org/10.2147/CIA.S41453>

Ekholm, J., Arborelius, U. P., & Nemeth, G. (1982). The load on the lumbo sacral joint and trunk muscle activity during lifting. *Ergonomics*. <https://doi.org/10.1080/00140138208924934>

Ekman, Gös. (1959). Weber's Law and Related Functions. *Journal of Psychology: Interdisciplinary and Applied*. <https://doi.org/10.1080/00223980.1959.9916336>

Elfeituri, F. E., & Taboun, S. M. (2002). An evaluation of the niosh lifting equation: A psychophysical and biomechanical investigation. *International Journal of Occupational Safety and Ergonomics*, 8(2), 243–258. <https://doi.org/10.1080/10803548.2002.11076527>

Englehart, K., & Hudgins, B. (2003). A Robust, Real-Time Control Scheme for Multifunction Myoelectric Control. *IEEE Transactions on Biomedical Engineering*. <https://doi.org/10.1109/TBME.2003.813539>

Farmer, A. D., Ban, V. F., Coen, S. J., Sanger, G. J., Barker, G. J., Gresty, M. A., Giampietro, V. P., Williams, S. C., Webb, D. L., Hellström, P. M., Andrews, P. L. R., & Aziz, Q. (2015). Visually induced nausea causes characteristic changes in cerebral, autonomic and endocrine

- function in humans. *Journal of Physiology*. <https://doi.org/10.1113/jphysiol.2014.284240>
- Farrow, M., Lutteroth, C., Rouse, P. C., & Bilzon, J. L. J. (2019). Virtual-reality exergaming improves performance during high-intensity interval training. *European Journal of Sport Science*. <https://doi.org/10.1080/17461391.2018.1542459>
- Ferrari, M. (1996). Observing the observer: Self-regulation in the observational learning of motor skills. *Developmental Review*, *16*(2), 203–240.  
<https://doi.org/10.1006/drev.1996.0008>
- Finkelstein, S., Nickel, A., Lipps, Z., Barnes, T., Wartell, Z., & Suma, E. A. (2011). Astrojumper: Motivating exercise with an immersive virtual reality exergame. *Presence: Teleoperators and Virtual Environments*, *20*(1), 78–92.  
[https://doi.org/10.1162/pres\\_a\\_00036](https://doi.org/10.1162/pres_a_00036)
- Firouzabadi, A., Arjmand, N., Pan, F., Zander, T., & Schmidt, H. (2021). Sex-Dependent Estimation of Spinal Loads During Static Manual Material Handling Activities—Combined in vivo and in silico Analyses. *Frontiers in Bioengineering and Biotechnology*, *9*(November), 1–14. <https://doi.org/10.3389/fbioe.2021.750862>
- Flanagan, J. R., & Beltzner, M. A. (2000). Independence of perceptual and sensorimotor predictions in the size- weight illusion. *Nature Neuroscience*. <https://doi.org/10.1038/76701>
- Fowler, N. E., Rodacki, A. L. F., & Rodacki, C. D. (2006). Changes in stature and spine kinematics during a loaded walking task. *Gait and Posture*.  
<https://doi.org/10.1016/j.gaitpost.2004.12.006>
- Freina, L., & Ott, M. (2015). A literature review on immersive virtual reality in education: State

of the art and perspectives. *Proceedings of ELearning and Software for Education (ELSE)(Bucharest, Romania, April 23--24, 2015)*, 1, 8. <https://doi.org/10.12753/2066-026X-15-020>

Frisoli, A., Salsedo, F., Bergamasco, M., Rossi, B., & Carboncini, M. C. (2009). A force-feedback exoskeleton for upper-limb rehabilitation in virtual reality. *Applied Bionics and Biomechanics*, 6(2), 115–126. <https://doi.org/10.1080/11762320902959250>

Gagnon, M., Chehade, A., Kemp, F., & Lortie, M. (1987). Lumbo-sacral loads and selected muscle activity while turning patients in bed. *Ergonomics*, 30(7), 1013–1032. <https://doi.org/10.1080/00140138708965992>

Gatti, C. J., Doro, L. C., Langenderfer, J. E., Mell, A. G., Maratt, J. D., Carpenter, J. E., & Hughes, R. E. (2008). Evaluation of three methods for determining EMG-muscle force parameter estimates for the shoulder muscles. *Clinical Biomechanics*. <https://doi.org/10.1016/j.clinbiomech.2007.08.026>

Goswami, S., Ghosh, S., & Sahu, S. (2017). Evaluation of ergonomic risk factors in manual patient handling tasks of Indian nurses. *Ergonomics SA*, 29(1), 2. <https://doi.org/10.4314/esa.v29i1.2>

Grady, S. M. (2003). *Virtual reality : simulating and enhancing the world with computers*. New ed. New York : Facts On File, 2003.

Granata, K. P., & Marras, W. S. (1995). An EMG-assisted model of trunk loading during free-dynamic lifting. *Journal of Biomechanics*. [https://doi.org/10.1016/0021-9290\(95\)00003-Z](https://doi.org/10.1016/0021-9290(95)00003-Z)

Grassini, S., & Laumann, K. (2020). Questionnaire Measures and Physiological Correlates of

Presence: A Systematic Review. *Frontiers in Psychology*.

<https://doi.org/10.3389/fpsyg.2020.00349>

Gray, H. (2000). *Anatomy of the human body*. Lea & Febiger.

Habes, D., Carlson, W., & Badger, D. (1985). Muscle fatigue associated with repetitive arm lifts:

Effects of height, weight and reach. *Ergonomics*.

<https://doi.org/10.1080/00140138508963156>

Halabi, O. (2020). Immersive virtual reality to enforce teaching in engineering education.

*Multimedia Tools and Applications*. <https://doi.org/10.1007/s11042-019-08214-8>

Halaki, M., & Gi, K. (2012). Normalization of EMG Signals: To Normalize or Not to Normalize

and What to Normalize to. In *Computational Intelligence in Electromyography Analysis - A*

*Perspective on Current Applications and Future Challenges* (pp. 175–194).

<https://doi.org/10.5772/49957>

Hall, S., Learning, O., & Hall, S. (1999). Kinematic concepts for analyzing human motion. *Basic*

*Biomechanics*. New York, NY: McGraw- ....

Hart, S. G., & Staveland, L. E. (1988). Development of NASA-TLX (Task Load Index): Results

of Empirical and Theoretical Research. *Advances in Psychology*, 52, 139–183.

[https://doi.org/10.1016/S0166-4115\(08\)62386-9](https://doi.org/10.1016/S0166-4115(08)62386-9)

Hashemi, J., Morin, E., Mousavi, P., & Hashtrudi-Zaad, K. (2015). Enhanced dynamic EMG-

force estimation through calibration and PCI modeling. *IEEE Transactions on Neural*

*Systems and Rehabilitation Engineering*. <https://doi.org/10.1109/TNSRE.2014.2325713>

Hein, D., Mai, C., & Hußmann, H. (2018). The Usage of Presence Measurements in Research: A

Review. *18th Conference of the International Society for Presence Research*.

- Hignett, S. (2003). Intervention strategies to reduce musculoskeletal injuries associated with handling patients: a systematic review. *Occupational and Environmental Medicine*, *60*(9), e6–e6.
- Hoareau, C., Querrec, R., Buche, C., & Ganier, F. (2017). Evaluation of Internal and External Validity of a Virtual Environment for Learning a Long Procedure. *International Journal of Human-Computer Interaction*, *33*(10), 786–798.  
<https://doi.org/10.1080/10447318.2017.1286768>
- Holden, M. K., & Todorov, E. (2002). Use of Virtual Environments in Motor Learning and Rehabilitation. *Handbook of Virtual Environments: Design, Implementation, and Applications*, *44*(0), 1–35. <http://web.mit.edu/bcs/bizzilab/publications/holden2002b.pdf>
- Hoozemans, M. J. M., & Van Dieën, J. H. (2005). Prediction of handgrip forces using surface EMG of forearm muscles. *Journal of Electromyography and Kinesiology*, *15*(4), 358–366.  
<https://doi.org/10.1016/j.jelekin.2004.09.001>
- Hou, W., Jiang, Y., Zheng, J., Zheng, X., Peng, C., & Xu, R. (2007). Handgrip Force Estimation Based on a Method Using Surface Electromyography (sEMG) of Extensor Carpi Radialis Longus. *IEEE/ICME International Conference on Complex Medical Engineering*.
- Howard, M. C. (2017). A meta-analysis and systematic literature review of virtual reality rehabilitation programs. *Computers in Human Behavior*, *70*(January), 317–327.  
<https://doi.org/10.1016/j.chb.2017.01.013>
- Hsu, W. L., Krishnamoorthy, V., & Scholz, J. P. (2006). An alternative test of electromyographic

normalization in patients. *Muscle and Nerve*, 33(2), 232–241.

<https://doi.org/10.1002/mus.20458>

Huang, H.-M., Rauch, U., & Liaw, S.-S. (2010). Investigating learners' attitudes toward virtual reality learning environments: Based on a constructivist approach [JOUR]. *Computers & Education*, 55(3), 1171–1182.

Hudgins, B., Parker, P., & Scott, R. N. (1993). A New Strategy for Multifunction Myoelectric Control. *IEEE Transactions on Biomedical Engineering*. <https://doi.org/10.1109/10.204774>

Hughes, R. E., Smutz, W. P., & Ms, G. N. (1997). Roles of deltoid and rotator shoulder elevation. *Clinical Biomechanics*, 12(1), 32–38. [https://doi.org/10.1016/S0268-0033\(96\)00047-2](https://doi.org/10.1016/S0268-0033(96)00047-2)

Hwang, J., Ari, H., Matoo, M., Chen, J., & Kim, J. H. (2020). Air-assisted devices reduce biomechanical loading in the low back and upper extremities during patient turning tasks. *Applied Ergonomics*. <https://doi.org/10.1016/j.apergo.2020.103121>

Hwang, J., Kuppam, V. A., Chodraju, S. S. R., Chen, J., & Kim, J. H. (2019). Commercially Available Friction-Reducing Patient-Transfer Devices Reduce Biomechanical Stresses on Caregivers' Upper Extremities and Low Back. *Human Factors*. <https://doi.org/10.1177/0018720819827208>

Ishii, C., Murooka, S., & Tajima, M. (2018). Navigation of an electric wheelchair using EMG, EOG and EEG. *International Journal of Mechanical Engineering and Robotics Research*. <https://doi.org/10.18178/ijmerr.7.2.143-149>

Jaromi, M., Nemeth, A., Kranicz, J., Laczko, T., & Betlehem, J. (2012). Treatment and

ergonomics training of work-related lower back pain and body posture problems for nurses. *Journal of Clinical Nursing*, 21(11-12), 1776–1784.

Jarrasse, N., Nicol, C., Touillet, A., Richer, F., Martinet, N., Paysant, J., & De Graaf, J. B. (2017). Classification of Phantom Finger, Hand, Wrist, and Elbow Voluntary Gestures in Transhumeral Amputees with sEMG. *IEEE Transactions on Neural Systems and Rehabilitation Engineering*. <https://doi.org/10.1109/TNSRE.2016.2563222>

Jauregui, D. A. G., Argelaguet, F., Olivier, A. H., Marchal, M., Multon, F., & Lecuyer, A. (2014). Toward “Pseudo-haptic avatars”: Modifying the visual animation of self-avatar can simulate the perception of weight lifting. *IEEE Transactions on Visualization and Computer Graphics*, 20(4), 654–661. <https://doi.org/10.1109/TVCG.2014.45>

Jebelli, H., & Lee, S. (2019). Feasibility of Wearable Electromyography (EMG) to Assess Construction Workers’ Muscle Fatigue. *Advances in Informatics and Computing in Civil and Construction Engineering*, January, 181–187. [https://doi.org/10.1007/978-3-030-00220-6\\_22](https://doi.org/10.1007/978-3-030-00220-6_22)

Jesus, I. R. T., Mello, R. G. T., & Nadal, J. (2016). Muscle fatigue assessment during cycle ergometer exercise using principal component analysis of electromyogram power spectra. *Journal of Applied Biomechanics*, 32(6), 593–598. <https://doi.org/10.1123/jab.2015-0253>

Johnson, G., Bogduk, N., Nowitzke, A., & House, D. (1994). Anatomy and actions of the trapezius muscle. *Clinical Biomechanics*, 9(1), 44–50. [https://doi.org/10.1016/0268-0033\(94\)90057-4](https://doi.org/10.1016/0268-0033(94)90057-4)

Jones, L. A. (1986). Perception of Force and Weight. Theory and Research. In *Psychological Bulletin*. <https://doi.org/10.1037/0033-2909.100.1.29>

- Kaiser, H. F. (1961). A NOTE ON GUTTMAN'S LOWER BOUND FOR THE NUMBER OF COMMON FACTORS. *British Journal of Statistical Psychology*.  
<https://doi.org/10.1111/j.2044-8317.1961.tb00061.x>
- Kamavuako, E. N., Farina, D., Yoshida, K., & Jensen, W. (2012). Estimation of grasping force from features of intramuscular EMG signals with mirrored bilateral training. *Annals of Biomedical Engineering*. <https://doi.org/10.1007/s10439-011-0438-7>
- Kang, M. H., Choi, S. H., & Oh, J. S. (2013). Postural taping applied to the low back influences kinematics and EMG activity during patient transfer in physical therapists with chronic low back pain. *Journal of Electromyography and Kinesiology*.  
<https://doi.org/10.1016/j.jelekin.2013.02.009>
- Keir, P. J., & MacDonell, C. W. (2004). Muscle activity during patient transfers: A preliminary study on the influence of lift assists and experience. *Ergonomics*, 47(3), 296–306.  
<https://doi.org/10.1080/0014013032000157922>
- Kennedy, R. S., Lane, N. E., Berbaum, K. S., & Lilienthal, M. G. (1993). Simulator Sickness Questionnaire: An Enhanced Method for Quantifying Simulator Sickness. *The International Journal of Aviation Psychology*. [https://doi.org/10.1207/s15327108ijap0303\\_3](https://doi.org/10.1207/s15327108ijap0303_3)
- Khokhar, Z. O., Xiao, Z. G., & Menon, C. (2010). Surface EMG pattern recognition for real-time control of a wrist exoskeleton. *BioMedical Engineering Online*.  
<https://doi.org/10.1186/1475-925X-9-41>
- Kim, H., Dropkin, J., Spaeth, K., Smith, F., & Moline, J. (2012). Patient handling and musculoskeletal disorders among hospital workers: Analysis of 7 years of institutional workers' compensation claims data. *American Journal of Industrial Medicine*, 55(8), 683–

690. <https://doi.org/10.1002/ajim.22006>

Kim, J. H., Kim, J. H., Jang, S. H., Jang, S. H., Kim, C. S., Kim, C. S., Jung, J. H., Jung, J. H., You, J. H., & You, J. H. (2009). Use of virtual reality to enhance balance and ambulation in chronic stroke: a double-blind, randomized controlled study. *American Journal of Physical Medicine & Rehabilitation / Association of Academic Physiatrists*.

<https://doi.org/10.1097/PHM.0b013e3181b33350>

Kim, J., Son, J., Ko, N., & Yoon, B. (2013). Unsupervised virtual reality-based exercise program improves hip muscle strength and balance control in older adults: A pilot study. *Archives of Physical Medicine and Rehabilitation*, 94(5), 937–943.

<https://doi.org/10.1016/j.apmr.2012.12.010>

Kim, K., Rosenthal, M. Z., Zielinski, D. J., & Brady, R. (2014). Effects of virtual environment platforms on emotional responses. *Computer Methods and Programs in Biomedicine*.

<https://doi.org/10.1016/j.cmpb.2013.12.024>

Kim, Y. Y., Kim, H. J., Kim, E. N., Ko, H. D., & Kim, H. T. (2005). Characteristic changes in the physiological components of cybersickness. *Psychophysiology*.

<https://doi.org/10.1111/j.1469-8986.2005.00349.x>

Klatzky, R. L., Wu, B., Shelton, D., & Stetten, G. (2008). Effectiveness of augmented-reality visualization versus cognitive mediation for learning actions in near space. *ACM Transactions on Applied Perception (TAP)*, 5(1), 1–23.

<https://doi.org/10.1145/1279640.1279641>

Kleim, J. A., & Jones, T. A. (2008). Principles of Experience-Dependent Neural Plasticity: Implications for Rehabilitation After Brain Damage. *Journal of Speech, Language, and*

- Hearing Research*, 51(1), 225–239. [https://doi.org/10.1044/1092-4388\(2008/018\)](https://doi.org/10.1044/1092-4388(2008/018))
- Kober, S. E., & Neuper, C. (2013). Personality and Presence in Virtual Reality: Does Their Relationship Depend on the Used Presence Measure? *International Journal of Human-Computer Interaction*. <https://doi.org/10.1080/10447318.2012.668131>
- Kolasinski, E. M. (1995). Simulator Sickness in Virtual Environments. In *United States Army Research Institute fo the Behavioral and Social Sciences*.
- Konard, P. (2012). The ABC of EMG. In *Noraxon: Scottsdale*.
- Korak, J. A., Bruininks, B. D., & Paquette, M. R. (2020). The influence of normalization technique on between-muscle activation during a back-squat. *International Journal of Exercise Science*, 13(1), 1098–1107.
- Kuhtz-Buschbeck, J. P., & Hagenkamp, J. (2020). Cold and heavy: grasping the temperature–weight illusion. *Experimental Brain Research*. <https://doi.org/10.1007/s00221-020-05794-y>
- Lafortune, J., Macuga, K. L., Lafortune, J., & Macuga, K. L. (2018). Learning Movements From a Virtual Instructor : Effects of Spatial Orientation , Immersion , and Expertise. *Journal of Experimental Psychology: Applied*, 24(4), 521–533.
- Lam, J. H., & Bordoni, B. (2019). Anatomy, Shoulder and Upper Limb, Arm Abductor Muscles. In *StatPearls*.
- Lavender, S. A., Lorenz, E. P., & Andersson, G. B. J. (2007). Can a new behaviorally oriented training process to improve lifting technique prevent occupationally related back injuries due to lifting? *Spine*, 32(4), 487–494. <https://doi.org/10.1097/01.brs.0000255203.96898.f2>
- LaViola Jr., J., Kruijff, E., McMahan, R., Bowman, D., & Poupyrev, I. (2017). *3D User*

*Interfaces Theory and Practice*. Addison-Wesley Professional.

LaViola Jr, J. J. (2000). A discussion of cybersickness in virtual environments. *ACM SIGCHI Bulletin*, 32(1), 47–56.

Lee, S. H., Yoon, C., Chung, S. G., Kim, H. C., Kwak, Y., Park, H. W., & Kim, K. (2015). Measurement of shoulder range of motion in patients with adhesive capsulitis using a Kinect. *PLoS ONE*, 10(6). <https://doi.org/10.1371/journal.pone.0129398>

Lewis, G. N., & Rosie, J. A. (2012). Virtual reality games for movement rehabilitation in neurological conditions: How do we meet the needs and expectations of the users. *Disability and Rehabilitation*. <https://doi.org/10.3109/09638288.2012.670036>

Lewis, J. R. (2002). Psychometric Evaluation of the PSSUQ Using Data from Five Years of Usability Studies. *International Journal of Human-Computer Interaction*, 14(3–4), 463–488. <https://doi.org/10.1080/10447318.2002.9669130>

Li, X., Fu, J., Xiong, L., Shi, Y., Davoodi, R., & Li, Y. (2015). Identification of finger force and motion from forearm surface electromyography. *IEEE International Conference on Multisensor Fusion and Integration for Intelligent Systems*. <https://doi.org/10.1109/MFI.2015.7295827>

Lim, J., Cho, J. J., Kim, J., Kim, Y., & Yoon, B. C. (2017). Design of virtual reality training program for prevention of falling in the elderly: A pilot study on complex versus balance exercises. *European Journal of Integrative Medicine*, 15(September), 64–67. <https://doi.org/10.1016/j.eujim.2017.09.008>

Lipscomb, A. H. J., Schoenfisch, A. L., Myers, D. J., Pompeii, L. A., Dement, J. M.,

- Occupational, S., Medicine, E., May, N., Lipscomb, H. J., Schoenfisch, A. L., Myers, D. J., Pompeii, L. A., & Dement, J. M. (2018). *Evaluation of direct workers ' compensation costs for musculoskeletal injuries surrounding interventions to reduce patient lifting* Stable URL : <https://www.jstor.org/stable/23218155> *Evaluation of direct workers ' compensation costs for musculoskeletal inj.* 69(5), 367–372. <https://doi.org/10.1136/oemed-2011-1Q0107>
- Liu, P., Martel, F., Rancourt, D., Clancy, E. A., & Brown, D. R. (2014). Fingertip force estimation from forearm muscle electrical activity. *ICASSP, IEEE International Conference on Acoustics, Speech and Signal Processing - Proceedings*. <https://doi.org/10.1109/ICASSP.2014.6853963>
- Liu, Z., Qin, H., Bu, S., Yan, M., Huang, J., Tang, X., & Han, J. (2015). 3D real human reconstruction via multiple low-cost depth cameras. *Signal Processing*. <https://doi.org/10.1016/j.sigpro.2014.10.021>
- Lohse, K. R., Boyd, L. A., Hodges, N. J., Lohse, K. R., Boyd, L. A., & Engaging, N. J. H. (2016). *Engaging Environments Enhance Motor Skill Learning in a Computer Gaming Task*. 2895(June). <https://doi.org/10.1080/00222895.2015.1068158>
- Lubeck, A. J. A., Bos, J. E., & Stins, J. F. (2015). Motion in images is essential to cause motion sickness symptoms, but not to increase postural sway. *Displays*. <https://doi.org/10.1016/j.displa.2015.03.001>
- Lucas, M. F., Gaufriau, A., Pascual, S., Doncarli, C., & Farina, D. (2008). Multi-channel surface EMG classification using support vector machines and signal-based wavelet optimization. *Biomedical Signal Processing and Control*. <https://doi.org/10.1016/j.bspc.2007.09.002>
- Makhoul, P. J., Sinden, K. E., MacPhee, R. S., & Fischer, S. L. (2017). Relative contribution of

- lower body work as a biomechanical determinant of spine sparing technique during common paramedic lifting tasks. *Journal of Applied Biomechanics*, 33(2), 137–143.  
<https://doi.org/10.1123/jab.2016-0178>
- Mao, A., Zhang, H., Liu, Y., Zheng, Y., Li, G., & Han, G. (2017). Easy and Fast Reconstruction of a 3D Avatar with an RGB-D Sensor. *Sensors*, 17(5), 1113.  
<https://doi.org/10.3390/s17051113>
- Martinez, I. J. R., Mannini, A., Clemente, F., Sabatini, A. M., & Cipriani, C. (2020). Grasp force estimation from the transient EMG using high-density surface recordings. *Journal of Neural Engineering*. <https://doi.org/10.1088/1741-2552/ab673f>
- Masin, S. C., Zudini, V., & Antonelli, M. (2009). Early alternative derivations of fechner's law. *Journal of the History of the Behavioral Sciences*. <https://doi.org/10.1002/jhbs.20349>
- Matallaoui, A., Koivisto, J., Hamari, J., & Zarnekow, R. (2017). How Effective Is “Exergamification”? A Systematic Review on the Effectiveness of Gamification Features in Exergames. *Proceedings of the 50th Hawaii International Conference on System Sciences (2017)*, 3316–3325. <https://doi.org/10.24251/hicss.2017.402>
- Mathiassen, S. E., Winkel, J., & Hägg, G. M. (1995). Normalization of surface EMG amplitude from the upper trapezius muscle in ergonomic studies - A review. In *Journal of Electromyography and Kinesiology*. [https://doi.org/10.1016/1050-6411\(94\)00014-X](https://doi.org/10.1016/1050-6411(94)00014-X)
- Mazzone, B., Lighthall Haubert, L., Mulroy, S., Requejo, P., Gotsis, M., Lympouridis, V., Lange, B., Profitt, R., & Winstein, C. (2013). Intensity of shoulder muscle activation during resistive exercises performed with and without virtual reality games. *2013 International Conference on Virtual Rehabilitation, ICVR 2013*, 127–133.

<https://doi.org/10.1109/ICVR.2013.6662091>

McGill, S. M. (1992). A myoelectrically based dynamic three-dimensional model to predict loads on lumbar spine tissues during lateral bending. *Journal of Biomechanics*.

[https://doi.org/10.1016/0021-9290\(92\)90259-4](https://doi.org/10.1016/0021-9290(92)90259-4)

Mehrfard, A., Fotouhi, J., Taylor, G., Forster, T., Navab, N., & Fuerst, B. (2019). A comparative analysis of virtual reality head-mounted display systems. In *arXiv*.

Melhorn, J. M. (1996). A prospective study for upper-extremity cumulative trauma disorders of workers in aircraft manufacturing. *Journal of Occupational and Environmental Medicine*, 38(12), 1264–1271.

Meng, W., Ding, B., Zhou, Z., Liu, Q., & Ai, Q. (2014). An EMG-based force prediction and control approach for robot-assisted lower limb rehabilitation. *Conference Proceedings - IEEE International Conference on Systems, Man and Cybernetics*, 2198–2203.

<https://doi.org/10.1109/smc.2014.6974250>

Milgram, P., & Colquhoun, H. W. (1999). A Framework for Relating Head-Mounted Displays to Mixed Reality Displays. *Proceedings of the Human Factors and Ergonomics Society Annual Meeting*. <https://doi.org/10.1177/154193129904302202>

Miller, J. D., Beazer, M. S., & Hahn, M. E. (2013). Myoelectric walking mode classification for transtibial amputees. *IEEE Transactions on Biomedical Engineering*.

<https://doi.org/10.1109/TBME.2013.2264466>

Mohammed, S., & Angell, L. C. (2004). Surface- and deep-level diversity in workgroups: Examining the moderating effects of team orientation and team process on relationship

- conflict. *Journal of Organizational Behavior*. <https://doi.org/10.1002/job.293>
- Moradi, M., Hadadnezhad, M., Letafatkar, A., Khosrokiani, Z., & Baker, J. S. (2020). Efficacy of throwing exercise with TheraBand in male volleyball players with shoulder internal rotation deficit: A randomized controlled trial. *BMC Musculoskeletal Disorders*, *21*(1), 376. <https://doi.org/10.1186/s12891-020-03414-y>
- Morris, A. D., Kemp, G. J., Lees, A., & Frostick, S. P. (1998). A study of the reproducibility of three different normalisation methods in intramuscular dual fine wire electromyography of the shoulder. *Journal of Electromyography and Kinesiology*. [https://doi.org/10.1016/S1050-6411\(98\)00002-9](https://doi.org/10.1016/S1050-6411(98)00002-9)
- Nagavarapu, S., Lavender, S. A., & Marras, W. S. (2017). Spine loading during the application and removal of lifting slings: the effects of patient weight, bed height and work method. *Ergonomics*, *60*(5), 636–648. <https://doi.org/10.1080/00140139.2016.1211750>
- Naik, G. R., Selvan, S. E., Gobbo, M., Acharyya, A., & Nguyen, H. T. (2016). Principal Component Analysis Applied to Surface Electromyography: A Comprehensive Review. *IEEE Access*, *4*, 4025–4037. <https://doi.org/10.1109/ACCESS.2016.2593013>
- Naranjo, J. E., Sanchez, D. G., Robalino-Lopez, A., Robalino-Lopez, P., Alarcon-Ortiz, A., & Garcia, M. V. (2020). A scoping review on virtual reality-based industrial training. In *Applied Sciences (Switzerland)*. <https://doi.org/10.3390/app10228224>
- NASA. (1986). NASA TASK LOAD INDEX - V 1.0. In *N.A.R. Center*.
- Nass, C., Moon, Y., Fogg, B. J., Reeves, B., & Dryer, C. (1995). Can computer personalities be human personalities? *Conference on Human Factors in Computing Systems - Proceedings*.

<https://doi.org/10.1145/223355.223538>

- Nazmi, N., Rahman, M. A. A., Yamamoto, S. I., Ahmad, S. A., Zamzuri, H., & Mazlan, S. A. (2016). A review of classification techniques of EMG signals during isotonic and isometric contractions. *Sensors, 16*(8), 1304. <https://doi.org/10.3390/s16081304>
- Nelson, A., & Baptiste, A. S. (2004). Evidence-based practices for safe patient handling and movement. In *Online Journal of Issues in Nursing*.
- Nielsen, J. (1993). *Usability engineering*.
- Nielsen, J. L. G., Holmgaard, S., Jiang, N., Englehart, K. B., Farina, D., & Parker, P. A. (2011). Simultaneous and proportional force estimation for multifunction myoelectric prostheses using mirrored bilateral training. *IEEE Transactions on Biomedical Engineering*. <https://doi.org/10.1109/TBME.2010.2068298>
- Nielsen, P. K., Andersen, L., & Jørgensen, K. (1998). The muscular load on the lower back and shoulders due to lifting at different lifting heights and frequencies. *Applied Ergonomics*. [https://doi.org/10.1016/S0003-6870\(98\)00005-2](https://doi.org/10.1016/S0003-6870(98)00005-2)
- NIOSH, & CDC. (2007). *Ergonomic guidelines for manual material handling*.
- Nussbaum, M. A., & Chaffin, D. B. (1998). Lumbar muscle force estimation using a subject-invariant 5-parameter EMG-based model. *Journal of Biomechanics*. [https://doi.org/10.1016/S0021-9290\(98\)00055-4](https://doi.org/10.1016/S0021-9290(98)00055-4)
- Occupational Safety & Health Administration. (n.d.). *Proper Lifting Techniques*.
- Oertel, C., Castellano, G., Chetouani, M., Nasir, J., Obaid, M., Pelachaud, C., & Peters, C. (2020). Engagement in Human-Agent Interaction: An Overview. *Frontiers in Robotics and*

AI. <https://doi.org/10.3389/frobt.2020.00092>

Olejnik, S., & Algina, J. (2003). Generalized Eta and Omega Squared Statistics: Measures of Effect Size for Some Common Research Designs. In *Psychological Methods*.

<https://doi.org/10.1037/1082-989X.8.4.434>

Oliveira, A. B., Silva, L. C. C. B., & Coury, H. J. C. G. (2011). How do low/high height and weight variation affect upper limb movements during manual material handling of industrial boxes? *Brazilian Journal of Physical Therapy*, *15*(6), 494–502.

<https://doi.org/10.1590/s1413-35552011005000017>

Ong, S. K., & Nee, A. Y. C. (2013). *Virtual and augmented reality applications in manufacturing*. Springer Science & Business Media.

Palmisano, S., Arcioni, B., & Stapley, P. J. (2018). Predicting vection and visually induced motion sickness based on spontaneous postural activity. *Experimental Brain Research*.

<https://doi.org/10.1007/s00221-017-5130-1>

Pantelidis, V. S. (2010). Reasons to Use Virtual Reality in Education and Training Courses and a Model to Determine When to Use Virtual Reality. *Themes in Science and Technology Education*.

Parekh, P., Patel, S., Patel, N., & Shah, M. (2020). Systematic review and meta-analysis of augmented reality in medicine, retail, and games. In *Visual Computing for Industry, Biomedicine, and Art*.

<https://doi.org/10.1186/s42492-020-00057-7>

Park, H., Branson, D., Kim, S., Warren, A., Jacobson, B., Petrova, A., Peksoz, S., & Kamenidis, P. (2014). Effect of armor and carrying load on body balance and leg muscle function. *Gait*

*and Posture*. <https://doi.org/10.1016/j.gaitpost.2013.08.018>

Paul, Y., Goyal, V., & Jaswal, R. A. (2017). Comparative analysis between SVM & KNN classifier for EMG signal classification on elementary time domain features. *4th IEEE International Conference on Signal Processing, Computing and Control, ISPCC 2017*. <https://doi.org/10.1109/ISPCC.2017.8269670>

Pausch, R., Proffitt, D., & Williams, G. (1997). Quantifying immersion in virtual reality. *Proceedings of the 24th Annual Conference on Computer Graphics and Interactive Techniques, SIGGRAPH 1997*. <https://doi.org/10.1145/258734.258744>

Perez, A. A., Hidalgo, M., Lediaeva, I., Mouloua, M., & Hancock, P. A. (2019). Considerations for the Usability and Implementation of Augmented Reality in Production Environments. *Proceedings of the Human Factors and Ergonomics Society Annual Meeting, 63(1)*, 2180–2184. <https://doi.org/10.1177/1071181319631453>

Perret, J., & Poorten, E. Vander. (2018). Touching Virtual Reality: A Review of Haptic Gloves. *ACTUATOR 2018; 16th International Conference on New Actuators*, 1–5. <https://ieeexplore.ieee.org/abstract/document/8470813>

Perry, J., & Bekey, G. A. (1981). EMG-FORCE RELATIONSHIPS IN SKELETAL MUSCLE. *Critical Reviews in Biomedical Engineering*.

Phinyomark, A., Thongpanja, S., Hu, H., Phukpattaranont, P., & Limsakul, C. (2012). The Usefulness of Mean and Median Frequencies in Electromyography Analysis. In *Computational Intelligence in Electromyography Analysis - A Perspective on Current Applications and Future Challenges* (pp. 195–220). <https://doi.org/10.5772/50639>

- Pirovano, M., Surer, E., Mainetti, R., Lanzi, P. L., & Alberto Borghese, N. (2016). Exergaming and rehabilitation: A methodology for the design of effective and safe therapeutic exergames. *Entertainment Computing, 14*, 55–65.  
<https://doi.org/10.1016/j.entcom.2015.10.002>
- Plaisier, M. A., & Smeets, J. B. J. (2012). Mass is all that matters in the size-weight illusion. *PLoS ONE*. <https://doi.org/10.1371/journal.pone.0042518>
- Pompeii, L. A., Lipscomb, H. J., Schoenfisch, A. L., & Dement, J. M. (2009). Musculoskeletal injuries resulting from patient handling tasks among hospital workers. *American Journal of Industrial Medicine, 52*(7), 571–578. <https://doi.org/10.1002/ajim.20704>
- Pratt, J. A., Hauser, K., Ugray, Z., & Patterson, O. (2007). Looking at human-computer interface design: Effects of ethnicity in computer agents. *Interacting with Computers*.  
<https://doi.org/10.1016/j.intcom.2007.02.003>
- Raaen, K. (2015). Measuring latency in virtual reality systems. *Lecture Notes in Computer Science (Including Subseries Lecture Notes in Artificial Intelligence and Lecture Notes in Bioinformatics)*. [https://doi.org/10.1007/978-3-319-24589-8\\_40](https://doi.org/10.1007/978-3-319-24589-8_40)
- Radwin, R. G., Chen, K. B., Ponto, K., & Tredinnick, R. D. (2013). Virtual exertions: Physical interactions in a virtual reality CAVE for simulating forceful tasks. *Proceedings of the Human Factors and Ergonomics Society, 57*(1), 967–971.  
<https://doi.org/10.1177/1541931213571216>
- Ragan, E. D., Bowman, D. A., Kopper, R., Stinson, C., Scerbo, S., & McMahan, R. P. (2015). Effects of field of view and visual complexity on virtual reality training effectiveness for a visual scanning task. *IEEE Transactions on Visualization and Computer Graphics*.

<https://doi.org/10.1109/TVCG.2015.2403312>

Rahman, S. A., & Rahman, A. (2010). Efficacy of Virtual Reality-Based Therapy on Balance in Children with Down Syndrome. *World Applied Sciences Journal*, 10(3), 254–261.

Ramadan, M. Z., Khalaf, T. M., Ragab, A. M., & Abdelgawad, A. A. (2018). Influence of shopping bags carrying on human responses while walking. *Journal of Healthcare Engineering*. <https://doi.org/10.1155/2018/5340592>

Ranstam, J., & Cook, J. A. (2018). LASSO regression. *British Journal of Surgery*, 105(10), 1348. <https://doi.org/10.1002/bjs.10895>

Reaz, M. B. I., Hussain, M. S., & Mohd-Yasin, F. (2006). Techniques of EMG signal analysis: Detection, processing, classification and applications. *Biological Procedures Online*, 8(1), 11–35. <https://doi.org/10.1251/bpo115>

Rebenitsch, L., & Owen, C. (2016). Review on cybersickness in applications and visual displays. *Virtual Reality*. <https://doi.org/10.1007/s10055-016-0285-9>

Riccio, G. E. (1995). Coordination of postural control and vehicular control: Implications for multimodal perception and simulation of self-motion. In *Local applications of the ecological approach to human-machine systems, Vol. 2*. (pp. 122–181).

Robertson, D. G. E., Caldwell, G. E., Hamill, J., Kamen, G., & Whittlesey, S. N. (2014). Research Methods in Biomechanics. In *Research Methods in Biomechanics*. <https://doi.org/10.5040/9781492595809>

Rose, F. D., Brooks, B. M., & Rizzo, A. A. (2005). Virtual reality in brain damage rehabilitation: Review. In *Cyberpsychology and Behavior*. <https://doi.org/10.1089/cpb.2005.8.241>

- Rose, T., Nam, C. S., & Chen, K. B. (2018). Immersion of virtual reality for rehabilitation - Review. In *Applied Ergonomics*. <https://doi.org/10.1016/j.apergo.2018.01.009>
- Roselyn Lee, J. E., Nass, C., Brave, S. B., Morishima, Y., Nakajima, H., & Yamada, R. (2007). The case for caring colearners: The effects of a computer-mediated colearner agent on trust and learning. *Journal of Communication*. <https://doi.org/10.1111/j.1460-2466.2007.00339.x>
- Saeed, B., Zia-ur-Rehman, M., Gilani, S. O., Amin, F., Waris, A., Jamil, M., & Shafique, M. (2021). Leveraging ANN and LDA Classifiers for Characterizing Different Hand Movements Using EMG Signals. *Arabian Journal for Science and Engineering*, 46(2), 1761–1769. <https://doi.org/10.1007/s13369-020-05044-x>
- Sapsanis, C., Georgoulas, G., Tzes, A., & Lymberopoulos, D. (2013). Improving EMG based classification of basic hand movements using EMD. *Proceedings of the Annual International Conference of the IEEE Engineering in Medicine and Biology Society, EMBS*. <https://doi.org/10.1109/EMBC.2013.6610858>
- Schmidt, R. A., Lee, T. D., Winstein, C. J., Wulf, G., & Zelaznik, H. (2019). Motor Control and Learning: A Behavioral Emphasis. In *Medicine & Science in Sports & Exercise*.
- Schuler, T., Brütsch, K., Müller, R., Van Hedel, H. J. A., & Meyer-Heim, A. (2011). Virtual realities as motivational tools for robotic assisted gait training in children: A surface electromyography study. *NeuroRehabilitation*, 28(4), 401–411. <https://doi.org/10.3233/NRE-2011-0670>
- Schultheis, M. T., & Rizzo, A. A. (2001). The application of virtual reality technology in rehabilitation. *Rehabilitation Psychology*, 46(3), 296–311. <https://doi.org/10.1037/0090-5550.46.3.296>

- Shao, Q., Bassett, D. N., Manal, K., & Buchanan, T. S. (2009). An EMG-driven model to estimate muscle forces and joint moments in stroke patients. *Computers in Biology and Medicine*. <https://doi.org/10.1016/j.compbiomed.2009.09.002>
- She, Q., Luo, Z., Meng, M., & Xu, P. (2010). Multiple kernel learning SVM-based EMG pattern classification for lower limb control. *11th International Conference on Control, Automation, Robotics and Vision, ICARCV 2010*.  
<https://doi.org/10.1109/ICARCV.2010.5707406>
- Shin, S., Langari, R., & Tafreshi, R. (2014). A performance comparison of emg classification methods for hand and finger motion. *ASME 2014 Dynamic Systems and Control Conference, DSCC 2014*. <https://doi.org/10.1115/DSCC2014-5993>
- Shingade, A., & Ghotkar, A. (2014). Animation of 3D Human Model Using Markerless Motion Capture Applied To Sports. *International Journal of Computer Graphics & Animation*.  
<https://doi.org/10.5121/ijcga.2014.4103>
- Sidner, C. L. (2008). Humanoid agents as hosts, advisors, companions and jesters. *Proceedings of the 21th International Florida Artificial Intelligence Research Society Conference, FLAIRS-21*.
- Sigrist, R., Rauter, G., Riener, R., & Wolf, P. (2013). Augmented visual, auditory, haptic, and multimodal feedback in motor learning: A review. In *Psychonomic Bulletin and Review*.  
<https://doi.org/10.3758/s13423-012-0333-8>
- Sinko, M., Kamencay, P., Hudec, R., & Benco, M. (2018). 3D registration of the point cloud data using ICP algorithm in medical image analysis. *12th International Conference ELEKTRO 2018, 2018 ELEKTRO Conference Proceedings*, 1–6.

<https://doi.org/10.1109/ELEKTRO.2018.8398245>

- Slater, M. (1999). Measuring presence: A response to the Witmer and Singer presence questionnaire. *Presence: Teleoperators and Virtual Environments*, 8(5), 560–565.
- Slater, M. (2018). Immersion and the illusion of presence in virtual reality. In *British Journal of Psychology*. <https://doi.org/10.1111/bjop.12305>
- Slater, M., Linakis, V., Usoh, M., & Kooper, R. (1995). Immersion , Presence , and Performance in Virtual Environments : An Experiment with Tri-Dimensional Chess. *Virtual Reality*. <https://doi.org/10.1.1.34.6594>
- Slater, M., Linakis, V., Usoh, M., & Kooper, R. (1996). Immersion, Presence, and Performance in Virtual Environments: An Experiment with Tri-Dimensional Chess. *Proceedings of the 3rd {ACM} Symposium on Virtual Reality Software and Technology ({VRST} 1996), Hong Kong, China*, 163–172. <https://doi.org/10.1.1.34.6594>
- Slater, M., & Usoh, M. (1993). Presence in immersive virtual environments. *1993 IEEE Annual Virtual Reality International Symposium*. <https://doi.org/10.1109/vrais.1993.380793>
- Smith, L. H., Hargrove, L. J., Lock, B. A., & Kuiken, T. A. (2011). Determining the optimal window length for pattern recognition-based myoelectric control: Balancing the competing effects of classification error and controller delay. *IEEE Transactions on Neural Systems and Rehabilitation Engineering*. <https://doi.org/10.1109/TNSRE.2010.2100828>
- So, R. H. Y., & Lo, W. T. (1999). Cybersickness: an experimental study to isolate the effects of rotational scene oscillations. *Virtual Reality, 1999. Proceedings., IEEE*, 237–241.
- So, R. H. Y., Lo, W. T., & Ho, A. T. K. (2001). Effects of navigation speed on motion sickness

caused by an immersive virtual environment. *Human Factors: The Journal of the Human Factors and Ergonomics Society*, 43(3), 452–461.

Sousa, A. S. P., & Tavares, J. M. R. S. (2012). Surface electromyographic amplitude normalization methods: A review. In *Electromyography: New Developments, Procedures and Applications*.

Spiewak, C. (2018). A Comprehensive Study on EMG Feature Extraction and Classifiers. *Open Access Journal of Biomedical Engineering and Biosciences*.  
<https://doi.org/10.32474/oajbeb.2018.01.000104>

Stanney, K. M., Hale, K. S., Nahmens, I., & Kennedy, R. S. (2003). What to Expect from Immersive Virtual Environment Exposure: Influences of Gender, Body Mass Index, and Past Experience. *Human Factors*. <https://doi.org/10.1518/hfes.45.3.504.27254>

Strickland, J. (2007). How Virtual Reality Works. *Howstuffwork.Com*.

Sveistrup, H. (2004). Motor rehabilitation using virtual reality. *Journal of NeuroEngineering and Rehabilitation*, 8, 1–8. <https://doi.org/10.1186/1743-0003-1-10>

Szczurowski, K., & Smith, M. (2018). Measuring presence: Hypothetical quantitative framework. *Proceedings of the 2017 23rd International Conference on Virtual Systems and Multimedia, VSMM 2017*. <https://doi.org/10.1109/VSMM.2017.8346261>

Tatić, D., & Tešić, B. (2017). The application of augmented reality technologies for the improvement of occupational safety in an industrial environment. *Computers in Industry*, 85, 1–10.

Terkildsen, T., & Makransky, G. (2019). Measuring presence in video games: An investigation

- of the potential use of physiological measures as indicators of presence. *International Journal of Human Computer Studies*. <https://doi.org/10.1016/j.ijhcs.2019.02.006>
- Tibshirani, R. (1997). The lasso method for variable selection in the cox model. *Statistics in Medicine*, 16(4), 385–395. [https://doi.org/10.1002/\(SICI\)1097-0258\(19970228\)16:4<385::AID-SIM380>3.0.CO;2-3](https://doi.org/10.1002/(SICI)1097-0258(19970228)16:4<385::AID-SIM380>3.0.CO;2-3)
- Toledo-Pérez, D. C., Rodríguez-Reséndiz, J., Gómez-Loenzo, R. A., & Jauregui-Correa, J. C. (2019). Support Vector Machine-based EMG signal classification techniques: A review. In *Applied Sciences (Switzerland)*. <https://doi.org/10.3390/app9204402>
- Too, J., Abdullah, A. R., & Saad, N. M. (2019). Classification of Hand movements based on discrete wavelet transform and enhanced feature extraction. *International Journal of Advanced Computer Science and Applications*, 10(6), 83–89. <https://doi.org/10.14569/ijacsa.2019.0100612>
- Total, D., Ojeda, L., Johnson, D. D., Gates, D., Provost, E. M., & Barton, K. (2018). Low-back electromyography (EMG) data-driven load classification for dynamic lifting tasks. *PLoS ONE*, 13(2), 1–14. <https://doi.org/10.1371/journal.pone.0192938>
- Trinkoff, A. M., Brady, B., & Nielsen, K. (2003). Workplace prevention and musculoskeletal injuries in nurses. *Journal of Nursing Administration*, 33(3), 153–158.
- U.S. Bureau of Labor Statistics. (2019). *2018 Survey of occupational injuries & illnesses*.
- U.S. Bureau of Labor Statistics. (2021). *HOUSEHOLD DATA ANNUAL AVERAGES Table 11. Employed persons by detailed occupation, sex, race, and Hispanic or Latino ethnicity*.
- Uppot, R. N., Laguna, B., McCarthy, C. J., De Novi, G., Phelps, A., Siegel, E., & Courtier, J.

- (2019). Implementing virtual and augmented reality tools for radiology education and training, communication, and clinical care. In *Radiology*.  
<https://doi.org/10.1148/radiol.2019182210>
- Vera-Garcia, F. J., Moreside, J. M., & McGill, S. M. (2010). MVC techniques to normalize trunk muscle EMG in healthy women. *Journal of Electromyography and Kinesiology*.  
<https://doi.org/10.1016/j.jelekin.2009.03.010>
- Vilkoniene, M. (2009). Influence of Augmented Reality Technology upon Pupils' Knowledge about Human Digestive System: The Results of the Experiment. [JOUR]. *Online Submission*, 6(1), 36–43.
- Weber-Fechner Law. (2005). In *Van Nostrand's Scientific Encyclopedia*.  
<https://doi.org/10.1002/0471743984.vse7496>
- Wellner, M., Schaufelberger, A., Zitzewitz, J. V., & Riener, R. (2008). Evaluation of visual and auditory feedback in virtual obstacle walking. *Presence: Teleoperators and Virtual Environments*. <https://doi.org/10.1162/pres.17.5.512>
- Westgaard, R. H., & Winkel, J. (1997). Ergonomic intervention research for improved musculoskeletal health: a critical review [JOUR]. *International Journal of Industrial Ergonomics*, 20(6), 463–500.
- Winkel, J., & Jørgensen, K. (1991). Significance of skin temperature changes in surface electromyography. *European Journal of Applied Physiology and Occupational Physiology*.  
<https://doi.org/10.1007/BF00364460>
- Winter, D. A., & Yack, H. J. (1987). EMG profiles during normal human walking: stride-to-

stride and inter-subject variability. *Electroencephalography and Clinical Neurophysiology*.  
[https://doi.org/10.1016/0013-4694\(87\)90003-4](https://doi.org/10.1016/0013-4694(87)90003-4)

Witmer, B. G., & Singer, M. J. (1998). Measuring presence in virtual environments: A presence questionnaire. *Presence*, 7, 225–240.

Wu, G., Van Der Helm, F. C. T., Veeger, H. E. J., Makhsous, M., Van Roy, P., Anglin, C., Nagels, J., Karduna, A. R., McQuade, K., Wang, X., Werner, F. W., & Buchholz, B. (2005). ISB recommendation on definitions of joint coordinate systems of various joints for the reporting of human joint motion - Part II: Shoulder, elbow, wrist and hand. *Journal of Biomechanics*, 38(5), 981–992. <https://doi.org/10.1016/j.jbiomech.2004.05.042>

Yang, J. F., & Winter, D. A. (1984). Electromyographic amplitude normalization methods: Improving their sensitivity as diagnostic tools in gait analysis. *Archives of Physical Medicine and Rehabilitation*.

Yasobant, S., & Rajkumar, P. (2014). Work-related musculoskeletal disorders among health care professionals: A cross-sectional assessment of risk factors in a tertiary hospital, India. *Indian Journal of Occupational and Environmental Medicine*. <https://doi.org/10.4103/0019-5278.146896>

Yates, J. W., & Karwowski, W. (1992). An electromyographic analysis of seated and standing lifting tasks. *Ergonomics*. <https://doi.org/10.1080/00140139208967369>

Yim, H. Bin, & Seong, P. H. (2010). Heuristic guidelines and experimental evaluation of effective augmented-reality based instructions for maintenance in nuclear power plants. *Nuclear Engineering and Design*, 240(12), 4096–4102.

<https://doi.org/10.1016/j.nucengdes.2010.08.023>

- Zhai, X., Jelfs, B., Chan, R. H. M., & Tin, C. (2016). Short latency hand movement classification based on surface EMG spectrogram with PCA. *Proceedings of the Annual International Conference of the IEEE Engineering in Medicine and Biology Society, EMBS*.  
<https://doi.org/10.1109/EMBC.2016.7590706>
- Zhang, D., Zhao, X., Han, J., & Zhao, Y. (2014). A comparative study on PCA and LDA based EMG pattern recognition for anthropomorphic robotic hand. *Proceedings - IEEE International Conference on Robotics and Automation*.  
<https://doi.org/10.1109/ICRA.2014.6907569>
- Zhang, Y., Fernando, T., Sotudeh, R., & Xiao, H. (2005). The use of visual and auditory feedback for assembly task performance in a virtual environment. *Proceedings of the International Conference on Information Visualisation*. <https://doi.org/10.1109/IV.2005.127>
- Zhao, Y., Bennett, C. L., Benko, H., Cutrell, E., Holz, C., Morris, M. R., & Sinclair, M. (2018). Enabling people with visual impairments to navigate virtual reality with a haptic and auditory cane simulation. *Conference on Human Factors in Computing Systems - Proceedings*. <https://doi.org/10.1145/3173574.3173690>
- Zyda, M. (2005). From visual simulation to virtual reality to games. *Computer*, 38(9), 25–32.

## **APPENDICES**

## Appendix A

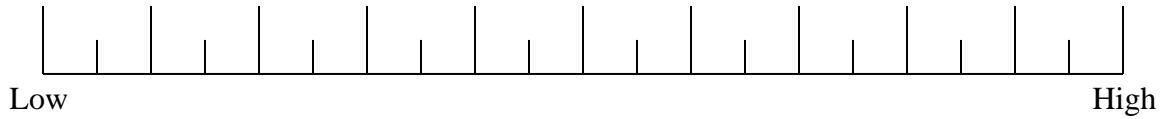
### Post-Study System Usability Questionnaire

Description	Strongly Agree				Strongly Disagree		
	1	2	3	4	5	6	7
1. Overall, I'm satisfied with the system.							
2. It was simple to use this system.							
3. I was able to complete the tasks and scenarios quickly using this system.							
4. I felt comfortable using this system.							
5. It was easy to learn to use this system.							
6. I believe I could become productive quickly using this system.							
7. The system gave error messages that clearly told me how to fix problems.							
8. Whenever I made a mistake using the system, I could recover easily and quickly.							
9. The information (such as online help, on-screen messages, and other documentation) provided with this system was clear.							
10. It was easy to find the information I needed.							
11. The information was effective in helping me complete the tasks and scenarios.							
12. The organization of information on the system screens was clear.							
13. The interface of this system was pleasant.							
14. I liked using the interface of this system.							
15. This system has all the functions and capabilities I expect it to have.							
16. Overall, I am satisfied with this system.							

## Appendix B

### NASA-TLX

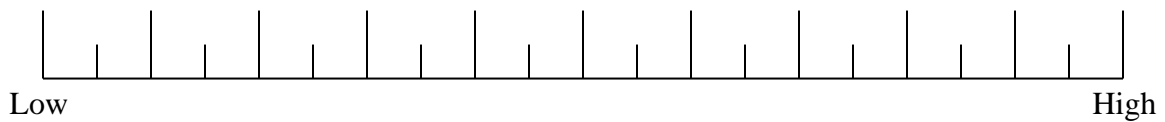
**MENTAL DEMAND:** How much mental and perceptual activity was required?



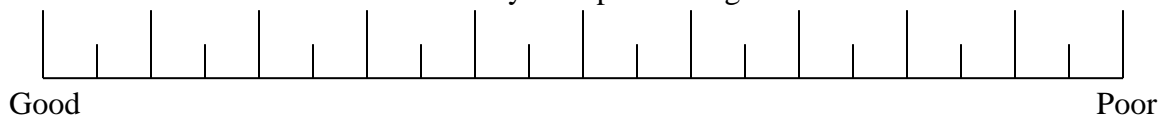
**PHYSICAL DEMAND:** How much physical activity was required?



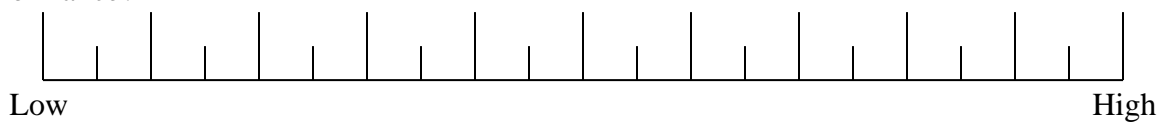
**TEMPORAL DEMAND:** How much time pressure did you feel due to the pace at which the tasks or task elements occurred?



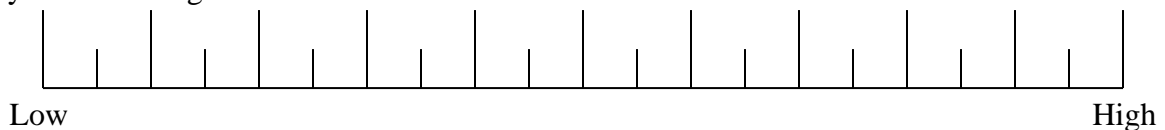
**PERFORMANCE:** How successful were you in performing the task?



**EFFORT:** How hard did you have to work (mentally and physically) to accomplish your level of performance?



**FRUSTRATION:** How irritated, stressed, and annoyed versus content, relaxed, and complacent did you feel during the task?



## Appendix C

### Borg rating of perceived exertion (RPE) in category ratio scale (CR-10 scale)

Scoring	Level of exertion
0	No Exertion
0.5	Very very Slight
1	Very Slight
2	Slight
3	Moderate
4	Somewhat Severe
5	Severe
6	
7	Very Severe
8	
9	Very very Severe
10	Maximal